Surface Girders

Jerzy Podgórski *Jarosław Bęc*

Lublin 2016

1. Introduction

Surface girders are a group of structures (or structural members) which are characterized by some similarity of shapes, i.e. three dimensional by nature members have got one of their dimensions significantly smaller than two others. This dimension, usually called “thickness” is in case of technical applications of theory of surface girders at least one order smaller (i.e. 10 times) smaller than dimensions measured in other perpendicular directions. Considering the working characteristics of these structures they are usually divided into: slabs, plates and surfaces. Slabs and plates are structures that ignoring the thickness may be treated as planar elements, while surfaces are curved elements.

Slabs are structures loaded in their planes, so the state of stresses occurring in them can be treated with high accuracy as planar in case they are “thin enough”. When we deal with massive (“thick”) slab we often can simplify the analysis of the state of strain assuming that this is a 2D state which simplifies the calculations. In both cases a slab can be considered as a two dimensional structure which decreases the number of the needed components of state of strain or stress.

A plate, though externally similar to a slab, yet it is loaded perpendicularly to its surface which produces its state of strain called bending. In the theory of thin plates there have been introduced assumptions similar in their nature to the theory of beams, i.e. assumption on straight normals to the surface before deflection which after deformation (bending of the plate) remain straight and normal to the deflected surface. This simplification proposed by Kirchhoff and Love is widely applied in engineering and contributes to simplification of essential equations needed to solve the states of stress and strain.

A surface is a structure which on the grounds of its curvature is usually subjected to compression and tension, as well as to bending. It is obviously much more complicated problem to obtain needful components of states of stress and strain in this case than for slabs or plates. This is why there are usually applied specific methods for specific cases of Surface geometry, i.e. cylindrical, revolutionary or surfaces in membrane state, which again lets the limitation of the effort needed for problem solution.

We will try to present the simplest approaches to solution of the problem of surface girders statics. There will be shown methods used in analyses of such structures and many examples of solution for specific engineering problems. We will discuss analytical and numerical methods used nowadays in engineering practice. Special attention will be paid to the issue of plate bending, which is essential in the process of civil engineering structures design and additionally profitable from the point of view of teaching and comparison of different computational methods.

At the end of this introduction, we should comment on the term in the title of this book "Surface Girders" which rather does not occur in English literature, but a compact and well characterizing the described structures' work. It is generally exact translation of the term proposed by Witold Nowacki in the tile of his Polish book „Dźwigary powierzchniowe", which may heve been inspires by other well-known book „Fläschentragwerke" by Karl Girkmann. In English literature there is usually employed term "Theory of plates and shells" – e.g. famous book by Stephen Timoshenko and S. Woinowsky-Krieger. The term „slab" for compressed plates is also rarely used, but we have decided to use it consistently to distinguish bended plates from compressed slabs.

The contents of this book mostly consist of the material used by the authors during lectures and classes conducted at the Faculty of Civil Engineering and Architecture of Lublin University of Technology over the period 2000-2012.

2. Theoretical Background – Introduction to Theory of Elasticity

Here we will present a few basic assumptions and theorems of mechanics which will be used in the subsequent chapters of this book.

2.1. Assumptions regarding the linear model of a structure

In this chapter and some subsequent ones we will be dealing with linear problems of mechanics. This means that the process of structural deformation can be written by linear differential equations. It involves the following consequences:

- Displacements of structure points which appear during deformation are small. Linear displacements are considerably smaller than the characteristic dimension of a structure (for example, the deflection of a beam is a few hundredths times smaller than its length) and angles of rotation are considerably smaller than one (for example, a nodal angle of rotation is smaller than 0.01 rad).
- Strains are small. It enables the relationship between strains and displacements to be expressed with the help of linear equations.
- The material is linear elastic which means that it satisfies Hook's law.

It may seem that such limits which are put on both geometry of a structure and material characteristics strongly restrict the application of the model. In effect these limits are realized for many structures (they can refer to most of them), so the range of usage of the model is very wide. The reader should know this when he proceeds with the description of any real problem in terms of mechanics equations.

2.2. Stresses and strains

We will denote components of the stress tensor traditionally as it occurs in most books on the finite element method. This means that components of direct stress will be denoted by letters σ_x , σ_y , σ_z and components of shear stress by τ_{xy} , τ_{xz} , τ_{yz} (Eqn. 2.1a). Because of the symmetry of the stress tensor ($\tau_{xy}= \tau_{yx}$, $\tau_{xz}= \tau_{zx}$, $\tau_{yz}= \tau_{zy}$) [Fung], [Timoshenko, Goodier], we will use only six components which when presented in a column matrix form the stress vector (Eqn 2.1b):

$$\text{a)}\quad \boldsymbol{\sigma} = \begin{bmatrix} \sigma_x & \tau_{xy} & \tau_{xz} \\ \tau_{yx} & \sigma_y & \tau_{yz} \\ \tau_{zx} & \tau_{zy} & \sigma_z \end{bmatrix}, \qquad \text{b)}\quad \boldsymbol{\sigma} = \begin{bmatrix} \sigma_x \\ \sigma_y \\ \sigma_z \\ \tau_{xy} \\ \tau_{xz} \\ \tau_{yz} \end{bmatrix}. \tag{2.1}$$

Denoting the components of the strain tensor traditionally (Eqn.2.2a) we assume the following definitions:

$$\begin{aligned} &\varepsilon_x = \frac{\partial u_x}{\partial x}, \quad \varepsilon_y = \frac{\partial u_y}{\partial y}, \quad \varepsilon_z = \frac{\partial u_z}{\partial z}, \\ &\gamma_{xy} = \gamma_{yx} = \frac{\partial u_x}{\partial y} + \frac{\partial u_y}{\partial x}, \quad \gamma_{xz} = \gamma_{zx} = \frac{\partial u_x}{\partial z} + \frac{\partial u_z}{\partial x}, \quad \gamma_{yz} = \gamma_{zy} = \frac{\partial u_y}{\partial z} + \frac{\partial u_z}{\partial y}, \end{aligned} \tag{2.2}$$

where $\varepsilon_x, \varepsilon_y, \varepsilon_z,$ are the components of direct strain (unit elongation) and $\gamma_{xy}, \gamma_{xz}, \gamma_{yz}$ the components of shear strain (they are the angles of the non-dilatation strain), u_x, u_y, u_z are the components of the displacement vector in the cartesian coordinate system.

We write the components of strain in the form of a column matrix - the strain vector (Eqn. 2.2b):

$$\text{a)}\quad \boldsymbol{\varepsilon} = \begin{bmatrix} \varepsilon_x & \gamma_{xy} & \gamma_{xy} \\ \gamma_{yx} & \varepsilon_y & \gamma_{yz} \\ \gamma_{zx} & \gamma_{zy} & \varepsilon_z \end{bmatrix}, \qquad \text{b)}\quad \boldsymbol{\varepsilon} = \begin{bmatrix} \varepsilon_x \\ \varepsilon_y \\ \varepsilon_z \\ \gamma_{xy} \\ \gamma_{xz} \\ \gamma_{yz} \end{bmatrix}. \tag{2.3}$$

We simplify the calculation of the internal work $\mathcal{W}$ if we take the components of the strain vector $\gamma_{\alpha\beta}$ (the angles of the volumetric strain) instead of usual tensor definitions:

$$\mathcal{W} = \int_{\mathcal{V}} \boldsymbol{\sigma}^{\mathrm{T}} \boldsymbol{\varepsilon} \, d\mathcal{V} = \int_{\mathcal{V}} \boldsymbol{\varepsilon}^{\mathrm{T}} \mathbf{D} \, \boldsymbol{\varepsilon} \, d\mathcal{V}, \tag{2.4}$$

where $\mathcal{V}$ means the volume of a body.

2.3. Constitutive equations

As we have noted in our introductory assumptions, the relationship between the components of the stress tensor and the components of the strain tensor (that is, between $\boldsymbol{\sigma}$ and $\boldsymbol{\varepsilon}$ in our notation) is expressed by the linear equation:

$$\boldsymbol{\sigma} = \mathbf{D} \cdot \boldsymbol{\varepsilon}, \tag{2.5}$$

$$\boldsymbol{\varepsilon} = \mathbf{D}^{-1} \cdot \boldsymbol{\sigma}, \tag{2.6}$$

where **D** is the square matrix with dimensions 6×6 containing the material constants:

$$\mathbf{D} = \begin{bmatrix} \lambda+2\mu & \lambda & \lambda & 0 & 0 & 0 \\ \lambda & \lambda+2\mu & \lambda & 0 & 0 & 0 \\ \lambda & \lambda & \lambda+2\mu & 0 & 0 & 0 \\ 0 & 0 & 0 & \mu & 0 & 0 \\ 0 & 0 & 0 & 0 & \mu & 0 \\ 0 & 0 & 0 & 0 & 0 & \mu \end{bmatrix}, \tag{2.7}$$

where λ and μ are the Lamé constants.

Since some other material constants like Young's modulus - E and Poisson's ratio ν are more often used, in practice we present the relationships between them and the Lamé constants by the following formulae:

$$\lambda = \frac{\nu E}{(1+\nu)(1-2\nu)}, \qquad \mu = \frac{E}{2(1+\nu)}. \tag{2.8}$$

The Lamé constant μ is noted by the letter G and is called Kirchhoff's (or shear) modulus.

The inverse matrix $\mathbf{D}^{-1}$ with the material constants has an unusually simple structure which is best shown by means of the constants E, ν:

$$\mathbf{D}^{-1} = \frac{1}{E}\begin{bmatrix} 1 & -\nu & -\nu & 0 & 0 & 0 \\ -\nu & 1 & -\nu & 0 & 0 & 0 \\ -\nu & -\nu & 1 & 0 & 0 & 0 \\ 0 & 0 & 0 & 2(1+\nu) & 0 & 0 \\ 0 & 0 & 0 & 0 & 2(1+\nu) & 0 \\ 0 & 0 & 0 & 0 & 0 & 2(1+\nu) \end{bmatrix}. \tag{2.9}$$

It should be noted that matrix **D** is symmetrical which means that the dependence $\mathbf{D}=\mathbf{D}^{\mathsf{T}}$ occurs. This dependence will often be used in conversions.

2.4. Plane stress

In two-dimensional problems of thin plates, the following simplification of the assumption is:

$$\sigma_z = 0, \quad \tau_{zx} = 0, \quad \tau_{zy} = 0, \tag{2.10}$$

which leads to the plane stress criterion.

If we put equation 1.10 into equation 1.5 taking into consideration data from equation 1.7 we obtain:

$$\varepsilon_z = -\frac{\nu}{1-\nu}\left(\varepsilon_x + \varepsilon_y\right),\ \gamma_{zx} = 0,\ \gamma_{zy} = 0. \tag{2.11}$$

In plane stress, the dimensions of the stress and strain vectors and the matrix of the material constants are reduced by half and thus:

$$\boldsymbol{\sigma} = \begin{bmatrix} \sigma_x \\ \sigma_y \\ \tau_{xy} \end{bmatrix}, \qquad \boldsymbol{\varepsilon} = \begin{bmatrix} \varepsilon_x \\ \varepsilon_y \\ \gamma_{xy} \end{bmatrix}, \qquad \boldsymbol{\sigma} = \mathbf{D}\cdot\boldsymbol{\varepsilon}, \qquad \boldsymbol{\varepsilon} = \mathbf{D}^{-1}\cdot\boldsymbol{\sigma} \tag{2.12}$$

$$\mathbf{D} = \frac{E}{1-\nu^2}\begin{bmatrix} 1 & \nu & 0 \\ \nu & 1 & 0 \\ 0 & 0 & \dfrac{1-\nu}{2} \end{bmatrix}, \tag{2.13}$$

$$\mathbf{D}^{-1} = \frac{1}{E}\begin{bmatrix} 1 & -\nu & 0 \\ -\nu & 1 & 0 \\ 0 & 0 & 2(1+\nu) \end{bmatrix}. \tag{2.14}$$

2.5. Plane strain

In problems regarding deformations of massive buildings, the plane strain criterion is often found and it is expressed by the equations:

$$\varepsilon_z = 0, \quad \gamma_{zx} = 0, \quad \gamma_{zy} = 0, \tag{2.15}$$

When we insert the above equations into 1.6 taking also into consideration 1.9 we get the following relations:

$$\sigma_z = \nu\left(\sigma_x + \sigma_y\right), \quad \tau_{zx} = 0, \quad \tau_{zy} = 0 \tag{2.16}$$

This is called the plane strain.

After taking into consideration the above equations 1.15 and 1.16, we can notice that the relationship between the reduced stress and strain vectors 1.12 leads to the following matrix of elastic constants:

$$\mathbf{D} = \frac{E}{(1+\nu)(1-2\nu)}\begin{bmatrix} 1-\nu & \nu & 0 \\ \nu & 1-\nu & 0 \\ 0 & 0 & \frac{1-2\nu}{2} \end{bmatrix}, \tag{2.17}$$

$$\mathbf{D}^{-1} = \frac{1-\nu^2}{E}\begin{bmatrix} 1 & \frac{-\nu}{1-\nu} & 0 \\ \frac{-\nu}{1-\nu} & 1 & 0 \\ 0 & 0 & \frac{2}{1-\nu} \end{bmatrix}. \tag{2.18}$$

3. Theory of Slabs

The 2D element can be defined as a solid of which one dimension (thickness) is considerably smaller than the two others and whose middle plane (the surface parallel to both external surfaces of an element) is a plane (Fig. 3.1). A plate element has also such a shape but the 2D element differs from a plate the way it is loaded. The 2D element can be loaded only with the load acting in its plane and by the temperature dependent upon the *x* and *y* coordinates. On the other hand, the plate can be loaded with a force perpendicular to its surface or any temperature field. Plate elements will be discussed in the following chapter.

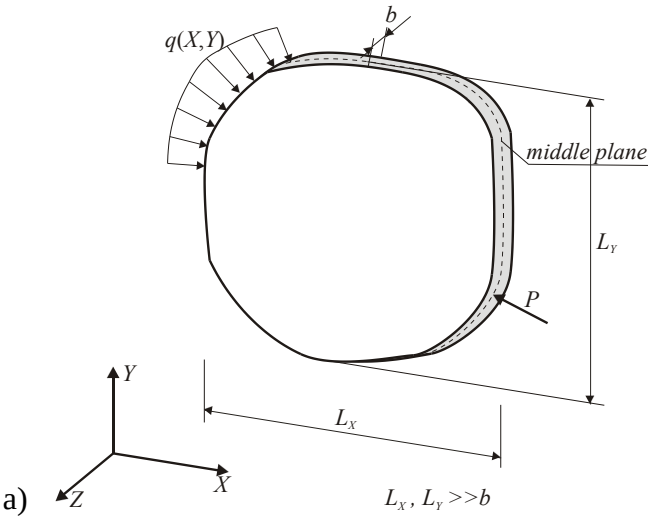

a)

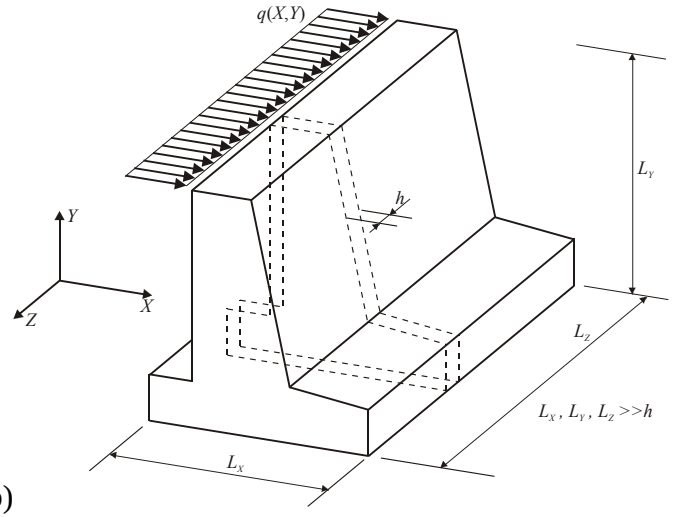

b)

Fig. 3.1. The exemplary application of a 2D element.

When external surfaces of a 2D element are free and this element is thin enough (Fig. 3.1a), we can assume that $\sigma_z = 0, \tau_{zx} = 0, \tau_{zy} = 0$ in reference to the whole thickness of the element. Then it is said that this is a plane stress problem. The thinner the 2D element (comp. Nowacki (1979), Timoshenko and Goodier (1962)), the better the approximation is. Hence only the components of stress shown in Fig. 3.2 are non-zero.

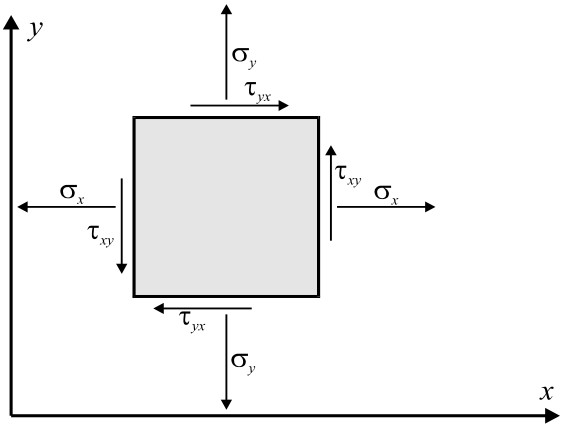

Fig. 3.2. Stress tensor components in plane stress.

With regard to the symmetry of a stress tensor components of shear stress τ_{xy} and τ_{yx} are equal, thus we have three independent components of stress which we compose in the stress vector:

$$\boldsymbol{\sigma} = \begin{bmatrix} \sigma_x \\ \sigma_y \\ \tau_{xy} \end{bmatrix}. \tag{3.1}$$

A completely different case occurs when the component L_Z in Fig. 3.1b is very significant, that is $h << L_X, L_Y, L_Z$, and the support and load conditions are constant along the axis which is perpendicular to the element. The structure satisfying these conditions can also be analysed by applying plane state which in fact is plane strain. Since the cross dimension of the structure shown in Fig. 3.1b prevents the structure deformation in the direction perpendicular to the cross section, the thin layer cut out from this structure is in the state described by the equation:

$$\varepsilon_z = 0, \quad \gamma_{zx} = 0, \quad \gamma_{zy} = 0. \tag{3.2}$$

$\sigma_z \neq 0$ comes from the above equations, but the first equation allows to calculate the component σ_z on the basis of two other components of a direct stress. Thus, we have

$$\sigma_z = \nu\left(\sigma_x + \sigma_y\right), \tag{3.3}$$

which allows to limit the number of searched components of the stress vector to three components given in Eqn. (3.1)

We also group independent components of the strain tensor in a column matrix which we have called a strain vector:

$$\boldsymbol{\varepsilon} = \begin{bmatrix} \varepsilon_x \\ \varepsilon_y \\ \gamma_{xy} \end{bmatrix}. \tag{3.4}$$

There is a relationship between vectors **σ** and **ε** described by constitutive equations whose form depends on the model of the material which the structure is made of. In this book we deal only with elastic isotropic materials which obey Hook's law. Hence we can write the constitutive equation as follows:

$$\boldsymbol{\sigma} = \mathbf{D} \cdot \boldsymbol{\varepsilon}, \tag{3.5}$$

where **D** is a square matrix containing material elastic constants described in Chapter 2.

For plane stress, the matrix **D** has the form written by Eqn. (2.13). Plane strain requires another matrix for elastic constants which is described by Eqn. (2.17).

3.1. Geometric relationships

A certain point can move only on the plane during the deformation process and then the displacement vector of this point **u**(*x*,*y*) has two components:

$$\mathbf{u}(x,y) = \begin{bmatrix} u_x(x,y) \\ u_y(x,y) \end{bmatrix}. \tag{3.6}$$

Some known relations exist (Timoshenko and Goodier (1962)) between the components of displacement and strain vectors:

$$\varepsilon_x = \frac{\partial u_x}{\partial x}, \quad \varepsilon_y = \frac{\partial u_y}{\partial y}, \quad \gamma_{xy} = \frac{\partial u_x}{\partial y} + \frac{\partial u_y}{\partial x}, \tag{3.7}$$

which can be presented in the form:

$$\boldsymbol{\varepsilon}=\mathscr{D}\,\mathbf{u}(x,y),\quad \mathscr{D}=\begin{bmatrix}\partial_x & 0\\ 0 & \partial_y\\ \partial_y & \partial_x\end{bmatrix},\quad \partial_x=\frac{\partial}{\partial x},\quad \partial_y=\frac{\partial}{\partial y}, \tag{3.8}$$

where $\mathscr{D}$ is the matrix of differential operators.

3.2. Equilibrium equations

Let us consider equilibrium of infinitely small part of a slab with dimensions $dx \times dy$ and Thickness b (Fig. 3.3). Assuming plane state of stress and consequently constant stresses at the plate thickness, we can write down equilibrium equations:

$$\sum X=0,\quad \sum Y=0,\quad \sum M=0, \tag{3.9}$$

which lead to the following relations:

$$\begin{aligned}
&\sum X=\left(\sigma_x+d\sigma_x-\sigma_x\right)b\,dy+\left(\tau_{xy}+d\tau_{xy}-\tau_{xy}\right)b\,dx+F_x\,b\,dx\,dy=0,\\
&\sum Y=\left(\sigma_y+d\sigma_y-\sigma_y\right)b\,dx+\left(\tau_{xy}+d\tau_{xy}-\tau_{xy}\right)b\,dy+F_y\,b\,dx\,dy=0,\\
&\sum M=\left(\tau_{xy}+d\tau_{xy}+\tau_{xy}\right)b\,dy\,dx/2-\left(\tau_{xy}+d\tau_{xy}+\tau_{xy}\right)b\,dy\,dx/2=0.
\end{aligned} \tag{3.10}$$

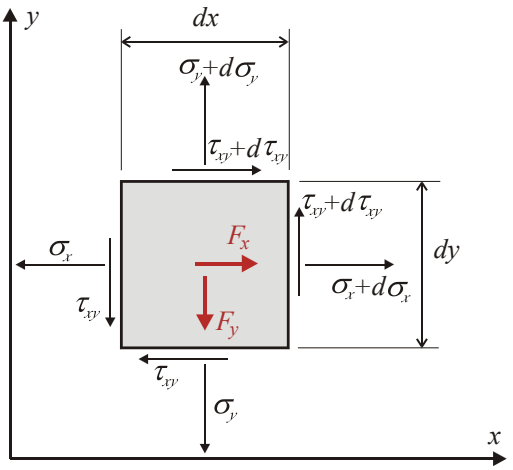

Fig. 3.3. Stress components and body forces in infinitesimal slab element.

Dividing two first equations (3.10) by the volume of the element ($\mathscr{V}=b\times dx\times dy$) we obtain:

$$\frac{d\sigma_x}{dx}+\frac{d\tau_{xy}}{dy}+F_x=0,$$
$$\frac{d\sigma_y}{dy}+\frac{d\tau_{xy}}{dx}+F_y=0. \tag{3.11}$$

The third equation is fulfilled automatically by assuming the stress tensor symmetry ($\tau_{xy}=\tau_{yx}$). Calculating the limit of the relation (3.11) at the dimensions of the element approaching zero ($dx \to 0$, $dy \to 0$) we obtain differential equilibrium equations:

$$\frac{\partial\sigma_x}{\partial x}+\frac{\partial\tau_{xy}}{\partial y}+F_x=0,$$
$$\frac{\partial\sigma_y}{\partial y}+\frac{\partial\tau_{xy}}{\partial x}+F_y=0. \tag{3.12}$$

System of two equations (3.12) contains three unknown components of stress vector which imposes the need of additional relation combining the quantities we want to find. It can be delivered by so-called compatibility condition, which utilizes the combination of three components of stress vector and two components of displacement vector through (3.6) the stress-strain constitutive relation (2.5). This method leading to the classical solution of the plane stress state with use of Airy's stress function will be shown in the next chapter.

Another method is writing down equilibrium equations (3.12) in such a way that the unknown quantities are components of displacement vector. Thanks to constitutive relations at the assumption of plane stress state, we obtain (comp.[Fung]):

$$G\left[\nabla^2 u_x+\frac{1+\nu}{1-\nu}\frac{\partial}{\partial x}\left(\frac{\partial u_x}{\partial x}+\frac{\partial u_y}{\partial y}\right)\right]+F_x=0,$$
$$G\left[\nabla^2 u_y+\frac{1+\nu}{1-\nu}\frac{\partial}{\partial y}\left(\frac{\partial u_x}{\partial x}+\frac{\partial u_y}{\partial y}\right)\right]+F_y=0, \tag{3.13}$$

where G is shear modulus (2.8), and ∇^2 is Laplace operator:

$$\nabla^2=\left(\frac{\partial^2}{\partial x^2}+\frac{\partial^2}{\partial y^2}\right). \tag{3.14}$$

Assumption of plane strain results in the following form of equations:

$$G\left[\nabla^2 u_x + \frac{1}{1-2\nu}\frac{\partial}{\partial x}\left(\frac{\partial u_x}{\partial x}+\frac{\partial u_y}{\partial y}\right)\right]+F_x=0,$$
$$G\left[\nabla^2 u_y + \frac{1}{1-2\nu}\frac{\partial}{\partial y}\left(\frac{\partial u_x}{\partial x}+\frac{\partial u_y}{\partial y}\right)\right]+F_y=0. \tag{3.15}$$

Comparison of relations (3.13) and (3.15) leads to the conclusion that after replacement of Poisson's coefficient by $\nu' = \nu/(1-\nu)$ in equations (3.15) we obtain relations (3.13). It allows simple conversion of the solutions obtained for plane stress into plane strain and other way around.

3.3. Compatibility equations

Condition of strain compatibility is resulting from relations (2.2), which define components of small strain tensor and vector. In case of plane strain we have:

$$u_z=0,\quad \varepsilon_x=\frac{\partial u_x}{\partial x},\quad \varepsilon_y=\frac{\partial u_y}{\partial y},\quad \varepsilon_z=\frac{\partial u_z}{\partial z}=0,\quad \sigma_z=\nu\left(\sigma_x+\sigma_y\right)$$
$$\gamma_{xy}=\gamma_{yx}=\frac{\partial u_x}{\partial y}+\frac{\partial u_y}{\partial x},\quad \gamma_{xz}=\gamma_{zx}=0,\quad \gamma_{yz}=\gamma_{zy}=0. \tag{3.16}$$

In case of plane stress the relations are slightly different:

$$\sigma_z=0,\quad \gamma_{xz}=0,\quad \gamma_{yz}=0,\quad \varepsilon_x=\frac{\partial u_x}{\partial x},\quad \varepsilon_y=\frac{\partial u_y}{\partial y},\quad \varepsilon_z=-\frac{\nu}{1-\nu}\left(\varepsilon_x+\varepsilon_y\right),$$
$$\gamma_{xy}=\gamma_{yx}=\frac{\partial u_x}{\partial y}+\frac{\partial u_y}{\partial x},\quad \gamma_{xz}=\gamma_{zx}=0,\quad \gamma_{yz}=\gamma_{zy}=0. \tag{3.17}$$

Common for both plane states is dependence of components of stress and strain only on two coordinates x, y. Because 3 independent components of strain tensor are obtained through derivation of 2 components of displacement vector (u_x, u_y), then there must occur the relation between them called compatibility relation.

It is obtained by comparison of the following derivatives:

$$\frac{\partial^2\varepsilon_x}{\partial y^2}=\frac{\partial^3 u_x}{\partial x\,\partial y^2},\quad \frac{\partial^2\varepsilon_y}{\partial x^2}=\frac{\partial^3 u_y}{\partial x^2},\quad \frac{\partial^2\gamma_{xy}}{\partial x\,\partial y}=\frac{\partial^3 u_x}{\partial x\,\partial y^2}+\frac{\partial^3 u_y}{\partial x^2\,\partial y}, \tag{3.18}$$

so

$$\frac{\partial^2 \varepsilon_x}{\partial y^2} + \frac{\partial^2 \varepsilon_y}{\partial x^2} = \frac{\partial^2 \gamma_{xy}}{\partial x \partial y}. \tag{3.17}$$

Substituting now constitutive relations of plane stress (2.12) into (3.17) we obtain the equation

$$\frac{\partial^2}{\partial y^2}\left(\sigma_x - \nu\sigma_y\right) + \frac{\partial^2}{\partial x^2}\left(\sigma_y - \nu\sigma_x\right) = \left(1+\nu\right)\frac{\partial^2 \tau_{xy}}{\partial x \partial y}, \tag{3.18}$$

which after taking equilibrium equations (3.12) into consideration obtains the following form:

$$\nabla^2\left(\sigma_x + \sigma_y\right) = -\left(1+\nu\right)\left(\frac{\partial F_x}{\partial x} + \frac{\partial F_y}{\partial y}\right). \tag{3.19}$$

Executing similar operations in plane strain we get:

$$\nabla^2\left(\sigma_x + \sigma_y\right) = -\frac{1}{1-\nu}\left(\frac{\partial F_x}{\partial x} + \frac{\partial F_y}{\partial y}\right). \tag{3.20}$$

Equation (3.19), in case of plane stress, or (3.20) in plane strain, together with equilibrium equations (3.12) forms a system of three equations which allows determination of three independent components of stress tensor. Solution of such systems of equations is most frequently performer through the stress function proposed by G. B. Airy and described in the next chapter.

3.4. Airy stress function

Airy's idea is based on the observation that the system of equilibrium equations (3.12) can be solved with use of substitution:

$$\sigma_x = \frac{\partial^2 \Phi}{\partial y^2}, \quad \sigma_y = \frac{\partial^2 \Phi}{\partial x^2}, \quad \tau_{xy} = -\frac{\partial^2 \Phi}{\partial x \partial y}, \tag{3.21}$$

where $\Phi(x,y)$ is a stress function, which automatically fulfills equilibrium conditions in case of mass forces F_x , F_y disappearance. Introduction of relations (3.21) into the compatibility equation (3.19) results with the condition that must be fulfilled by the stress function:

$$\frac{\partial^4 \Phi}{\partial x^4} + 2\frac{\partial^4 \Phi}{\partial x^2 \partial y^2} + \frac{\partial^4 \Phi}{\partial y^4} = 0. \tag{3.22}$$

When mass forces are not equal to zero, but fulfill the potential condition, i.e. are derivatives of some function $\Psi(x,y)$:

$$F_x = -\frac{\partial \Psi}{\partial x}, \quad F_y = -\frac{\partial \Psi}{\partial y}, \tag{3.23}$$

Airy's approach can be applied as well, but it needs now some correction:

$$\sigma_x - \Psi = \frac{\partial^2 \Phi}{\partial y^2}, \quad \sigma_y - \Psi = \frac{\partial^2 \Phi}{\partial x^2}, \quad \tau_{xy} = -\frac{\partial^2 \Phi}{\partial x \partial y}. \tag{3.24}$$

The compatibility equation after substitution of these relations in the plane stress condition obtains the following form:

$$\frac{\partial^4 \Phi}{\partial x^4} + 2\frac{\partial^4 \Phi}{\partial x^2 \partial y^2} + \frac{\partial^4 \Phi}{\partial y^4} = -(1-\nu)\nabla^2 \Psi. \tag{3.25}$$

Plane strain condition gives us compatibility equation in similar form:

$$\frac{\partial^4 \Phi}{\partial x^4} + 2\frac{\partial^4 \Phi}{\partial x^2 \partial y^2} + \frac{\partial^4 \Phi}{\partial y^4} = -\frac{1-2\nu}{1-\nu}\nabla^2 \Psi. \tag{3.26}$$

The stress function described by equation (3.22) is named the biharmonic function. The family of biharomonic functions contains polynomials, exponential, trigonometric and hyperbolic functions. Application of these functions to solution of analytical problems of slab statics will be shown in the next chapters.

3.5. Analytical solutions of 2D elasticity problems

Examples of solution for problems of slabs statics, shown in this chapter, will deal with problems without mass forces. This will simplify solutions and make it easier to understand analytical methods used here:

$$\frac{\partial^4 \Phi}{\partial x^4} + 2\frac{\partial^4 \Phi}{\partial x^2 \partial y^2} + \frac{\partial^4 \Phi}{\partial y^4} = 0, \quad \text{lub} \quad \nabla^2 \nabla^2 \Phi = 0, \tag{3.27}$$

where $\nabla^2 \nabla^2 = \left(\frac{\partial^4}{\partial x^4} + 2\frac{\partial^4}{\partial x^2 \partial y^2} + \frac{\partial^4}{\partial y^4} \right)$ is a biharmonic operator.

Biharmonic functions fulfilling homogenous equation (3.27) can be selection from a wide group of functions:

$$\begin{aligned} &\Phi(x,y) = \\ &a_0 + a_1 x + a_2 x^2 + a_3 x^3 + \ldots + b_1 y + b_2 y^2 + b_3 y^3 + \ldots + c_1 xy + c_2 x^2 y + c_3 x y^2 + \ldots \\ &Ae^{\pm \alpha x} \sin \alpha y, \quad Ae^{\pm \alpha x} \cos \alpha y, \quad Axe^{\pm \alpha x} \sin \alpha y, \quad Axe^{\pm \alpha x} \cos \alpha y, \\ &Ae^{\pm \beta y} \sin \beta x, \quad Ae^{\pm \beta y} \cos \beta x, \quad Aye^{\pm \beta y} \sin \beta x, \quad Aye^{\pm \beta y} \cos \beta x. \end{aligned} \tag{3.28}$$

Now we will show their usage in solving problems which usually occur in civil engineering and are important from practical point of view.

3.5.1. Rectangular slab. Solution in the polynomial form

Let us accept the Airy stress function as a full 3rd degree polynomial:

$$\Phi(x,y) = a_0 + a_1 x + a_2 y + a_3 x^2 + a_4 xy + a_5 y^2 + a_6 x^3 + a_7 x^2 y + a_8 x y^2 + a_9 y^3, \tag{3.29}$$

where $a_0 \ldots a_9$ are constants that can be selected in such a manner that the boundary conditions are fulfilled. The stress function in the shape of (3.29) fulfills the biharmonic equation (3.27) for any values of these constants. After its derivation we obtain the components of the stress vector:

$$\begin{aligned} \sigma_x &= \frac{\partial^2 \Phi}{\partial y^2} = 2a_5 + 2a_8 x + 6a_9 y, \\ \sigma_y &= \frac{\partial^2 \Phi}{\partial x^2} = 2a_3 + 6a_6 x + 2a_7 y, \\ \tau_{xy} &= -\frac{\partial^2 \Phi}{\partial x \partial y} = -\left(a_4 + 2a_7 x + 2a_8 y\right). \end{aligned} \tag{3.30}$$

Accepting a rectangular slab of the h height and the l span (Fig. 3.4), we indicate: $\zeta = y/h$, $\xi = x/l$ and $\lambda = l/h$. Now we will see what is the influence of each constant occurring in equations (3.30) on the boundary conditions. To do so we will compose the stress diagrams in the slab area: $-l/2 \le x \le +l/2$; $-h/2 \le y \le +h/2$, assuming $l = 5h$.

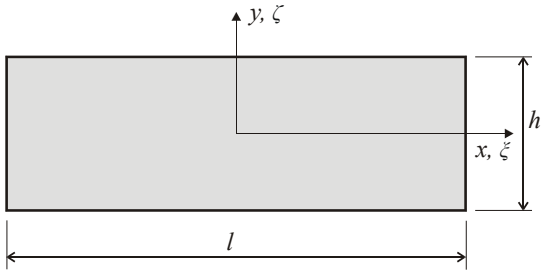

Fig. 3.4. Coordinate system and geometry of the rectangular slab

Because 3 first coefficients $a_0 \ldots a_2$ of the polynomial (3.29) have no influence on the stress field in the slab (comp. eq. 3.30) we can narrow down to seven diagrams with coefficients $a_3 \ldots a_9$ not equal to 0. For the sake of convenience, we will assume that these coefficients, one by one, take unit values, keeping in mind that the stress fields obtained in such a way should be multiplied by the values, which fulfill the boundary conditions of the problem.

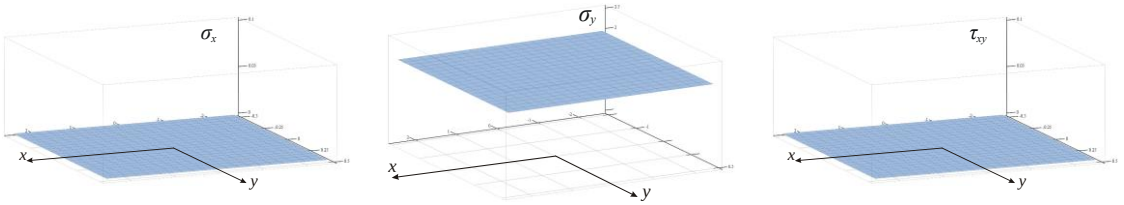

a) a_3=1, other coefficients a_i=0

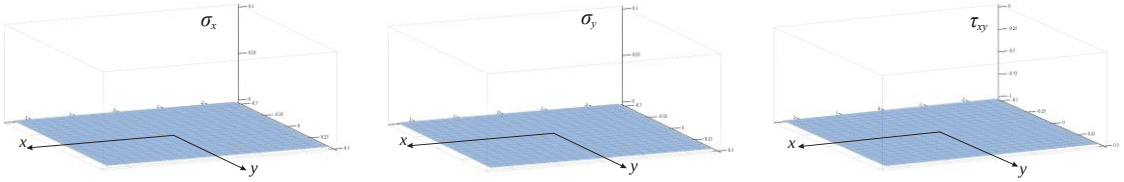

b) a_4=1, other coefficients a_i=0

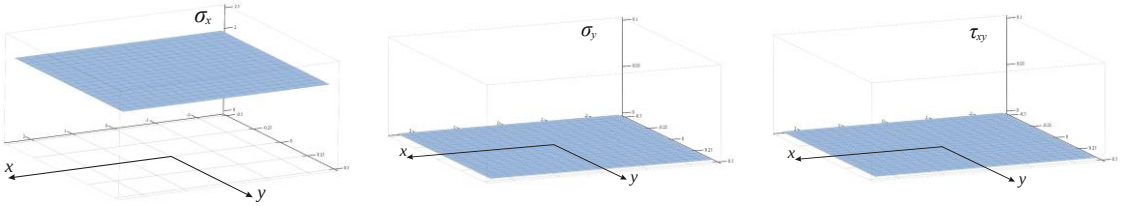

c) a_5=1, other coefficients a_i=0

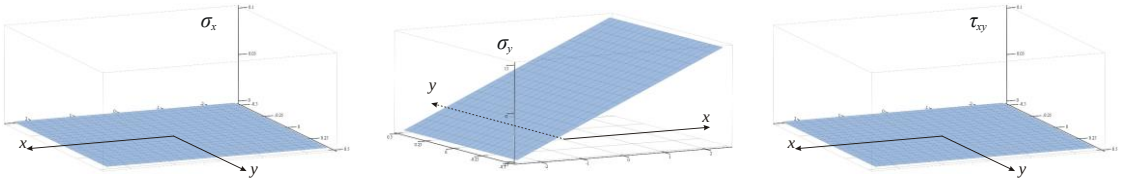

d) a_6=1, other coefficients a_i=0

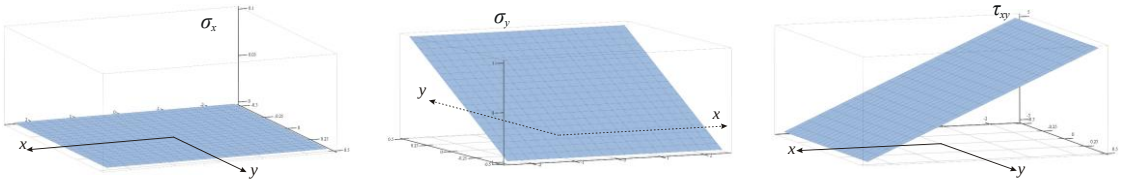

e) a_7=1, other coefficients a_i=0

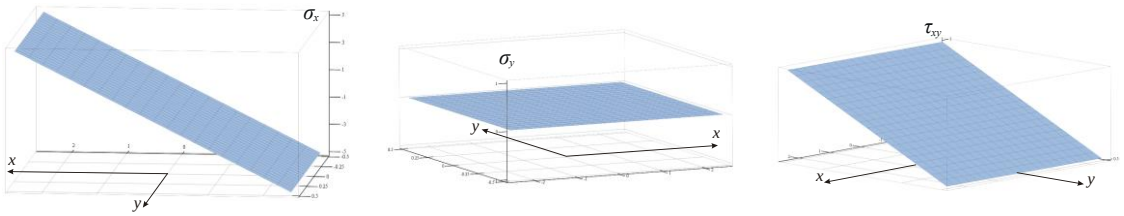

f) a_8=1, other coefficients a_i=0

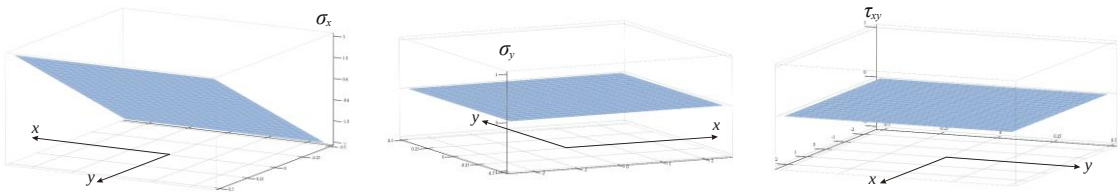

g) a_9=1, other coefficients a_i=0

Fig. 3.5. The influence of the Airy function coefficients on the stress distribution in rectangular slab

The analysis of the diagrams shown in Fig. 3.5 leads to the conclusion, that the stress function in the shape of the 3rd degree polynomial allows solving the problems of compression, tension, shearing and simple bending. Details for such applications may be followed through the examples shown in the book by Timoshenko and Goodier.

We will now show an example of the 5th degree polynomial application to the problem referring to bending of simply supported slab-beam loaded with uniform load distributed at the top edge (Fig. 3.6).

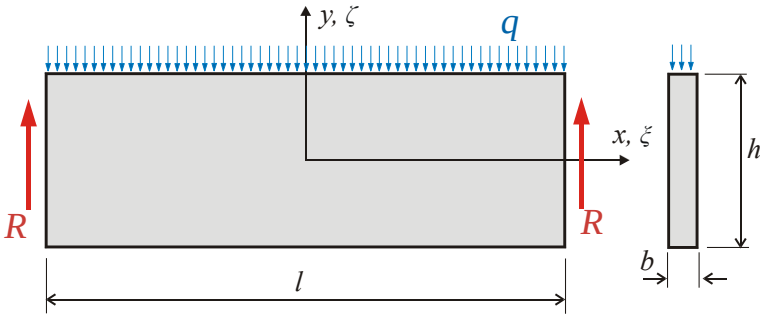

Fig. 3.6. Bending of the rectangular beam-slab

The boundary conditions of the problem are:

$$\sigma_y(x,h/2)=-q/b,\ \ \tau_{xy}(x,\tfrac{1}{2}h)=0,\quad \sigma_y(x,-h/2)=0,\ \ \tau_{xy}(x,-h/2)=0,$$
$$\int_{-h/2}^{h/2}\sigma_x(l/2,y)\,dy=0,\ \int_{-h/2}^{h/2}\sigma_x(l/2,y)\,y\,dy=0,\ \int_{-h/2}^{h/2}\tau_{xy}(l/2,y)\,b\,dy=R=ql/2, \tag{3.31}$$
$$\int_{-h/2}^{h/2}\sigma_x(-l/2,y)\,dy=0,\ \int_{-h/2}^{h/2}\sigma_x(-l/2,y)\,y\,dy=0,\ \int_{-h/2}^{h/2}\tau_{xy}(-l/2,y)\,b\,dy=-R=-ql/2,$$

where b is the beam cross-section width and q [kN/m] is the load intensity.

At the vertical edges ($x=\pm l/2$) there have been applied boundary conditions in the integral form, because it is not possible that the polynomial form of the stress function fulfills the boundary conditions fully. In the present form this means that the horizontal forces and the bending moments disappear at the beam ends.

We will now accept the stress function as a 5th degree polynomial:

$$\begin{aligned}\Phi(x,y) &= a_1x^2 + a_2xy + a_3y^2 + a_4x^3 + a_5x^2y + a_6xy^2 + a_7y^3 + a_8x^4 + a_9x^3y + \\ &+ a_{10}x^2y^2 + a_{11}xy^3 + a_{12}y^4 + a_{13}x^5 + a_{14}x^4y + a_{15}x^3y^2 + a_{16}x^2y^3 + a_{17}xy^4 + a_{18}y^5,\end{aligned} \tag{3.32}$$

where a_1... a_{18} are the constants accepted to fulfill the compatibility equation (3.26) and the boundary conditions (3.31). There have been omitted constant and linear components in the equation (3.32) because they have no influence on the equations describing the components of stress vector (3.21).

Substitution of the polynomial (3.32) to the condition (3.26) leads to:

$$\begin{aligned}&\nabla^2\nabla^2\Phi(x,y) = \\ &4\left(6a_8 + a_{10} + 6a_{12}\right) + 12x\left(10a_{13} + 10a_{17} + a_{15}\right) + 12y\left(2a_{14} + a_{16} + 10a_{18}\right) = 0.\end{aligned} \tag{3.33}$$

Components of the stress vector are obtained after the Airy function derivation:

$$\begin{aligned}\sigma_x &= \frac{\partial^2\Phi}{\partial y^2} = 2a_3 + 2a_6x + 6a_7y + 2a_{10}x^2 + 6a_{11}xy + 12a_{12}y^2 + 2a_{15}x^3 + 3a_{16}x^2y + \\ &\quad + 12a_{17}xy^2 + 20a_{18}y^3 \\ \sigma_y &= \frac{\partial^2\Phi}{\partial x^2} = 2a_1 + 6a_4x + 2a_5y + 12a_8x^2 + 6a_9xy + 2a_{10}y^2 + 20a_{13}x^3 + 12a_{14}x^2y + \\ &\quad + 6a_{15}xy^2 + 2a_{16}y^3 \\ \tau_{xy} &= -\frac{\partial^2\Phi}{\partial x\partial y} = -\left(\begin{matrix}a_2 + 2a_5x + 2a_6y + 3a_9x^2 + 4a_{10}xy + 3a_{11}y^2 + 4a_{14}x^3 + 6a_{15}x^2y + \\ + 6a_{16}xy^2 + 4a_{17}y^3\end{matrix}\right).\end{aligned} \tag{3.34}$$

The condition (3.33) gives 3 equation allowing calculation of the a_i coefficients, which come from the independence of the polynomials occurring in (3.33):

$$\begin{aligned}&6a_8 + a_{10} + 6a_{12} = 0, \\ &10a_{13} + 10a_{17} + a_{15} = 0, \\ &2a_{14} + a_{16} + 10a_{18} = 0.\end{aligned} \tag{3.35}$$

The remaining equations are obtained after using of the boundary conditions (3.31). Conditions $\sigma_y(x, h/2) = -\frac{q}{b}$ and $\sigma_y(x, -h/2) = 0$ give the system of equations:

$$
\begin{aligned}
&2a_1 + a_5 h + a_{10}\frac{h^2}{2} + a_{16}\frac{h^3}{4} = -\frac{q}{b}, && 6a_4 + 3a_9 h + \frac{3}{2}a_{15}h^2 = 0,\\
&2a_1 - a_5 h + a_{10}\frac{h^2}{2} - a_{16}\frac{h^3}{4} = 0, && 6a_4 - 3a_9 h + \frac{3}{2}a_{15}h^2 = 0,\\
&12a_8 + 6a_{14}h = 0,\\
&12a_8 - 6a_{14}h = 0, && a_{13} = 0.
\end{aligned}
\tag{3.36}
$$

The conditions of the shear stress disappearance at the top and bottom Edge of the slab $\tau_{xy}(x, \frac{1}{2}h) = 0$ and $\tau_{xy}(x, -\frac{1}{2}h) = 0$, produce the following system of equations:

$$
\begin{aligned}
&a_2 + a_6 h + 3a_{11}\frac{h^2}{4} + a_{17}\frac{h^3}{2} = 0, && 2a_5 + 2a_{10}h + 3a_{16}\frac{h^2}{2} = 0,\\
&a_2 - a_6 h + 3a_{11}\frac{h^2}{4} - a_{17}\frac{h^3}{2} = 0, && 2a_5 + 2a_{10}h + 3a_{16}\frac{h^2}{2} = 0,\\
&3a_9 + 3a_{15}h = 0,\\
&3a_9 - 3a_{15}h = 0, && a_{14} = 0.
\end{aligned}
\tag{3.37}
$$

The integral conditions leading to moments and horizontal resultant forces disappearance at the edges $x=\pm l/2$: $\int_{-h/2}^{h/2} \sigma_x(\pm l/2, y)\, dy = 0$, $\int_{-h/2}^{h/2} \sigma_x(\pm l/2, y)\, y\, dy = 0$, give the system of equations:

$$
\begin{aligned}
&4a_3 h + 2a_6 hl + a_{10} hl^2 + 2a_{12}h^3 + a_{17}h^3 l = 0,\\
&4a_3 h - 2a_6 hl + a_{10} hl^2 + 2a_{12}h^3 - a_{17}h^3 l = 0,\\
&8a_7 h^3 + 4a_{11}h^3 l + a_{16}h^3 l^2 + 4a_{18}h^5 = 0,\\
&8a_7 h^3 - 4a_{11}h^3 l + a_{16}h^3 l^2 + 4a_{18}h^5 = 0.
\end{aligned}
\tag{3.38}
$$

Conditions $\int_{-h/2}^{h/2} \tau_{xy}(\pm l/2, y)\, b\, dy = \pm ql/2,$ describing the resultant of the shear stress at the left and right edges of the slab give equations:

$$
\begin{aligned}
&4a_2 + 4a_5 l + 3a_9 l^2 + a_{11}h^2 + 2a_{14}l^3 + a_{16}h^2 l = -2\frac{ql}{bh},\\
&4a_2 - 4a_5 l + 3a_9 l^2 + a_{11}h^2 - 2a_{14}l^3 - a_{16}h^2 l = 2\frac{ql}{bh}.
\end{aligned}
\tag{3.39}
$$

Conditions (3.35, 3.36, 3.37, 3.38, 3.39) contain 23 equations with 18 unknown coefficients. Five of these equations are fulfilled identically. Other 18 can be easily simplified to the system of five equations. The coefficients a_2, a_3, a_4, a_6, a_8, a_9, a_{10}, a_{11}, a_{12}, a_{13}, a_{14}, a_{15} a_{17} are equal to zero, and others can be calculated after solution of the system of equations which will be shown in the matrix form:

$$\begin{bmatrix} 16 & 0 & 0 & 0 & 0 \\ 0 & 8 & 0 & h^2 & 0 \\ 0 & 0 & 8 & l^2 & 4h^2 \\ 0 & 0 & 0 & 5h^2 & 0 \\ 0 & 0 & 0 & 1 & 10 \end{bmatrix} \cdot \begin{bmatrix} a_1 \\ a_5 \\ a_7 \\ a_{16} \\ a_{18} \end{bmatrix} = 4\frac{q}{bh} \begin{bmatrix} -h \\ -1 \\ 0 \\ 1 \\ 0 \end{bmatrix}. \tag{3.40}$$

After solution of this system we obtain the components of the stress vector in the form:

$$\begin{aligned} \sigma_x &= \frac{-3q}{2bh^3} y\left(l^2 - 4x^2 + \tfrac{8}{3}y^2 - \tfrac{2}{5}h^2\right) = \frac{-3q}{2b}\zeta\left[\lambda^2\left(1-4\xi^2\right) + \tfrac{8}{3}\zeta^2 - \tfrac{2}{5}\right], \\ \sigma_y &= \frac{-q}{6bh^3}\left(12y^3 - h^2 y + h^3\right) = \frac{-q}{2b}\left(1 - 4\zeta^3 + 3\zeta\right), \\ \tau_{xy} &= \frac{3q}{2bh^2}\left(h^2 - 4y^2\right)x = \frac{3q}{2b}\left(1-4\zeta^2\right)\lambda\xi, \end{aligned} \tag{3.41}$$

This solution allows interpretation of the classic problem of beam bending. The normal stress σ_x distribution, as it can be seen in Fig. 3.7a, is non-linear, but includes the component depending on y^3, with small influence at the high beam slenderness. We observe stress σ_x at the left and right edges with the resultant $N_x = 0$ and the resultant bending moment $M_z = 0$. According to de Saint Venant theorem, the influence of this stress distribution becomes negligibly small at the distances higher than the dimension of the area at which this stress field occurs, i.e. h – the slab height. We also obtain the shear stress τ_{xy} distribution in the cross-section and the normal stress σ_y distribution at the slab height, which is usually neglected in the classic Bernoulli solution. The diagrams of stresses described with use of equations (3.41) are presented in Fig. 3.7. More of this problem analysis can be found in the book by Timoshenko and Goodier.

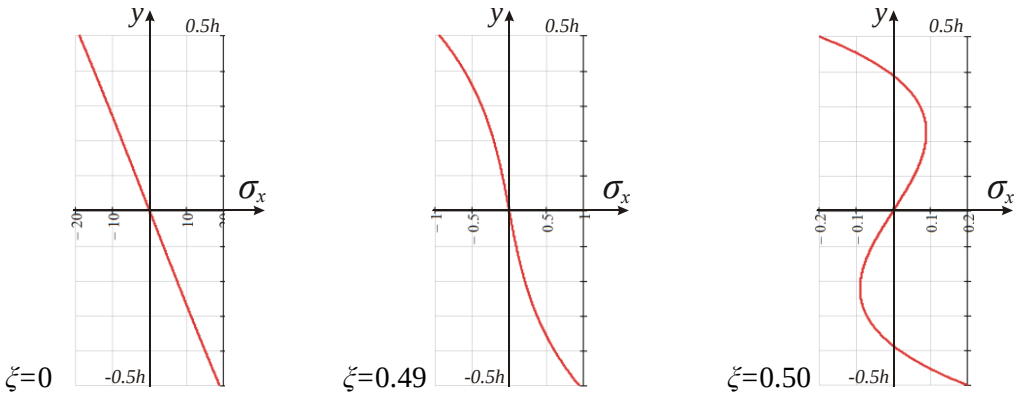

a) σ_x stress on 3 different cross-section: ξ=0; 0.49; 0.5

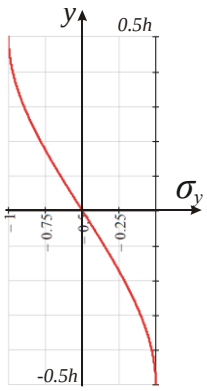

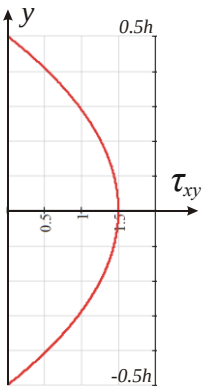

b) σ_y stress at ξ=0 c) τ_{xy} stress at ξ=0.5

Fig. 3.7. Graphs of stress fields in the rectangular slab

3.5.2. Rectangular slab. Solution in the Fourier series form

Assuming the stress function as a combination of trigonometric and exponential functions, we will solve the same problem as it has been solved with use of polynomials in the previous paragraph. There will be surely some differences in fulfilling the boundary conditions. The geometry is shown in Fig. 3.6 and the boundary conditions are described by the equations (3.31).

Because of the problem symmetry we assume the stress function as a cosine Fouries series:

$$\Phi(x,y)=\sum_{i=0}^{n} f_i(y)\cos\alpha_i x, \tag{3.42}$$

where $f_i(y)$ are unknown so far functions, which are taken in such a form to fulfill the biharmonic equation (3.27), α_i are constants needed to fulfill the boundary conditions, n is the number of the summed terms of the Fourier series allowing the needed precision of the solution. Calculating adequate derivatives, we substitute (3.42) to the equation (3.27).

$$\begin{aligned}
\frac{\partial^4\Phi}{\partial x^4}&=\sum_{i=0}^{n}\alpha_i^4 f_i(y)\cos\alpha_i x,\\
\frac{\partial^4\Phi}{\partial x^2\partial y^2}&=-\sum_{i=0}^{n}\alpha_i^2 f_i^{II}(y)\cos\alpha_i x,\\
\frac{\partial^4\Phi}{\partial y^4}&=\sum_{i=0}^{n} f_i^{IV}(y)\cos\alpha_i x,\\
\nabla^2\nabla^2\Phi&=\sum_{i=0}^{n}\left[\alpha_i^4 f_i(y)-2\alpha_i^2 f_i^{II}(y)+ f_i^{IV}(y)\right]\cos\alpha_i x=0,
\end{aligned} \tag{3.43}$$

where $f^{II}(y)=\dfrac{d^2 f(y)}{dy^2}$, $f^{IV}(y)=\dfrac{d^4 f(y)}{dy^4}$.

To fulfill the compatibility equation (3.27) we need fulfillment of the ordinary linear differential equation:

$$\alpha_i^4 f_i(y)-2\alpha_i^2 f_i^{II}(y)+ f_i^{IV}(y)=0. \tag{3.44}$$

The solution to the equation (3.44) may be given as functions in the shape:

$$f_i(y)=A_i\cosh\alpha_i y+B_i\sinh\alpha_i y+C_i\alpha_i y\cosh\alpha_i y+D_i\alpha_i y\sinh\alpha_i y, \tag{3.45}$$

where A_i, B_i, C_i, D_i are constants, which should be accepted in such a manner to fulfill the boundary conditions. Now we calculate the components of stress vector:

$$\begin{aligned}
\sigma_x &= \sum_{i=0}^{n}\alpha_i^2\begin{bmatrix} A_i\cosh\alpha_i y+B_i\sinh\alpha_i y+ \\ C_i\left(2\sinh\alpha_i y+\alpha_i y\cosh\alpha_i y\right)+ \\ D_i\left(2\cosh\alpha_i y+\alpha_i y\sinh\alpha_i y\right)\end{bmatrix}\cos\alpha_i x, \\
\sigma_y &= -\sum_{i=0}^{n}\alpha_i^2\left(A_i\cosh\alpha_i y+B_i\sinh\alpha_i y+C_i\alpha_i y\cosh\alpha_i y+D_i\alpha_i y\sinh\alpha_i y\right)\cos\alpha_i x, \\
\tau_{xy} &= -\sum_{i=0}^{n}\alpha_i^2\begin{bmatrix} A_i\sinh\alpha_i y+B_i\cosh\alpha_i y+ \\ C_i\left(\cosh\alpha_i y+\alpha_i y\sinh\alpha_i y\right)+ \\ D_i\left(\sinh\alpha_i y+\alpha_i y\cosh\alpha_i y\right)\end{bmatrix}\sin\alpha_i x.
\end{aligned} \tag{3.46}$$

The next step is substitution of the boundary conditions in order to calculate the constants A_i, B_i, C_i, D_i. In different way as we have done it in the previous paragraph we will start from the left and right edges of the slab. We will also strengthen the boundary conditions by demanding of the disappearance of stresses at the vertical edges:

$$\sigma_x(l/2,y)=\sum_{i=0}^{n}\alpha_i^2\begin{bmatrix} A_i\cosh\alpha_i y+B_i\sinh\alpha_i y+ \\ C_i\left(2\sinh\alpha_i y+\alpha_i y\cosh\alpha_i y\right)+ \\ D_i\left(2\cosh\alpha_i y+\alpha_i y\sinh\alpha_i y\right)\end{bmatrix}\cos\left(\frac{\alpha_i l}{2}\right)=0. \tag{3.47}$$

To make the condition (3.47) be fulfilled at any value of y, the following equation must be in force:

$$\cos\left(\frac{\alpha_i l}{2}\right)=0 \;\rightarrow\; \frac{\alpha_i l}{2}=\frac{i\pi}{2} \;\rightarrow\; \alpha_i=\frac{i\pi}{l},\quad i=1,3,5,\ldots n, \tag{3.48}$$

which gives automatic fulfillment of the condition $\sigma_x(-l/2,y) = 0$ at the left slab edge.

Knowing the α_i values we can analyze the conditions at the top and bottom edges of the slab

$$\sigma_y(x,h/2)=-\frac{q}{b},$$

$$\sum_{i=1,3,5}^{n}\alpha_i^2\left(A_i\cosh\beta_i+B_i\sinh\beta_i+C_i\beta_i\cosh\beta_i+D_i\beta_i\sinh\beta_i\right)\cos\alpha_i x=\sum_{i=1,3,5}^{n}p_i\cos\alpha_i x$$

$$\tau_{xy}(x,h/2)=-\sum_{i=1,3,5}^{n}\alpha_i^2\begin{bmatrix}A_i\sinh\beta_i+B_i\cosh\beta_i+\\ C_i\left(\cosh\beta_i+\beta_i\sinh\beta_i\right)+\\ D_i\left(\sinh\beta_i+\beta_i\cosh\beta_i\right)\end{bmatrix}\sin\alpha_i x=0, \tag{3.49}$$

$$\sigma_y(x,-h/2)=0$$

$$\sum_{i=1,3,5}^{n}\alpha_i^2\left(A_i\cosh\beta_i-B_i\sinh\beta_i-C_i\beta_i\cosh\beta_i+D_i\beta_i\sinh\beta_i\right)\cos\alpha_i x=0,$$

$$\tau_{xy}(x,-h/2)=-\sum_{i=1,3,5}^{n}\alpha_i^2\begin{bmatrix}-A_i\sinh\beta_i+B_i\cosh\beta_i+\\ C_i\left(\cosh\beta_i+\beta_i\sinh\beta_i\right)+\\ -D_i\left(\sinh\beta_i+\beta_i\cosh\beta_i\right)\end{bmatrix}\sin\alpha_i x=0,$$

where $\beta_i=\alpha_i\frac{h}{2}=\frac{i\pi}{2\lambda}$, $p_i=\frac{2q}{l\,b}\int_{-l/2}^{l/2}\cos\alpha_i x\,dx=\frac{4q}{i\pi\,b}(-1)^{\frac{i-1}{2}}$ is the solution of the uniformly distributed load and taken as the Fourier series.

After solution of this system of equations we obtain the values of constants A_i, B_i, C_i, D_i:

$$D_i=\frac{p_i}{2\alpha_i^2}\frac{1}{\beta_i\sinh\beta_i-\cosh\beta_i\left(1+\frac{\beta_i}{\operatorname{tgh}\beta_i}\right)},\quad A_i=-D_i\left(1+\frac{\beta_i}{\operatorname{tgh}\beta_i}\right), \tag{3.50}$$

$$C_i=\frac{p_i}{2\alpha_i^2}\frac{1}{\beta_i\cosh\beta_i-\sinh\beta_i\left(1+\beta_i\operatorname{tgh}\beta_i\right)},\quad B_i=-C_i\left(1+\beta_i\operatorname{tgh}\beta_i\right),$$

which allow calculation of the components of stress vector on the basis of equations (3.46).

The stress diagrams are shown in Fig. 3.8. For comparison of both solutions (polynomial and based on Fourier series) both diagrams have been juxtaposed in Fig. 3.8b. There you can see the more detailed representation of the boundary condition $\sigma_x(l/2,y)=0$. The differences in both solutions are quickly disappearing according to Saint Venant's theorem and in the middle of slab no differences can be observed.

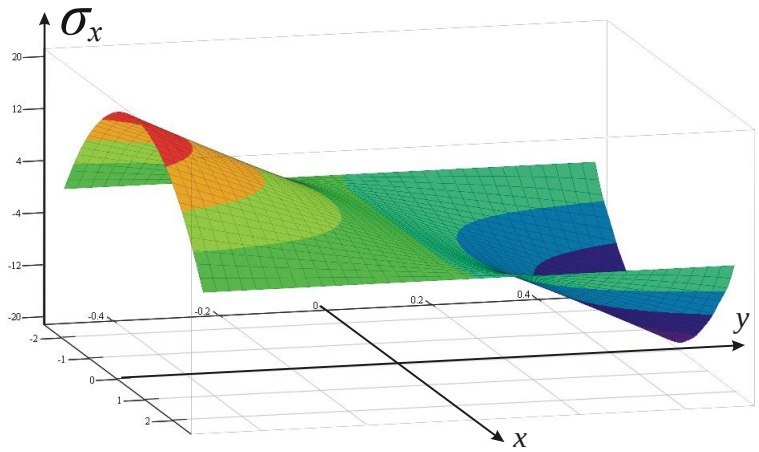

a) σ_x stress field over the slab area

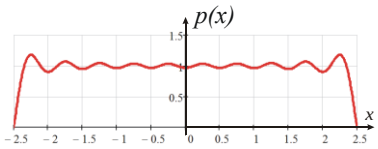

b) load of the upper slab edge expanded in Fourier series

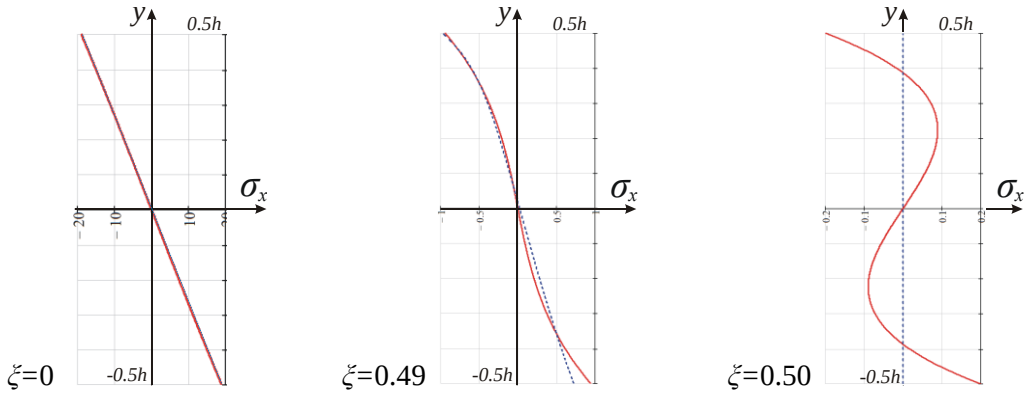

c) σ_x stress on 3 different cross-section: ξ=0; 0.49; 0.5; red line —— polynomial solution; blue line ----- solution by Fourier series

Fig. 3.8. Graphs of stress fields in the rectangular slab obtained by Fourier series

3.5.3. Solutions in polar coordinate system

Many interesting solutions can be obtained by using the assumption of rotational symmetry. We will now show, without going into details, some solutions obtained on the basis of Airy function in polar coordinate system. More of such solutions can be found in the previously presented books by Timoshenko and Goodier, Fung, Nowacki. Especially the first one contains many examples of solution to problems important from practical point of view.

The polar coordinate system shown in Fig. 3.9 is connected with Cartesian coordinate system by the following relations:

$$r^2 = x^2 + y^2, \quad \vartheta = \arctan\frac{y}{x}, \quad x = r\cos\vartheta, \quad y = r\sin\vartheta,$$
$$\frac{\partial r}{\partial x} = \cos\vartheta, \quad \frac{\partial r}{\partial y} = \sin\vartheta, \quad \frac{\partial \vartheta}{\partial x} = -\frac{\sin\vartheta}{r}, \quad \frac{\partial \vartheta}{\partial y} = \frac{\cos\vartheta}{r}. \tag{3.51}$$

Introducing them into relations (3.21) and (3.22), we obtain:

$$\sigma_r = \frac{1}{r}\frac{\partial \Phi}{\partial r} + \frac{1}{r^2}\frac{\partial^2 \Phi}{\partial \vartheta^2}, \quad \sigma_\vartheta = \frac{\partial^2 \Phi}{\partial r^2}, \quad \tau_{r\vartheta} = \frac{1}{r^2}\frac{\partial \Phi}{\partial \vartheta} - \frac{1}{r}\frac{\partial^2 \Phi}{\partial r \partial \vartheta},$$
$$\nabla^2\nabla^2\Phi = \left(\frac{\partial^2}{\partial r^2} + \frac{1}{r^2}\frac{\partial}{\partial r} + \frac{1}{r^2}\frac{\partial^2}{\partial \vartheta^2}\right)\left(\frac{\partial^2 \Phi}{\partial r^2} + \frac{1}{r^2}\frac{\partial \Phi}{\partial r} + \frac{1}{r^2}\frac{\partial^2 \Phi}{\partial \vartheta^2}\right) = 0, \tag{3.52}$$

where σ_r, σ_ϑ, $\tau_{r\vartheta}$ are the stress tensor components in the polar coordinate system.

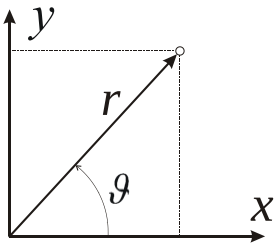

Fig. 3.9. Relationship between Cartesian and polar coordinate systems

We will now show 3 solutions for important problems which have solutions in polar coordinate system:

- problem of pressure analysis in thick-walled pipe,
- compression of the half-space with concentrated force,
- circular slab compressed with use of two forces remaining in equilibrium state.

■ *Stress in thick-walled pipe as a result of internal pressure p_1 and external pressure p_0*

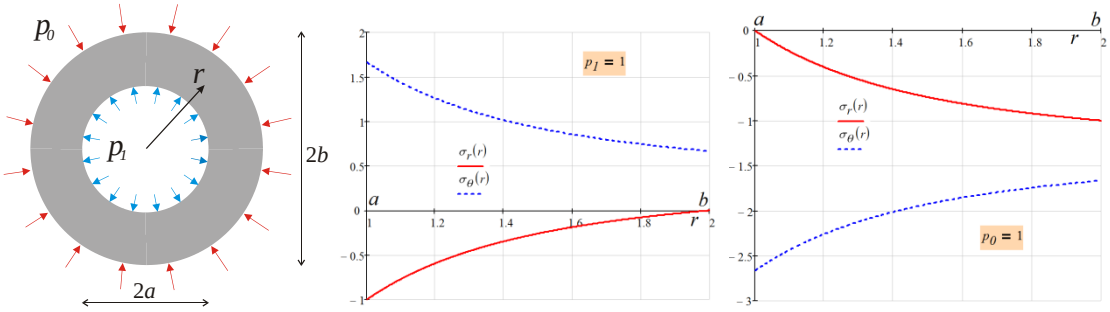

Fig. 3.10. The cross-section of the pipe subjected to the action of external and internal pressure

Components of stress are described with use of equations:

$$\sigma_r = \frac{a^2 b^2 (p_0 - p_1)}{b^2 - a^2} \cdot \frac{1}{r^2} - \frac{p_0 b^2 - p_1 a^2}{b^2 - a^2},$$
$$\sigma_\vartheta = -\frac{a^2 b^2 (p_0 - p_1)}{b^2 - a^2} \cdot \frac{1}{r^2} - \frac{p_0 b^2 - p_1 a^2}{b^2 - a^2}, \qquad (3.53)$$
$$\tau_{r\vartheta} = 0,$$

where a is the internal radius, b is the external radius of the pipe (Fig. 3.10), shear stress $\tau_{r\vartheta}$ disappears because of the rotational symmetry in the problem.

The stress diagrams σ_r and σ_ϑ for 2 load cases: p_0=0, p_1=1 and p_0=1, p_1=0 are shown in Fig. 3.10b and Fig. 3.10c.

■ *Compression of the half-space with concentrated force*

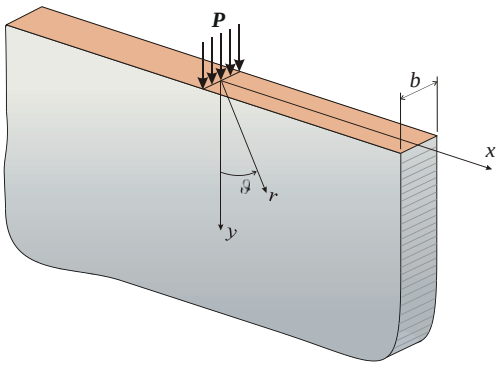

Fig. 3.11. Concentrated force acting on the edge of the half infinite slab

The problem is solved with use of relatively simple stress function:

$$\Phi(r,\vartheta) = -\frac{P}{b\pi} r\vartheta \sin\vartheta$$
$$\sigma_r = \frac{1}{r}\cdot\frac{\partial\Phi}{\partial r} + \frac{1}{r^2}\cdot\frac{\partial^2\Phi}{\partial\vartheta^2} = -\frac{2P}{b\pi}\frac{\cos\vartheta}{r}, \quad \sigma_\vartheta = \frac{\partial^2\Phi}{\partial r^2} = 0, \quad \tau_{r\vartheta} = -\frac{\partial}{\partial r}\left(\frac{1}{r}\cdot\frac{\partial\Phi}{\partial\vartheta}\right) = 0, \qquad (3.54)$$

and the stress vector has got only one component not equal to 0. Such a distribution of stresses is called a simple radial distribution.

It is convenient to use Cartesian stress components. They can be obtained by the second equation (3.54) transformation into Cartesian coordinate system:

$$\sigma_x = \sigma_r \sin^2 \vartheta = -\frac{2P}{yb\pi} \sin^2 \vartheta \cos^2 \vartheta,$$

$$\sigma_y = \sigma_r \cos^2 \vartheta = -\frac{2P}{yb\pi} \cos^4 \vartheta, \tag{3.55}$$

$$\tau_{xy} = \sigma_r \sin \vartheta \cos \vartheta = -\frac{2P}{yb\pi} \sin \vartheta \cos^3 \vartheta.$$

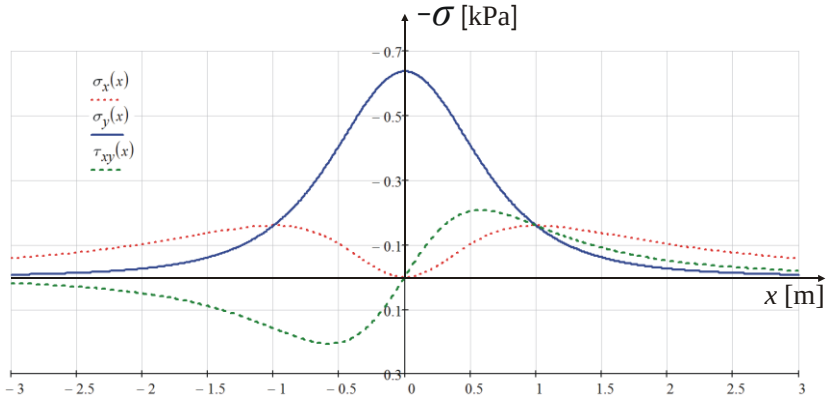

Fig. 3.12. Stress graph at the depth y=1m for the force P=1kN and the bandwidth b=1m

The stress graph for stresses described with equation (3.51) when assuming values P=1 kN, y=1 m, b=1 m, is shown in Fig. 2.12.

Simple radial distribution has got an interesting feature, which will be used in the next solution. The stress σ_r at the side of the circular tangent do the plane y=0 is constant and equal to $\sigma_r = -\frac{2P}{bd\pi}$, where d is the cylinder radius, because $d = \frac{r}{\cos \vartheta}$ (comp. Fig. 3.13).

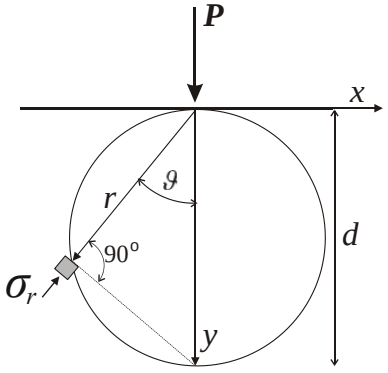

Fig. 3.13. Stress σ_r on the cylinder surface

■ *Circular slab compressed with two forces remaining in equilibrium*

Adding together two solutions for radial distribution, which have been shown in previous problem, we will obtain stress distribution in a circular slab compressed with two forces in equilibrium (Fig. 3.14). Two added radial stresses acting in perpendicular direction to each other, generate the state of even pressure $\sigma_r = -\dfrac{2P}{b\,d\,\pi}$ at the side of the cylinder. Because the slab shown in Fig 3.14 has two edges unaffected by stresses then to get rid of this pressure we need to apply the balancing positive stress of the same value.

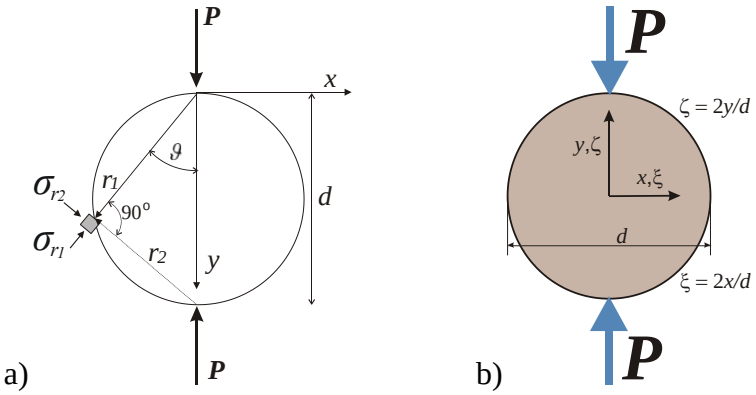

Fig. 3.14. Circular disk compressed by two balancing forces, so-called Brazilian test

Finally, we obtain the stress distribution, which is described with equations:

$$\sigma_x = -\frac{4P}{\pi\,d\,b}\left[\frac{(1-\zeta)\xi^2}{\left((1-\zeta)^2+\xi^2\right)^2}+\frac{(1+\zeta)\xi^2}{\left((1+\zeta)^2+\xi^2\right)^2}-\frac{1}{2}\right],$$
$$\sigma_y = -\frac{4P}{\pi\,d\,b}\left[\frac{(1-\zeta)^3}{\left((1-\zeta)^2+\xi^2\right)^2}+\frac{(1+\zeta)^3}{\left((1+\zeta)^2+\xi^2\right)^2}-\frac{1}{2}\right], \qquad (3.56)$$
$$\tau_{xy} = \frac{-4P}{\pi d b}\left[\frac{(1-\zeta)^2\xi}{\left((1-\zeta)^2+\xi^2\right)^2}+\frac{(1+\zeta)^2\xi}{\left((1+\zeta)^2+\xi^2\right)^2}\right],$$

where ξ and ζ are dimensionless coordinates in the coordinate system shown in Fig. 3.14b. Graphs of stress distribution described with these equations are shown in Fig. 3.15. There can be seen a singularity of the stress field in the point where the concentrated force is applied. The stress tends toward infinity at this point. A very interesting stress σ_x distribution is obtained along the vertical symmetry axis of the slab

(Fig. 3.15e), which at the long stretch has got constant value $\sigma_x = \frac{2P}{\pi db}$. This is why a laboratory test of cylinder compression with use of two loads distributed along side lines and remaining in equilibrium is used to evaluate tensile strength of material. Such a test is called *Brazilian test* and it is executed for brittle materials, i.e. rocks, concrete etc. which have got many times smaller tensile strength than the compressive one. Existence of 3 times bigger compressive stresses $\sigma_y = \frac{-6P}{\pi db}$ in the middle of the test specimen (comp. Fig. 3.15d) has minor influence on the effort of material, then.

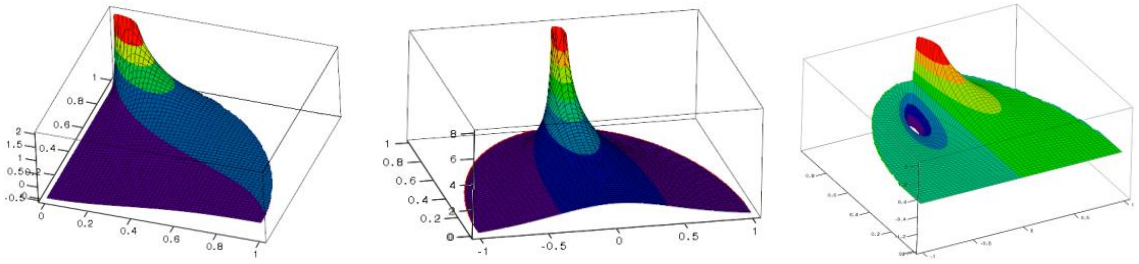

a) $\sigma_x(\xi, \zeta)$ b) $\sigma_y(\xi, \zeta)$ c) $\tau_{xy}(\xi, \zeta)$

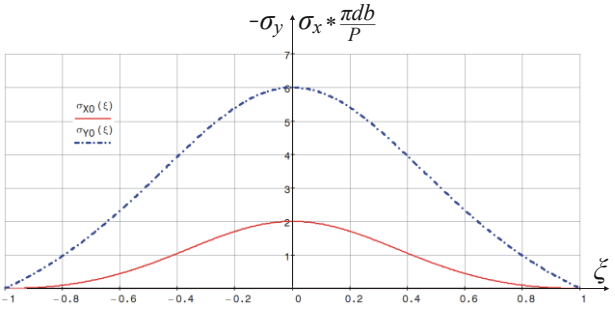

d) $\zeta=0 \rightarrow \sigma_x(\xi,0)$, $\sigma_y(\xi,0)$

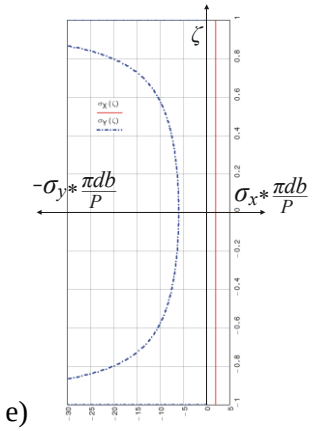

e) $\zeta=0$ $\sigma_x(0,\zeta)$ $\sigma_y(0,\zeta)$

Fig. 3.15. Stress distribution in the circular disc compressed with two balanced forces

3.6. Numerical solutions of the slab static problems with FEM

Analytical solutions shown in the previous chapters unfortunately cannot be applied to any problem, e.g. a slab of any shape or with any boundary conditions. These limitations of analytical methods have caused their smaller fitness to everyday engineering practice. Numerical methods are not affected by such drawbacks. Popularity of such methods grew in the 2nd half of the 20th century thanks to the

development of computational techniques and certainly lasts nowadays. Numerical methods have their own drawbacks such as numerical model errors, discretization errors, limited possibility of singularity in stress fields modelling, etc. However, we can control them and narrow down their influence, which gives the basis for using the results of calculations in engineering practice. From among many numerical methods used for problem solutions and shown in this chapter, the most universal and convenient, thus for this reason nowadays the most popular if finite element method (FEM). It will be shown in short here, however the reader who wants to learn this method in depth should be referred to the excellent book by O. C. Zienkiewicz. Another method, with usage presented here, is older than FEM – finite difference method (FDM). Its applications in solid body mechanics are nowadays rare, but it is worth to know this universal and simple in the idea method of solving differential equations. FDM in application of slab statics is described in detail in the book by F. Anderman.

3.6.1. The stiffness matrix of an elastic element

Let us divide a continuum into finite elements. We will discuss only a triangular 2D element in this book and we will choose such elements during discretization (Fig. 3.16).

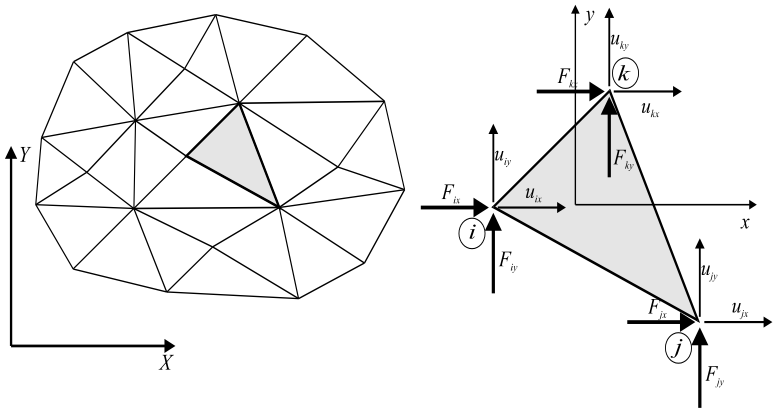

Fig. 3.16. Nodal forces and displacements for the 2D element in the global coordinate system.

According to assumption Eqn. (3.6) it is seen that every node of an element has two degrees of freedom and all nodal forces have two components. The local coordinate system *xy* is chosen in such a way that its axes are parallel to the axes of the global coordinate system. Hence distinguishing components of local and global vectors and matrices is insignificant.

Now we group nodal displacements and forces in the vectors of:

- nodal and element displacements

$$\mathbf{u}_i = \begin{bmatrix} u_{ix} \\ u_{iy} \end{bmatrix},\ \mathbf{u}_j = \begin{bmatrix} u_{jx} \\ u_{jy} \end{bmatrix},\ \mathbf{u}_k = \begin{bmatrix} u_{kx} \\ u_{ky} \end{bmatrix}, \quad \mathbf{u}^e = \begin{bmatrix} \mathbf{u}_i \\ \mathbf{u}_j \\ \mathbf{u}_k \end{bmatrix} = \begin{bmatrix} u_{ix} \\ u_{iy} \\ u_{jx} \\ u_{jy} \\ u_{kx} \\ u_{ky} \end{bmatrix} \tag{3.57}$$

- nodal and element forces

$$\mathbf{f}_i = \begin{bmatrix} F_{ix} \\ F_{iy} \end{bmatrix},\ \mathbf{f}_j = \begin{bmatrix} F_{jx} \\ F_{jy} \end{bmatrix},\ \mathbf{f}_k = \begin{bmatrix} F_{kx} \\ F_{ky} \end{bmatrix}, \quad \mathbf{f}^e = \begin{bmatrix} \mathbf{f}_i \\ \mathbf{f}_j \\ \mathbf{f}_k \end{bmatrix} = \begin{bmatrix} F_{ix} \\ F_{iy} \\ F_{jx} \\ F_{jy} \\ F_{kx} \\ F_{ky} \end{bmatrix}. \tag{3.58}$$

Since we look for the dependence between nodal displacement and nodal forces vectors of an element we apply the principle of virtual work which requires giving the relation between displacements of points lying within the element and displacements of nodes. Accepting errors coming from approximation, we assume that this relationship can be written by the function of two variables:

$$\begin{aligned} u_x(x,y) &= N_i(x,y)u_{ix} + N_j(x,y)u_{jx} + N_k(x,y)u_{kx} \quad \text{and} \\ u_y(x,y) &= N_i(x,y)u_{iy} + N_j(x,y)u_{jy} + N_k(x,y)u_{ky}, \end{aligned} \tag{3.59}$$

or the general matrix form:

$$\mathbf{u}(x,y) = \mathbf{N}^e(x,y)\mathbf{u}^e, \tag{3.60}$$

where $\mathbf{N}^e(x,y)$ is the matrix of shape functions of the element:

$$\mathbf{N}^e(x,y) = \begin{bmatrix} N_i(x,y)\,\mathbf{I} & N_j(x,y)\,\mathbf{I} & N_k(x,y)\,\mathbf{I} \end{bmatrix}, \tag{3.61}$$

where $\mathbf{I}$ is a unit diagonal matrix and $N_i(x,y)$, $N_j(x,y)$, $N_k(x,y)$ are the shape functions for nodes i, j, k.

Let us now assume the simplest of all possible forms of the shape function for the node i

$$N_i(x,y) = a_i + b_i x + c_i y, \tag{3.629}$$

where a_i, b_i, c_i are constants which we determine on the basis of consistency conditions

$$N_i(x_i,y_i)=1,\ N_i(x_j,y_j)=0,\ N_i(x_k,y_k)=0. \tag{3.63}$$

After inserting these conditions into Eqn. (3.62), we obtain the set of equations:

$$\begin{bmatrix} 1 & x_i & y_i \\ 1 & x_j & y_j \\ 1 & x_k & y_k \end{bmatrix} \begin{bmatrix} a_i \\ b_i \\ c_i \end{bmatrix} = \begin{bmatrix} 1 \\ 0 \\ 0 \end{bmatrix} \tag{3.64}$$

which, after being solved, give the values of coefficients of the shape function.

Equation (3.64) can also be written in the general form:

$$\mathbf{M}\boldsymbol{\alpha}_i = \boldsymbol{\delta}_i \text{ , where } \boldsymbol{\delta}_i = \begin{bmatrix} \delta_{i1} \\ \delta_{i2} \\ \delta_{i3} \end{bmatrix} \tag{3.6510}$$

which, after modification depending on the change of *i* into *j* (or *k*), allows us to determine the coefficients of the shape functions for the subsequent nodes. δ_{ij} means the Kronecker's delta in this equation.

We solve the set of Eqn. (3.65) by the Cramer method

$$W = \det \mathbf{M} = \begin{vmatrix} 1 & x_i & y_i \\ 1 & x_j & y_j \\ 1 & x_k & y_k \end{vmatrix} = \begin{vmatrix} x_j & y_j \\ x_k & y_k \end{vmatrix} - \begin{vmatrix} x_i & y_i \\ x_k & y_k \end{vmatrix} + \begin{vmatrix} x_i & y_i \\ x_j & y_j \end{vmatrix},$$

$$W_{a_i} = \begin{vmatrix} 1 & x_i & y_i \\ 0 & x_j & y_j \\ 0 & x_k & y_k \end{vmatrix} = \begin{vmatrix} x_j & y_j \\ x_k & y_k \end{vmatrix}, \tag{3.66}$$

$$W_{b_i} = \begin{vmatrix} 1 & 1 & y_i \\ 1 & 0 & y_j \\ 1 & 0 & y_k \end{vmatrix} = -\begin{vmatrix} 1 & y_i \\ 1 & y_k \end{vmatrix} = y_j - y_k,$$

$$W_{c_i} = \begin{vmatrix} 1 & x_i & 1 \\ 1 & x_j & 0 \\ 1 & x_k & 0 \end{vmatrix} = \begin{vmatrix} 1 & x_j \\ 1 & x_k \end{vmatrix} = x_k - x_j$$

then $a_i = \frac{W_{a_i}}{W}$, $b_i = \frac{W_{b_i}}{W}$, $c_i = \frac{W_{c_i}}{W}$.

Similarly, if we change the index *i* into *j* and we find $\boldsymbol{\delta}_j = \begin{bmatrix} 0 \\ 1 \\ 0 \end{bmatrix}$,

$$W_{a_j} = \begin{vmatrix} 0 & x_i & y_i \\ 1 & x_j & y_j \\ 0 & x_k & y_k \end{vmatrix} = -\begin{vmatrix} x_i & y_i \\ x_k & y_k \end{vmatrix},$$

$$W_{b_j} = \begin{vmatrix} 1 & 0 & y_i \\ 1 & 1 & y_j \\ 1 & 0 & y_k \end{vmatrix} = y_k - y_i, \tag{11}$$

$$W_{c_j} = \begin{vmatrix} 1 & x_i & 0 \\ 1 & x_j & 1 \\ 1 & x_k & 0 \end{vmatrix} = x_i - x_k,$$

$$a_j = \frac{W_{a_j}}{W}, \quad b_j = \frac{W_{b_j}}{W}, \quad c_j = \frac{W_{c_j}}{W}.$$

Finally, we have

$$\boldsymbol{\delta}_k = \begin{bmatrix} 0 \\ 0 \\ 1 \end{bmatrix},$$

$$W_{a_k} = \begin{vmatrix} 0 & x_i & y_i \\ 0 & x_j & y_j \\ 1 & x_k & y_k \end{vmatrix} = \begin{vmatrix} x_i & y_i \\ x_j & y_j \end{vmatrix},$$

(3.68)

$$W_{b_k} = \begin{vmatrix} 1 & 0 & y_i \\ 1 & 0 & y_j \\ 1 & 1 & y_k \end{vmatrix} = y_i - y_j,$$

$$W_{c_k} = \begin{vmatrix} 1 & x_i & 0 \\ 1 & x_j & 0 \\ 1 & x_k & 1 \end{vmatrix} = x_j - x_i,$$

$$a_k = \frac{W_{a_k}}{W},\ b_k = \frac{W_{b_k}}{W},\ c_k = \frac{W_{c_k}}{W}.$$

for node *k*.

Constants a_i, a_j, a_k are insignificant for further transformations (because they are connected with the rigid motion of a 2D element) and they can be neglected when solving the set of Eqn. (3.65).

After determining the shape functions of the element, let us come back to its strains. We insert Eqn. (3.60) in (3.8):

$$\boldsymbol{\varepsilon} = \mathscr{D}\mathbf{N}^e(x,y)\mathbf{u}^e = \mathbf{B}^e(x,y)\mathbf{u}^e, \tag{3.69}$$

obtaining the dependence between the nodal displacements of the element and its strains. The matrix **B** in Eqn. (3.69) is called a geometric matrix and it can be expressed as follows:

$$\mathbf{B}^e(x,y) = \left[\mathbf{B}_i(x,y) \quad \mathbf{B}_j(x,y) \quad \mathbf{B}_k(x,y)\right],$$

where $\mathbf{B}_n = \mathscr{D}\mathbf{N}_n(x,y) = \begin{bmatrix} b_n & 0 \\ 0 & c_n \\ c_n & b_n \end{bmatrix}$ (3.70)

is the geometric matrix of any node *n*.

Thus, we have all components which are necessary to write an element equilibrium equation. We apply the principle of virtual work which says that the external work (done by external forces – here nodal forces) has to be equal to internal work (done by stress) of a 2D element:

$$\left(\mathbf{u}^e\right)^{\mathsf{T}}\mathbf{f}^e = \int_{\mathscr{V}} \boldsymbol{\varepsilon}^{\mathsf{T}}\boldsymbol{\sigma}\, d\mathscr{V}. \tag{3.71}$$

We transform this equation first substituting the constitutive relation Eqn. (3.5) for **δ** and next substituting geometric relations (3.69) for **ε**:

$$\left(\mathbf{u}^e\right)^{\mathsf{T}}\mathbf{f}^e = \int_{\mathscr{V}} \left(\mathbf{B}^e\mathbf{u}^e\right)^{\mathsf{T}}\mathbf{D}\mathbf{B}^e\mathbf{u}^e\, d\mathscr{V} = \left(\mathbf{u}^e\right)^{\mathsf{T}}\int_{\mathscr{V}} \left(\mathbf{B}^e\right)^{\mathsf{T}}\mathbf{D}\mathbf{B}^e\, d\mathscr{V}\mathbf{u}^e. \tag{3.72}$$

In this equation the nodal displacement vectors of the element being independent of variables *x* and *y*, are taken to the front and back of the integral. Eqn. (3.72) can be solved independently of element displacements only when

$$\mathbf{f}^e = \int_{\mathcal{V}} \left(\mathbf{B}^e\right)^{\mathsf{T}} \mathbf{D}\mathbf{B}^e \, d\mathcal{V} \; \mathbf{u}^e \,, \tag{3.73}$$

which, after comparison with the known relation:

$$\mathbf{f}^e = \mathbf{K}^e \, \mathbf{u}^e \,,$$

gives us the equation determining coefficients of the element stiffness matrix:

$$\mathbf{K}^e = \int_{\mathcal{V}} \left(\mathbf{B}^e\right)^{\mathsf{T}} \mathbf{D}\mathbf{B}^e \, d\mathcal{V} \,. \tag{3.74}$$

Building the element stiffness matrix can be considerably easy if we note that this matrix divides into blocks:

$$\mathbf{K}^e = \begin{bmatrix} \mathbf{K}_{ii} & \mathbf{K}_{ij} & \mathbf{K}_{ik} \\ \mathbf{K}_{ji} & \mathbf{K}_{jj} & \mathbf{K}_{jk} \\ \mathbf{K}_{ki} & \mathbf{K}_{kj} & \mathbf{K}_{kk} \end{bmatrix}, \tag{12.75}$$

in which any of them, for example $\mathbf{K}_{ij}$, can be calculated from the equation:

$$\mathbf{K}_{ij} = \int_{\mathcal{V}} \left(\mathbf{B}_i\right)^{\mathsf{T}} \mathbf{D}\mathbf{B}_j \, d\mathcal{V} \,, \tag{3.76}$$

and others coming from analogous equations formed after suitable changes of indices have been made.

The insertion of the geometric matrices $\mathbf{B}_i$ and $\mathbf{B}_j$ given by Eqn.(3.70) and the matrix **D** given by Eqn. (2.13) into (3.76) results in

$$\mathbf{K}_{ij} = \left(\mathbf{B}_i\right)^{\mathsf{T}} \mathbf{D}\mathbf{B}_j \int_{\mathcal{V}} d\mathcal{V} = \left(\mathbf{B}_i\right)^{\mathsf{T}} \mathbf{D}\mathbf{B}_j \, Ab =$$

$$= \frac{EAb}{1-\nu^2} \begin{bmatrix} b_i b_j + c_i c_j \dfrac{1-\nu}{2} & b_i c_j \nu + b_j c_i \dfrac{1-\nu}{2} \\ b_j c_i \nu + b_i c_j \dfrac{1-\nu}{2} & c_i c_j + b_i b_j \dfrac{1-\nu}{2} \end{bmatrix}, \tag{3.77}$$

where *A* is the surface of a slab element and *b* is the its thickness.

The above matrix is the stiffness matrix for plane stress.

Note that matrices $\mathbf{B}_i$, $\mathbf{B}_j$ and $\mathbf{D}$ do not contain components dependent on variables x, y, z, thus we can take them outside the integral.

We obtain the block of the stiffness matrix for plane strain accepting the matrix of material constants according to Eqn. (2.17):

$$\mathbf{K}_{ij} = \frac{EAb}{(1+\nu)(1-2\nu)} \begin{bmatrix} (1-\nu)b_i b_j + c_i c_j \dfrac{1-2\nu}{2} & b_i c_j \nu + b_j c_i \dfrac{1-2\nu}{2} \\ b_j c_i \nu + b_i c_j \dfrac{1-2\nu}{2} & (1-\nu)c_i c_j + b_i b_j \dfrac{1-2\nu}{2} \end{bmatrix}. \tag{3.78}$$

Since the local coordinate system is assumed in such a way that its axes are parallel to the global coordinate system, then we do not have to transform the stiffness matrix.

We also calculate element strains. They are given by Eqn. (3.69) and taking into consideration Eqn. (3.70) we have

$$\varepsilon_x = \sum_{n=i,j,k} b_n u_{nx}\,,\ \varepsilon_y = \sum_{n=i,j,k} b_n u_{ny}\,,\ \gamma_{xy} = \sum_{n=i,j,k} \left(c_n u_{nx} + b_n u_{ny}\right). \tag{3.79}$$

We see that components of the strain vector are constant within the element which is the consequence of the assumption of linear shape functions. This element is called CST (*constant strain triangle*).

We determine element stresses from the constitutive Eqn. (3.5) and Eqn. (2.13) or (2.17) according to the kind of variant that we deal with. It is obvious that strains, just as stresses are constant within the CST element.

3.6.2. Nodal force vector for a distributed load

Loads on slab elements can be treated as loads on plane trusses which means that they can be applied to the nodes of a structure. But if a distributed load acting on the boundary of an element is given, then it should be converted to concentrated forces acting on the nodes of an element (Fig. 3.17).

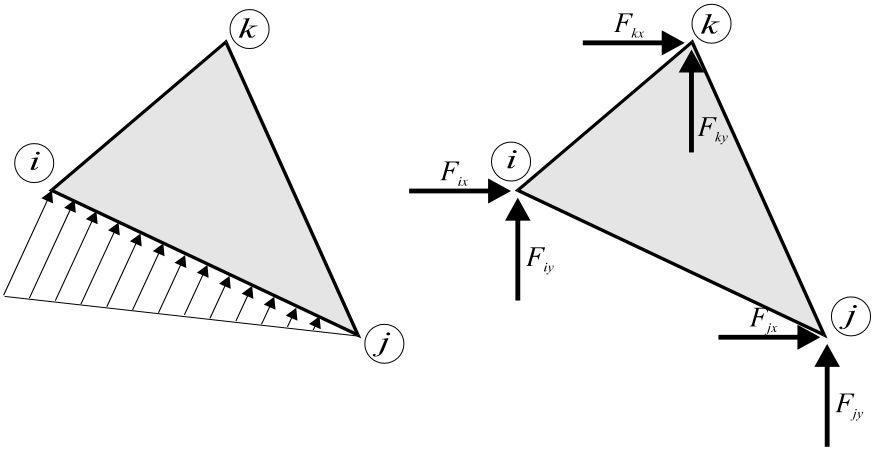

Fig. 3.17. Nodal forces representing continuous loads.

Similarly, as in previous chapters, we apply the principal of virtual work giving the following equilibrium equation for this case:

$$\left(\mathbf{u}^e\right)^{\mathrm{T}}\mathbf{f}^e + L_{ij}\int_0^1 \mathbf{u}(\xi)^{\mathrm{T}}\mathbf{q}(\xi)d\xi = 0\,, \tag{3.80}$$

where $\mathbf{u}(\xi)$ contains functions describing the displacement of the loaded edge and $\mathbf{q}(\xi)=\begin{bmatrix} q_x(\xi) \\ q_y(\xi) \end{bmatrix}$ contains functions describing the load on the edge, L_{ij} is the length of the edge *i-j*, ξ is the non-dimensional coordinate taking zero value at the node *i* and value 1 at the node *j*. Since we assume linear shape functions for the element, then we write the vector $\mathbf{u}(\xi)$ as follows:

$$\mathbf{u}(\xi) = \mathbf{N}_{ij}^e\mathbf{u}^e, \tag{3.81}$$

where $\mathbf{N}_{ij}^e$ is the matrix of shape functions for displacements of the boundary.

$$\mathbf{N}_{ij}^e = \left[N_i^o(\xi)\mathbf{I} \quad N_j^o(\xi)\mathbf{I} \quad N_k^o(\xi)\mathbf{0}\right], \tag{3.82}$$

where $N_i^o(\xi)=1-\xi$, $N_j^o(\xi)=\xi$, or in the developed form

$$\mathbf{N}_{ij}^e = \begin{bmatrix} 1-\xi & 0 & \xi & 0 & 0 & 0 \\ 0 & 1-\xi & 0 & \xi & 0 & 0 \end{bmatrix}. \tag{3.83}$$

After inserting relation Eqn. (3.81) into Eqn. (3.80), we obtain

$$\mathbf{f}^e = -L_{ij}\int_0^1 \left(\mathbf{N}_{ij}^e\right)^{\mathrm{T}}\mathbf{q}(\xi)d\xi. \tag{3.84}$$

After taking into consideration the shape functions described by Eqn. (3.83), we obtain

$$\mathbf{f}^e = -L_{ij}\int_0^1 \begin{bmatrix} (1-\xi)q_x(\xi) \\ (1-\xi)q_y(\xi) \\ \xi q_x(\xi) \\ \xi q_y(\xi) \\ 0 \\ 0 \end{bmatrix} d\xi \,. \tag{3.85}$$

For example, let us calculate the nodal force vector due to the linear distributed load on the edge *i-j* of value q_{ix}, q_{iy} - at the node *i* and q_{jx}, q_{jy} - at the node *j*. We write such a load with the help of a non-dimensional coordinate ξ:

$$\mathbf{q}(\xi) = \begin{bmatrix} q_{ix}(1-\xi) + q_{jx}\xi \\ q_{iy}(1-\xi) + q_{jy}\xi \end{bmatrix}, \tag{3.86}$$

and after inserting the above equation into Eqn. (3.85), we obtain

$$\mathbf{f}^e = -L_{ij}\begin{bmatrix} q_{ix}\int_0^1 (1-\xi)^2 d\xi + q_{jx}\int_0^1 (1-\xi)\xi d\xi \\ q_{iy}\int_0^1 (1-\xi)^2 d\xi + q_{jy}\int_0^1 (1-\xi)\xi d\xi \\ q_{ix}\int_0^1 (1-\xi)\xi d\xi + q_{jx}\int_0^1 \xi^2 d\xi \\ q_{iy}\int_0^1 (1-\xi)\xi d\xi + q_{jy}\int_0^1 \xi^2 d\xi \\ 0 \\ 0 \end{bmatrix}, \tag{3.87}$$

which after integration gives

$$\mathbf{f}^e = -\frac{L_{ij}}{6}\begin{bmatrix} 2q_{ix} + q_{jx} \\ 2q_{iy} + q_{jy} \\ q_{ix} + 2q_{jx} \\ q_{iy} + 2q_{jy} \\ 0 \\ 0 \end{bmatrix}. \tag{3.88}$$

For a particular case when the load is constant and equal to $\mathbf{q}(\xi) = \begin{bmatrix} q_{ox} \\ q_{oy} \end{bmatrix}$, on the basis of Eqn. (3.88) we obtain

$$\mathbf{f}^e = -\frac{L_{ij}}{2}\begin{bmatrix} q_{ox} \\ q_{oy} \\ q_{ox} \\ q_{oy} \\ 0 \\ 0 \end{bmatrix}. \tag{3.89}$$

It should be remembered that the calculated forces are forces acting on the element. We obtain the necessary nodal forces changing the sense of vectors which means:

$$\mathbf{p}^e = -\mathbf{f}^e, \tag{3.90}$$

where $\mathbf{p}^e$ is the nodal force vector for the nodes touching the element *e*.

3.6.3. A Nodal force vector due to a temperature load

As in the previous section, we apply the principal of virtual work to calculate alternative nodal forces replacing a temperature load. In accordance with the features of a CST element we will take into consideration only a constant temperature field within the element.

The suitable equation of virtual work has the form:

$$\left(\mathbf{u}^e\right)^{\mathrm{T}} \mathbf{f}^{et} = \int_{\mathcal{V}} \boldsymbol{\varepsilon}^{\mathrm{T}} \boldsymbol{\sigma}_t \, d\mathcal{V} = \int_{\mathcal{V}} \boldsymbol{\varepsilon}^{\mathrm{T}} \mathbf{D}\, \boldsymbol{\varepsilon}_t \, d\mathcal{V}, \tag{3.91}$$

where $\boldsymbol{\sigma}_t$ is the stress field in the element which is caused by the temperature and $\boldsymbol{\varepsilon}_t$ is the strain of the element caused by the change of a temperature.

Assuming isotropy of a 2D element we obtain

$$\boldsymbol{\varepsilon}_t = \alpha_t \Delta t \begin{bmatrix} 1 \\ 1 \\ 0 \end{bmatrix}, \tag{3.92}$$

After inserting geometric relation Eqn.(3.69) into Eqn. (3.91), we obtain

$$\mathbf{f}^{et} = \alpha_t \Delta t \int_{\mathcal{V}} \left(\mathbf{B}^e\right)^{\mathsf{T}} \mathbf{D} \begin{bmatrix} 1 \\ 1 \\ 0 \end{bmatrix} d\mathcal{V} = \alpha_t \Delta t A b \left(\mathbf{B}^e\right)^{\mathsf{T}} \mathbf{D} \begin{bmatrix} 1 \\ 1 \\ 0 \end{bmatrix}. \tag{3.93}$$

For a plane stress problem this equation is simplified to the following relation:

$$\mathbf{f}^{et}_{\mathrm{PSN}} == \frac{\alpha_t \Delta t E A b}{1-\nu} \begin{bmatrix} b_i \\ c_i \\ b_j \\ c_j \\ b_k \\ c_k \end{bmatrix}, \tag{3.94}$$

where b_i ... c_k are coefficients of shape functions of the CST element.

Plane strain gives a slightly different nodal force vector:

$$\mathbf{f}^{et}_{\mathrm{PSO}} == \frac{\alpha_t \Delta t E A b}{(1+\nu)(1-2\nu)} \begin{bmatrix} b_i \\ c_i \\ b_j \\ c_j \\ b_k \\ c_k \end{bmatrix}. \tag{3.95}$$

As in previous sections, we should change the signs of components of nodal forces before applying them to the nodes:

$$\mathbf{p}^{et} = -\mathbf{f}^{et}. \tag{3.96}$$

We calculate stresses in the element undergoing the action of a temperature taking into consideration strains caused by the thermal expansion of the element:

$$\boldsymbol{\sigma}_t = \mathbf{D}(\boldsymbol{\varepsilon} - \boldsymbol{\varepsilon}_t) = \mathbf{D}\left(\mathbf{B}\mathbf{u}^e - \alpha_t \Delta t \begin{bmatrix} 1 \\ 1 \\ 0 \end{bmatrix}\right). \tag{3.97}$$

3.6.4. Boundary conditions of a 2D element

Boundary conditions of a two-dimensional structure can be treated analogously to the conditions in a plane truss because the nodes of both systems have two degrees of freedom on the *XY* plane.

Hence we have: fixed supports (at the node r_1 in Fig. 3.18) and supports which can move along the X axis (at the node r_2), next supports which can move along the Y axis (at the node r_4) or skew supports (at the node r_3). The boundary conditions for these supports are as follows:

- node r_1: $u_{r_1X}=0$, $u_{r_1Y}=0$,
- node r_2: $u_{r_2Y}=0$,
- node r_4: $u_{r_4X}=0$,
- for node r_3, where constraints are not consistent with the axes of the global coordinate system we propose the use of boundary elements described in [Podgórski, Gontarz] or [Podgórski, Błazik].

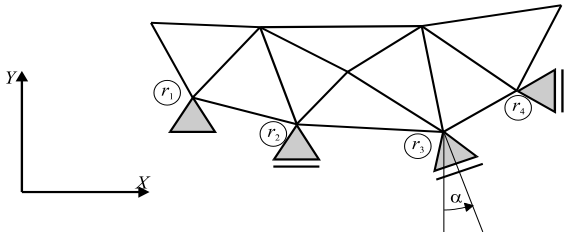

Fig. 3.18. Slab structure divided into triangle finite elements.

3.6.5. Example of solving the problem of bending the rectangular slab

Let us solve with use of FEM the problem which has been previously calculated with analytical methods, to compare the results. We will make use of the stiffness matrix of CST element shown in previous paragraphs and use, for sake if comparison, more complex quadrilateral element. Autodesk Simulation Mechanical will be used to obtain the solution.

The slab shown in Fig. 3.19 is divided into 640 triangular elements (Fig. 3.19), which gives 369 nodes with 2 degrees of freedom at each node. Composition of the stiffness matrix for triangular elements and collation of nodal forces into equilibrium equations results in generation of system of 738 equations.

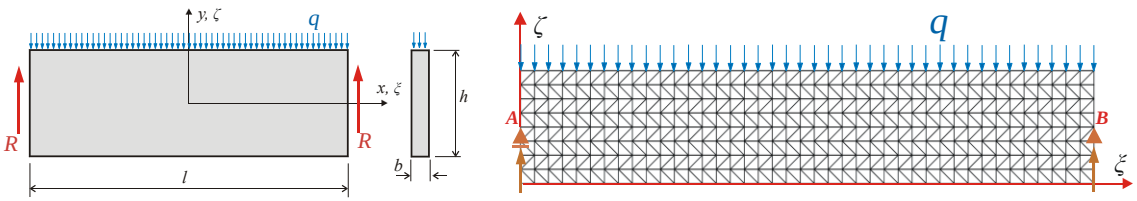

Fig. 3.19. Slab FEM model, built with CST elements.

Thanks to boundary conditions: u_{yA}=0, u_{xB}=0, u_{yB}=0 we can eliminate or modify 3 equations, which allows solution of the system. After determination of displacements, we calculate stress in elements. We have used CST, so at the triangular area we obtain constant values of stresses. To smooth the stress field, we average the calculated stress at each node. Figure 3.20a shows normal stress σ_x field at the slab surface and the diagram of these stresses in the cross-section $\xi = 0.5$, which has been generated with use of Autodesk Simulation Mechanical 2015. Figure 3.20b shows the same stress field obtained with use of quadrilateral elements. There are observed differences at the graph in Fig. 3.20a, which is diverged from the expected linear relation. It is caused by less dense mesh of triangular CST elements and smaller accuracy of solutions obtained with use of such elements in comparison to the ones when quadrilateral elements are used.

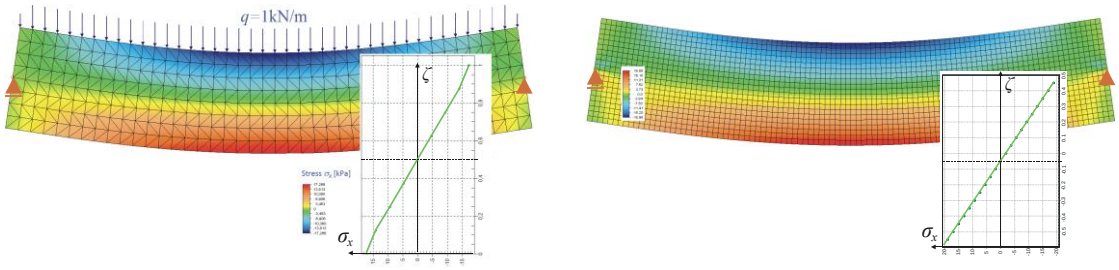

a) Slab model 1 b) Slab model 2

Fig. 3.20. Stress graph at ξ=0 for two FEM models

It is apparently visible in the cross-section, which is close to a support. Figure 3.21 shows stress diagrams in the cross-section located in the 0.25m distance from the right support of the slab. The diagrams have been prepared for both models of slab and for comparison there have been additionally given diagrams resulting from analytical solutions: polynomial and based on Fourier series (Fig. 3.7, Fig. 3.8).

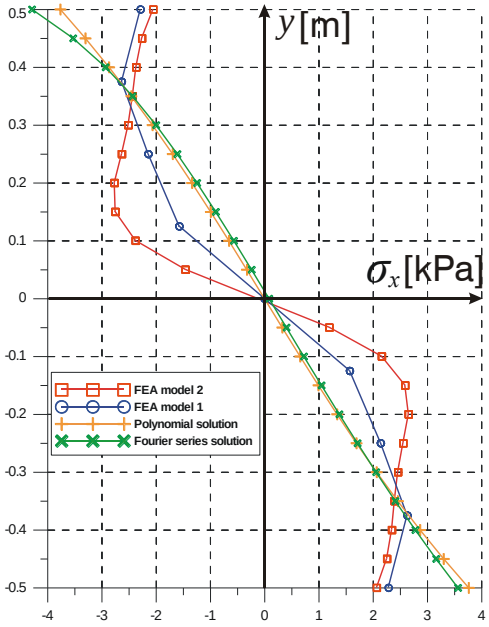

Fig. 3.21. Normal stresses σ_x in the cross-section at ξ=0.45 calculated by various methods.

3.7. Numerical solutions of the slab static problems with FDM

Finite difference method (FDM) is one of the simplest methods of solving problems described with use of systems of differentia equations. The idea in this method is based on the replacement of derivatives occurring in these equations with the appropriate difference quotients. Some difficulty in application of this method is generated by boundary conditions and irregular shape of an edge.

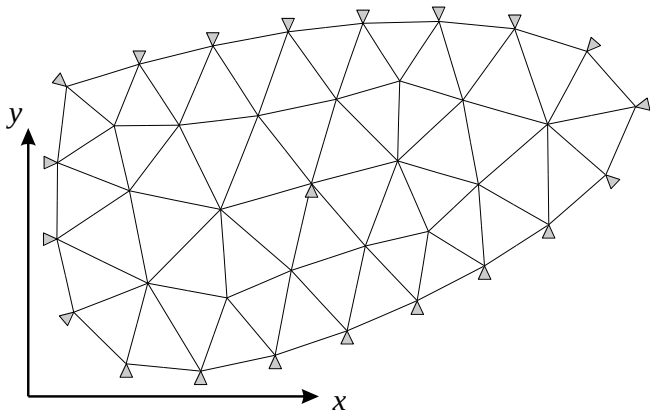

Fig. 3.22 Grid of the nodes and boundary conditions

We overlay mesh of nodal points (as regular as possible) (Fig. 3.22) to the area where the calculated equation should be fulfilled. The values of the analyzed function in

the nodes of the mesh are the set of unknowns. Now, difference quotients adequate to the order of differential equation should be set down, which will allow us to transform differential equation into the system of algebraic equations. The simple method of getting these quotients is expansion of the analyzed function into Taylor series at the nodal points.

3.7.1. One variable function

Expansion into Taylor series of the analyzed function $u(x)$ around the point at the coordinate x_i (Fig. 3.23.), may be presented in the following form:

$$u_{i+1} = u_i + \Delta_x \left.\frac{du}{dx}\right|_i + \frac{\Delta_x^2}{2!}\left.\frac{d^2u}{dx^2}\right|_i + \frac{\Delta_x^3}{3!}\left.\frac{d^3u}{dx^3}\right|_i + \frac{\Delta_x^4}{4!}\left.\frac{d^4u}{dx^4}\right|_i + \frac{\Delta_x^5}{5!}\left.\frac{d^5u}{dx^5}\right|_i + \dots \tag{3.98}$$

$$u_{i-1} = u_i - \Delta_x \left.\frac{du}{dx}\right|_i + \frac{\Delta_x^2}{2!}\left.\frac{d^2u}{dx^2}\right|_i - \frac{\Delta_x^3}{3!}\left.\frac{d^3u}{dx^3}\right|_i + \frac{\Delta_x^4}{4!}\left.\frac{d^4u}{dx^4}\right|_i - \frac{\Delta_x^5}{5!}\left.\frac{d^5u}{dx^5}\right|_i + \dots \tag{3.99}$$

Transformation of equations (3.98) and (3.99) leads to:

$$\left.\frac{du}{dx}\right|_i = \frac{u_{i+1} - u_i}{\Delta_x} + O(\Delta_x) \qquad \text{- forward finite difference} \tag{3.100}$$

$$\left.\frac{du}{dx}\right|_i = \frac{u_i - u_{i-1}}{\Delta_x} + O(\Delta_x) \qquad \text{- backward finite difference} \tag{3.101}$$

and calculating the mean from (3.100) and (3.101) or subtracting (3.99) from (3.98) we get:

$$\left.\frac{du}{dx}\right|_i = \frac{u_{i+1} - u_{i-1}}{2\Delta_x} + O(\Delta_x^2) \quad \text{- central finite difference,} \tag{3.102}$$

which is characterized by smaller error. In these equations Δ_x is the distance between mesh nodes in the x direction, and $O(\Delta_x)$ means the remainder of the Δ_x order, $O(\Delta_x^2)$ is the remainder of the Δ_x^2 order, $\left.\frac{du}{dx}\right|_i$ is the value of the derivative calculated in the point at the x_i coordinate.

This result can be also obtained by approximation of the analyzed function in the range $2\Delta_x$ with 2nd order polynomial: $u(x) = a_2 x^2 + a_1 x + a_0$ (Fig. 3.23). The constants

a_i should be evaluated with use of conditions: $u(0) = u_i$, $u(-\Delta_x) = u_{i-1}$, $u(\Delta_x) = u_{i+1}$, which leads to the equation:

$$u(x) \approx (u_{i+1} - 2u_i + u_{i-1}) \frac{x^2}{2\Delta_x{}^2} + (u_{i+1} - u_{i-1}) \frac{x}{2\Delta_x} + u_i \,, \tag{3.103}$$

which after derivation in regard to x and calculation of the derivative in the „i" point, (x=0) gives central finite difference (3.102).

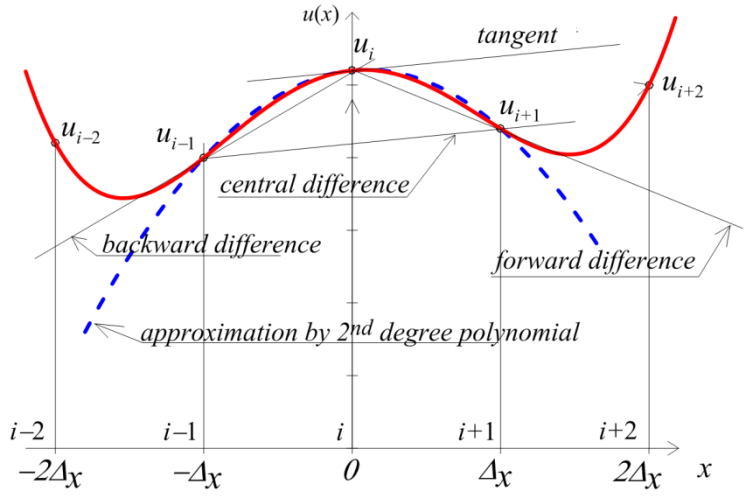

Fig. 3.23. Function *u(x)* approximation by 2nd degree polynomial

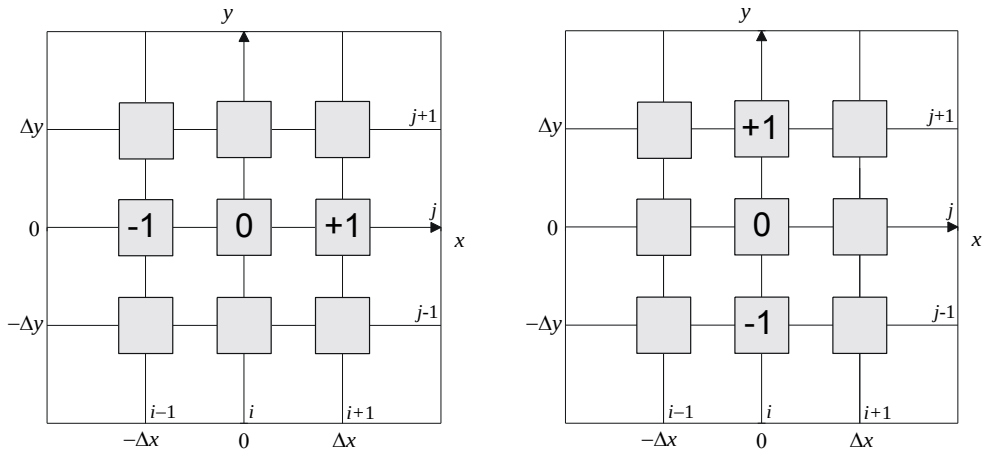

a) $2\Delta x\, du/dx$ b) $2\Delta y\, du/dy$

Fig. 3.24 Differential schemes: *du/dx* (a) and *du/dy* (b)

As it can be easily calculated, taking first 5 terms of the Taylor series (up to the term containing x^4), the second derivative can be expressed with use of the differential formula:

$$\left.\frac{d^2u}{dx^2}\right|_i = \frac{u_{i+1} - 2u_i + u_{i-1}}{\Delta_x{}^2} + O(\Delta_x{}^2)\,. \tag{3.104}$$

Taking first terms of the Taylor series up to the term containing x^6 and averaging in the same manner as we have done in equation (6), we obtain the expressions for central finite differences:

$$\left.\frac{d^2u}{dx^2}\right|_i = \frac{-u_{i+2} + 16u_{i+1} - 30u_i + 16u_{i-1} - u_{i-2}}{12\Delta_x{}^2} + O(\Delta_x{}^4)\,, \tag{3.105}$$

$$\left.\frac{d^3u}{dx^3}\right|_i = \frac{u_{i+2} - 2u_{i+1} + 2u_{i-1} - u_{i-2}}{2\Delta_x{}^3} + O(\Delta_x{}^2)\,, \tag{3.106}$$

$$\left.\frac{d^4u}{dx^4}\right|_i = \frac{u_{i+2} - 4u_{i+1} + 6u_i - 4u_{i-1} + u_{i-2}}{\Delta_x{}^4} + O(\Delta_x{}^2)\,. \tag{3.107}$$

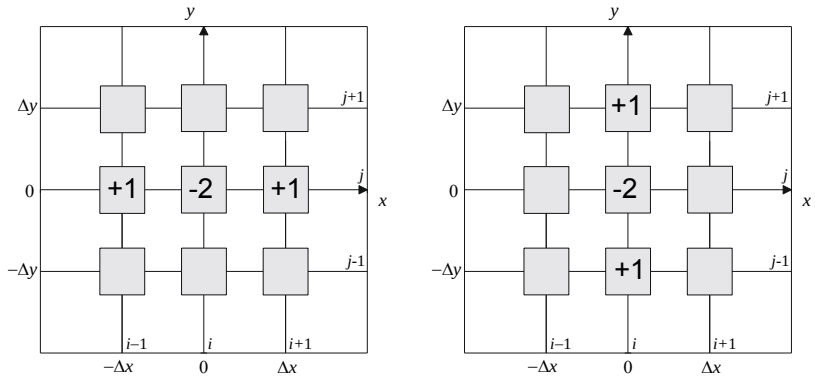

a) $\Delta x^2\, d^2u/dx^2$ b) $\Delta y^2\, d^2u/dy^2$

Fig. 3.25 Differential schemes: d^2u/dx^2 (a) and d^2u/dy^2 (b)

3.7.2. Case of two-variable function

By analogy to the differences in one-dimensional case, marking with i the order of distances Δ_x in the x axis direction, and with j the order of distances Δ_y in the y axis direction, we write down expressions for appropriate finite differences:

$$\left.\frac{\partial u}{\partial x}\right|_{i,j} = \frac{u_{i+1,j} - u_{i-1,j}}{2\Delta_x} + O(\Delta_x{}^2) \tag{3.108}$$

$$\left.\frac{\partial u}{\partial y}\right|_{i,j} = \frac{u_{i,j+1} - u_{i,j-1}}{2\Delta_y} + O(\Delta_y{}^2)\,, \tag{3.109}$$

$$\left.\frac{\partial^2 u}{\partial x^2}\right|_{i,j} = \frac{u_{i+1,j} - 2u_{i,j} + u_{i-1,j}}{\Delta_x{}^2} + O(\Delta_x{}^2), \tag{3.110}$$

$$\left.\frac{\partial^2 u}{\partial y^2}\right|_{i,j} = \frac{u_{i,j+1} - 2u_{i,j} + u_{i,j-1}}{\Delta_y{}^2} + O(\Delta_y{}^2). \tag{3.111}$$

Mixed derivatives may be replaced with finite differences calculated by combining formulae (3.108) and (3.109), which gives:

$$\left.\frac{\partial^2 u}{\partial x \partial y}\right|_{i,j} = \frac{u_{i+1,j+1} - u_{i+1,j-1} - u_{i-1,j+1} + u_{i-1,j-1}}{4\Delta_x \Delta_y} + O(\Delta_x{}^2, \Delta_y{}^2) \tag{3.112}$$

Adding differential schemes (3.110) and (3.111) we obtain already previously used Laplace operator:

$$\nabla^2 u(x,y) = \frac{u_{i-1,j} - 2u_{i,j} + u_{i+1,j}}{\Delta_x{}^2} + \frac{u_{i,j-1} - 2u_{i,j} + u_{i,j+1}}{\Delta_y{}^2} + O(\Delta_x{}^2, \Delta_y{}^2), \tag{3.113}$$

and calculation of the 4th order derivative calculation leads to the biharmonic operator which occurs in the equation of the Airy stress function:

$$\begin{aligned}\nabla^2\nabla^2 u(x,y) = {} & \frac{6u_{i,j} - 4\left(u_{i-1,j} + u_{i+1,j}\right) + \left(u_{i-2,j} + u_{i+2,j}\right)}{\Delta_x^4} + \\ & + \frac{8u_{i,j} - 4\left(u_{i-1,j} + u_{i+1,j} + u_{i,j-1} + u_{i,j+1}\right) + 2\left(u_{i-1,j-1} + u_{i+1,j-1} + u_{i-1,j+1} + u_{i+1,j+1}\right)}{\Delta_x^2 \Delta_y^2} + \\ & + \frac{6u_{i,j} - 4\left(u_{i,j-1} + u_{i,j+1}\right) + \left(u_{i,j-2} + u_{i,j+2}\right)}{\Delta_y^4} + O(\Delta_x{}^4, \Delta_y{}^4).\end{aligned} \tag{3.114}$$

In the case of the quadrilateral differential mesh, when $\Delta_x=\Delta_y$, the biharmonic operator obtains much simpler for, which will be used in further consideration. Indicating $\Delta=\Delta_x=\Delta_y$ we have:

$$\nabla^2\nabla^2 u(x,y) = \frac{1}{\Delta^4}\begin{bmatrix} 20u_{i,j} - 8\left(u_{i-1,j} + u_{i+1,j} + u_{i,j-1} + u_{i,j+1}\right) + \\ + 2\left(u_{i-1,j-1} + u_{i+1,j-1} + u_{i-1,j+1} + u_{i+1,j+1}\right) + \\ + u_{i-2,j} + u_{i+2,j} + u_{i,j-2} + u_{i,j+2} \end{bmatrix} + O(\Delta_x{}^4, \Delta_y{}^4). \tag{3.115}$$

It is convenient to present differential quotients as graphic schemes. Schemes referring to equations (3.108)...(3.115) are presented in figures: 3.23...3.27.

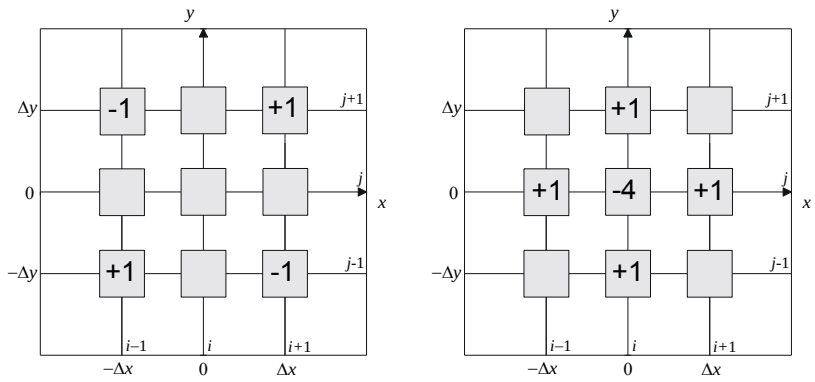

a) $4\Delta x\Delta y\,\partial^2 u/\partial x\partial y$ b) $\Delta_{xy}^2\left(\partial^2 u/\partial x^2+\partial^2 u/\partial y^2\right)$

Fig. 3.26 Differential schemes: $\partial^2 u/\partial x\partial y$ (a) and $\nabla^2 u$ for $\Delta x=\Delta y=\Delta_{xy}$ (b)

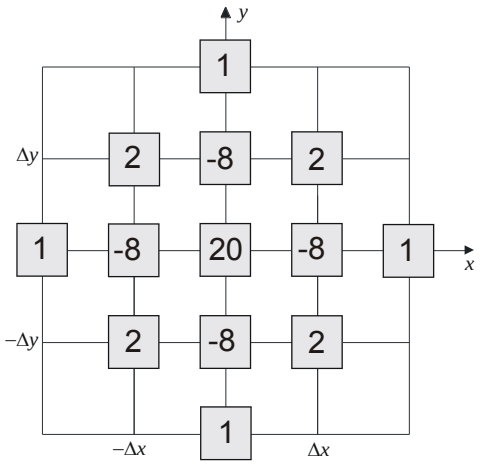

Fig. 3.27 Differential scheme for biharmonic operator $\nabla^2\nabla^2 u$ for $\Delta x=\Delta y=\Delta$

In the chapter devoted to plate theory we will show another method of obtaining the differential operator formula for the biharmonic equation, which can be useful when differential mesh is irregular.

Application of Taylor series to determine differential quotients of higher orders has been described in details in the wide monograph by T. J. Chung [2002]. Usage of irregular meshes has been presented by J. Orkisz in the third part of monograph (Kleiber et al. [1995]). Differential operators of higher orders used for solving equations of plate theory and methods of boundary conditions application are given in extensive form in monograph by Z. Kączkowski [1980].

3.7.3. Boundary conditions application

First order differential equations where the only boundary conditions are values of the analyzed function in the boundary nodes of the mesh (Dirichlet's condition), are no difficulty when composing system of equations for FDM. If we limit our consideration to first and second order differential equations then as it can be seen in figures 3.24 and 3.25, differential operators contain only function values in the nodes directly neighboring the node in which operator is written down. Because the function values in the boundary points in Dirichlet's conditions are given, then we do not have to write down differential equations for these points. The only remaining points are inside the area (Fig. 3.28). Thus the formed system of equations will not contain any function values in points located outside the area of solution.

Difficulties are rising when we analyze higher order equations, where the differential operators contain function values in neighboring points, but also located in distances $2\Delta_x$ and further from the central point (comp. Kączkowski [1980]). Of other nature, but similar in the effect difficulties are generated, when there are defined derivatives of the function in the boundary points (Neumann's conditions). First order differential quotient (equation 3.108) written down for a boundary point introduces the function value from the point located outside the solution area into the system of equations. These values should be calculated on the basis of the derivative value in the boundary point:

$$\left.\frac{\partial u}{\partial x}\right|_{i,j} = \psi \quad \rightarrow \quad \frac{u_{i+1,j} - u_{i-1,j}}{2\Delta} = \psi \quad \rightarrow \quad u_{i+1,j} = u_{i-1,j} + 2\Delta\psi \,. \tag{3.116}$$

In the example shown in Fig. 3.28 we have Dirichlet's conditions in the points at the area's circumference and the Neumann's condition in the point 14. If we want to use central differences to describe a derivative at this point then this state generates the necessity of introduction of additional node *"16"* located outside of the calculation area. The additional equation allowing evaluation of the function value at the new node is expressed as follows: $u_{16} = u_{11} + 2a\psi$.

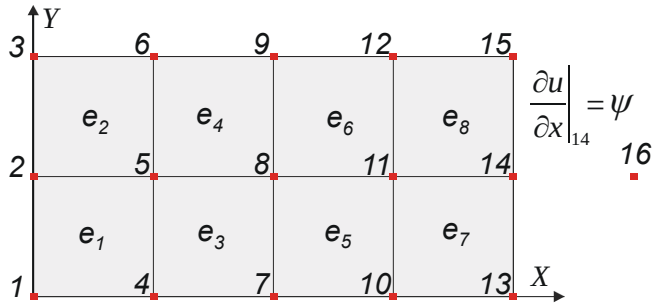

$u_1,\ u_2,\ u_3,\ u_6,\ u_9,\ u_{12} = 0$
$u_4,\ u_7,\ u_{10},\ u_{13} = 0,\ u_{15} = u_O$

Fig. 3.28 Rectangular area $2a \times 4a$ and the Dirichlet and Neumann boundary conditions

In case of searching for the Airy stress function, we will deal with both types of boundary conditions. This may seem odd, since the natural conditions at the slab edge are referring to stresses which are described with use of 2nd order derivatives of the Airy function. We will show the method of consideration of boundary with use of the previously shown example of the problem presented in Fig. 3.29 and boundary conditions 3.31, which will be now slightly modified to make the obtained result similar to the one calculated with use of the polynomial stress function:

$$\begin{aligned}
&1)\ \sigma_y(x,h) = -q/b, \quad 2)\ \tau_{xy}(x,h) = 0,\\
&3)\ \sigma_y(x,0) = 0, \qquad 4)\ \tau_{xy}(x,0) = 0,\\
&5)\ \sigma_x(0,y) = 0, \qquad 6)\ -\int_0^h \tau_{xy}(0,y)\, b\, dy = R = ql/2,\\
&7)\ \sigma_x(l,y) = 0, \qquad 8)\ \int_0^h \tau_{xy}(l,y)\, b\, dy = R = ql/2\,.
\end{aligned} \tag{3.117}$$

The stresses τ_{xy} at both vertical edges of the slab have got parabolic distribution: $\tau_{xy} = \frac{3ql}{4bh}\left(1 - 4\zeta^2\right)$, which corresponds to the result obtained in the equation 3.41. Maximum value occurs at the horizontal axis of the slab an is equal to $\tau_{\max} = \frac{3ql}{4hb}$, at the right edge and $\tau_{\min} = -\frac{3ql}{4hb}$ at the left edge, which fulfills equilibrium conditions:

$$\int_{-h/2}^{h/2} \tau_{xy}(l,y)\, b\, dy = ql/2 \ \text{ for } x = l/2 \ \text{ and } \ -\int_{-h/2}^{h/2} \tau_{xy}(0,y)\, b\, dy = ql/2 \ \text{ for } x = l/2$$

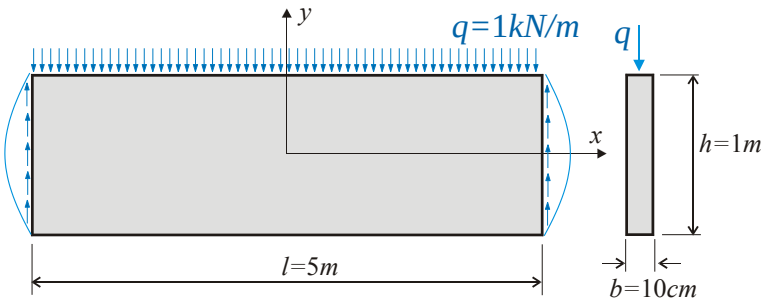

Fig. 3.29 Rectangular slab and stress boundary conditions

Writing down the boundary condition $\sigma_y(x,h) = p(x)$ in the relation to the Airy function, we have: $\sigma_y = \dfrac{\partial^2 \Phi}{\partial x^2} = p(x)$. Replacement of the 2nd order derivative with the differentia quotient (3.110) we obtain for the point *i,j* located at the top edge of the slab the following equation: $\left.\dfrac{\partial^2 \Phi}{\partial x^2}\right|_{i,j} = \dfrac{\Phi_{i+1,j} - 2\Phi_{i,j} + \Phi_{i-1,j}}{\Delta_x^{\,2}} = p_{i,j}$, which combines the nearby boundary points, as well. By using similarity of the boundary condition to the relation of bending moment and shear load, which is known from beam theory, leads to the significant simplification of this condition (comp. Andermann): $\dfrac{\partial^2 M}{\partial x^2} = p(x) \;\rightarrow\; \Phi \sim M$, which yields: $\Phi_{i,j} \sim M_{i,j}$, where $M_{i,j}$ is the value of the bending moment in the *i,j* point assigned for the fictional rod of the shape of the slab circumference (Fig. 3.30).

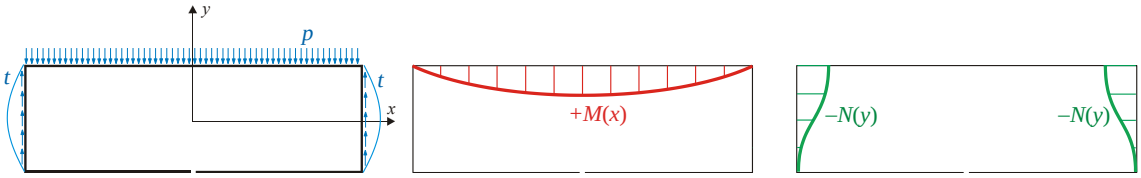

a) b) c)

Fig. 3.30 Rectangular slab and its fictional edge rod (a), bending moment (b) and axial force (c) charts

The rod, for easy calculation of internal forces, may be cut at any point. Internal forces in the cross-section may be arbitrary. This does not influence the calculated in this way stresses because only constant and linear components of stress function are changed, and the stresses are expressed with use of 2nd order derivatives. The moment should be positive since it generated elongation of fictional rod fiber inside the slab area (Fig. 3.30).

The boundary condition for shear stresses at the right edge of the slab: $\tau_{xy}(l,y)=t(y)$ written down with use of Airy function $\tau_{xy}=-\frac{\partial^2\Phi}{\partial x\partial y}=t(y)$ gives the following differential quotient: $-\left.\frac{\partial^2\Phi}{\partial x\partial y}\right|_{i,j}=-\frac{\Phi_{i+1,j+1}-\Phi_{i+1,j-1}-\Phi_{i-1,j+1}+\Phi_{i-1,j-1}}{4\Delta_x\Delta_y}=t_{i,j}$. In similar way as before, by using beam analogy (comp. Andermann) we obtain: $\frac{\partial N(y)}{\partial y}=-t(y)$. Integration of this equation leads to $N(y)=-\int t(y)\,dy$, which allows simplification of the boundary condition to the following relation $\frac{\partial\Phi(x,y)}{\partial x}=N(y)$ and it leads to the differential quotient in the shape $\frac{\Phi_{i+1,j}-\Phi_{i-1,j}}{2\Delta_x}=N_{i,j}$, which gives the value of the stress function in the point outside the slab area: $\Phi_{i+1,j}=2\Delta_x N_{i,j}+\Phi_{i-1,j}$, where $N_{i,j}$ is axial force in the point *i,j* calculated for the fictional rod.

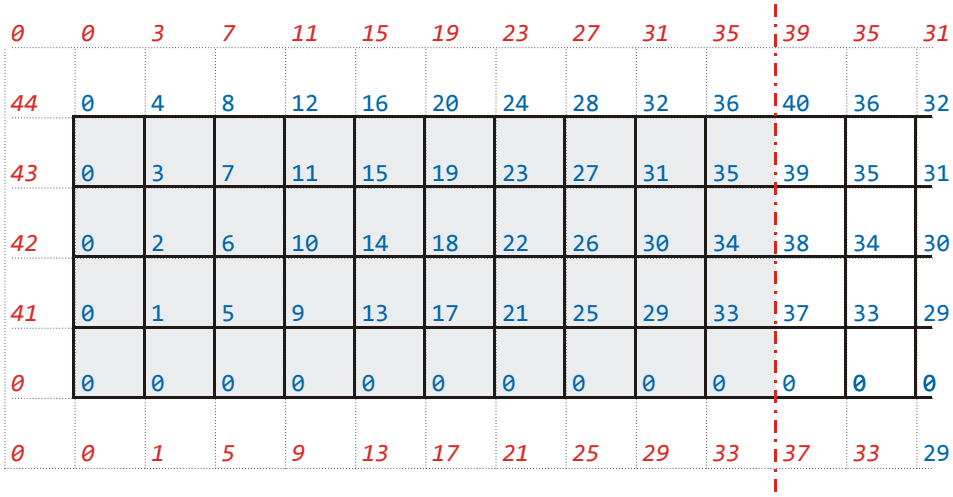

Fig. 3.31 Grid nodes of finite difference method, symmetry of the problem was used

We will show the application of this method in the example of quadrilateral mesh of nodal points. Dividing shorter edge of the slab shown in figure 3.29 into four sections, we obtain the mesh of the side length of 25 cm (comp. Fig. 3.31). The numbering scheme shown in figure uses the problem symmetry, i.e. nodes located at both sides of the symmetry axis have got the same numbers. Zero boundary conditions for stress function have been used as well (Dirichlet's conditions) by numbering these nodes as `0` (comp. Fig. 3.30b). Zero values of the stress function derivatives have also been introduced (Neumann's conditions) by numbering nodes outside the slab area with

the same values as for the nodes inside the area symmetrically across the slab edge (comp. Fig. 3.30c). This method allows limitation of the number of unknown nodal values.

The function values will be calculated in all boundary points. We will apply here analogy of the bending moments diagram in the fictional rod (Fig. 3.30b). Distribution of the bending moment is described with the equation: $\Phi(\xi)=M(\xi)=\frac{q\,l^2}{8b}\left(1-4\xi^2\right)$, where $\xi=x/l$. Table 1 gives values of dimensionless stress function $\mu(\xi)$ in points located at the top edge of the slab. The function $\mu(\xi)$ is described with equation: $\mu(\xi)=\frac{1}{8}\left(1-4\xi^2\right)$. The values μ_i given in Table 1 indicate: $\mu_i = \mu(\xi_i)$.

Table 1.

Node i	μ_i	Node i	μ_i	Node i	μ_i
0	0.00000	16	0.08000	32	0.12000
4	0.02375	20	0.09375	36	0.12375
8	0.04500	24	0.10500	40	0.12500
12	0.06375	28	0.11375		

In the same way we calculate the values of derivative $\frac{\partial\Phi}{\partial x}=N(y)$ in the points of vertical edge ($x=l/2$). Integrating shear stresses at the left edge we obtain the equation of the axial force in the fictional rod: $N(y)=\int\tau_{xy}(y)\,dy$ or the other way by using non-dimensional coordinates $N(\zeta)=\frac{-ql}{4b}\left(3\zeta-4\zeta^3+C\right)$ where $\zeta=y/h$ and C is the integration constant taken to make $N(-h/2)=0$. Finally, the function of axial force in the fictional rod can be described with the following equation: $N(\zeta)=\frac{-ql}{4b}\left(1+3\zeta-4\zeta^3\right)$. This equation allows calculation of the derivative values in boundary points $\left.\frac{\partial\Phi}{\partial x}\right|_{i,j}$, and then the stress function values in the external points located in the opposite direction to x: $\Phi_{i-1,j}=\Phi_{i+1,j}-2\Delta_x N_{i,j}$. Because the side dimension of the mesh in this case is equal to $\Delta_x=l/n$ (n=20 in the presented case which gives Δ_x=25cm), the function values in the points located on the left side of the edge are

calculated with use of the equation: $\Phi_{i-1,j} = \Phi_{i+1,j} + \frac{q l^2}{2nb}\left(1 + 3\zeta_{i,j} - 4\zeta_{i,j}{}^3\right)$ or $\Phi_{i-1,j} = \Phi_{i+1,j} + \frac{q l^2}{b}\eta_{i-1,j}$, where $\eta_{i,j} = \frac{1}{2n}\left(1 + 3\zeta_{i,j} - 4\zeta_{i,j}{}^3\right)$ is the non-dimensional increment of the function values in the *x* axis direction. Table 2 shows values of these increments for *n*=20.

Table 2.

Node *i*	η_i	Node *i*	η_i	Node *i*	η_i
0	0.0000000	42	0.0250000	44	0.0500000
41	0.0078125	43	0.0421875		

We will write down differential quotients for all internal points of the slab:

Node *i*	$\nabla^2\nabla^2\Phi\|_i$	= 0
1	$20\Phi_1-8(\Phi_0+\Phi_5+\Phi_2+\Phi_0)+2(\Phi_0+\Phi_6+\Phi_0+\Phi_0)+\Phi_1+\Phi_9+\Phi_3+\Phi_{41}$	= 0
2	$20\Phi_2-8(\Phi_1+\Phi_6+\Phi_3+\Phi_0)+2(\Phi_5+\Phi_7+\Phi_0+\Phi_0)+\Phi_0+\Phi_{10}+\Phi_4+\Phi_{42}$	= 0
3	$20\Phi_3-8(\Phi_2+\Phi_7+\Phi_4+\Phi_0)+2(\Phi_6+\Phi_8+\Phi_0+\Phi_0)+\Phi_1+\Phi_{11}+\Phi_3+\Phi_{43}$	= 0
5	$20\Phi_5-8(\Phi_0+\Phi_9+\Phi_6+\Phi_1)+2(\Phi_0+\Phi_{10}+\Phi_2+\Phi_0)+\Phi_5+\Phi_{13}+\Phi_7+\Phi_0$	= 0
6	$20\Phi_6-8(\Phi_5+\Phi_{10}+\Phi_7+\Phi_2)+2(\Phi_9+\Phi_{11}+\Phi_3+\Phi_1)+\Phi_0+\Phi_{14}+\Phi_8+\Phi_0$	= 0
7	$20\Phi_7-8(\Phi_6+\Phi_{11}+\Phi_8+\Phi_3)+2(\Phi_{11}+\Phi_{11}+\Phi_3+\Phi_3)+\Phi_5+\Phi_{15}+\Phi_7+\Phi_0$	= 0
..*i*..	$20\Phi_i-8(...)+2(...)+1(...)$	= 0
37	$20\Phi_{37}-8(\Phi_0+\Phi_{33}+\Phi_{38}+\Phi_{33})+2(\Phi_0+\Phi_{34}+\Phi_{34}+\Phi_0)+\Phi_{37}+\Phi_{29}+\Phi_{39}+\Phi_{29}$	= 0
38	$20\Phi_{38}-8(\Phi_{37}+\Phi_{34}+\Phi_{39}+\Phi_{34})+2(\Phi_{33}+\Phi_{35}+\Phi_{35}+\Phi_{33})+\Phi_0+\Phi_{30}+\Phi_{40}+\Phi_{30}$	= 0
39	$20\Phi_{39}-8(\Phi_{38}+\Phi_{35}+\Phi_{40}+\Phi_{35})+2(\Phi_{34}+\Phi_{36}+\Phi_{36}+\Phi_{34})+\Phi_{37}+\Phi_{31}+\Phi_{39}+\Phi_{31}$	= 0

and Dirichlet's boundary conditions $\Phi_i = \frac{q l^2}{b}\mu_i$ for points at the top edge, where values μ_i are given in Table 1. Neumann's conditions: $\Phi_i = \Phi_{i-40} + \frac{q l^2}{b}\eta_i$ for the external points at the left edge where the values η_i are given in Table 2.

After rearrangement we obtain system of 44 equations which will be written down in matrix form: $\mathbf{B}\boldsymbol{\Phi} = \frac{q l^2}{b}\mathbf{b}$, where $\boldsymbol{\Phi}$ is the vector of nodal values of the stress function, $\mathbf{b}$ is the right-hand side vector containing non-dimensional values μ_i and η_i.

Matrix $\mathbf{B}$ because of its dimensions will be shown in two pieces - blocks $\mathbf{B}_1$, $\mathbf{B}_2$ located at the diagonal of the matrix $\mathbf{B} = \begin{bmatrix} \mathbf{B}_1 & \mathbf{B}_3 \\ \mathbf{B}_4 & \mathbf{B}_2 \end{bmatrix}$ (Fig. 3.33).

Solution of this system of equation in the shape of the stress function $\Phi(x, y)$ graph over the slab area is shown in Fig. 3.32

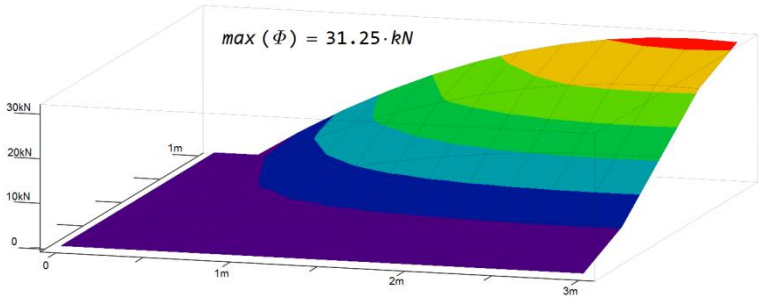

Fig.3.32 Chart of the Airy stress function over the slab surface

$\mathbf{B}_1 =$

	0	1	2	3	4	5	6	7	8	9	10	11	12	13	14	15	16	17	18	19	20	21	22
0	1	0	0	0	0	0	0	0	0	0	0	0	0	0	0	0	0	0	0	0	0	0	0
1	-10	21	-8	1	0	-8	2	0	0	1	0	0	0	0	0	0	0	0	0	0	0	0	0
2	-3	-8	20	-8	1	2	-8	2	0	0	1	0	0	0	0	0	0	0	0	0	0	0	0
3	-4	1	-8	21	-8	0	2	-8	2	0	0	1	0	0	0	0	0	0	0	0	0	0	0
4	0	0	0	0	1	0	0	0	0	0	0	0	0	0	0	0	0	0	0	0	0	0	0
5	-3	-8	2	0	0	21	-8	1	0	-8	2	0	0	1	0	0	0	0	0	0	0	0	0
6	2	2	-8	2	0	-8	20	-8	1	2	-8	2	0	0	1	0	0	0	0	0	0	0	0
7	1	0	2	-8	2	1	-8	21	-8	0	2	-8	2	0	0	1	0	0	0	0	0	0	0
8	0	0	0	0	0	0	0	0	1	0	0	0	0	0	0	0	0	0	0	0	0	0	0
9	-4	1	0	0	0	-8	2	0	0	21	-8	1	0	-8	2	0	0	1	0	0	0	0	0
10	1	0	1	0	0	2	-8	2	0	-8	20	-8	1	2	-8	2	0	0	1	0	0	0	0
11	0	0	0	1	0	0	2	-8	2	1	-8	21	-8	0	2	-8	2	0	0	1	0	0	0
12	0	0	0	0	0	0	0	0	0	0	0	0	1	0	0	0	0	0	0	0	0	0	0
13	-4	0	0	0	0	1	0	0	0	-8	2	0	0	21	-8	1	0	-8	2	0	0	1	0
14	1	0	0	0	0	0	1	0	0	2	-8	2	0	-8	20	-8	1	2	-8	2	0	0	1
15	0	0	0	0	0	0	0	1	0	0	2	-8	2	1	-8	21	-8	0	2	-8	2	0	0
16	0	0	0	0	0	0	0	0	0	0	0	0	0	0	0	0	1	0	0	0	0	0	0
17	-4	0	0	0	0	0	0	0	0	1	0	0	0	-8	2	0	0	21	-8	1	0	-8	2
18	1	0	0	0	0	0	0	0	0	0	1	0	0	2	-8	2	0	-8	20	-8	1	2	-8
19	0	0	0	0	0	0	0	0	0	0	0	1	0	0	2	-8	2	1	-8	21	-8	0	2
20	0	0	0	0	0	0	0	0	0	0	0	0	0	0	0	0	0	0	0	0	1	0	0
21	-4	0	0	0	0	0	0	0	0	0	0	0	0	1	0	0	0	-8	2	0	0	21	-8
22	1	0	0	0	0	0	0	0	0	0	0	0	0	0	1	0	0	2	-8	2	0	-8	20

$\mathbf{B}_2 =$

	23	24	25	26	27	28	29	30	31	32	33	34	35	36	37	38	39	40	41	42	43	44
22	-8	1	2	-8	2	0	0	1	0	0	0	0	0	0	0	0	0	0	0	0	0	0
23	21	-8	0	2	-8	2	0	0	1	0	0	0	0	0	0	0	0	0	0	0	0	0
24	0	1	0	0	0	0	0	0	0	0	0	0	0	0	0	0	0	0	0	0	0	0
25	0	0	21	-8	1	0	-8	2	0	0	1	0	0	0	0	0	0	0	0	0	0	0
26	2	0	-8	20	-8	1	2	-8	2	0	0	1	0	0	0	0	0	0	0	0	0	0
27	-8	2	1	-8	21	-8	0	2	-8	2	0	0	1	0	0	0	0	0	0	0	0	0
28	0	0	0	0	0	1	0	0	0	0	0	0	0	0	0	0	0	0	0	0	0	0
29	0	0	-8	2	0	0	21	-8	1	0	-8	2	0	0	1	0	0	0	0	0	0	0
30	0	0	2	-8	2	0	-8	20	-8	1	2	-8	2	0	0	1	0	0	0	0	0	0
31	1	0	0	2	-8	2	1	-8	21	-8	0	2	-8	2	0	0	1	0	0	0	0	0
32	0	0	0	0	0	0	0	0	0	1	0	0	0	0	0	0	0	0	0	0	0	0
33	0	0	1	0	0	0	-8	2	0	0	22	-8	1	0	-8	2	0	0	0	0	0	0
34	0	0	0	1	0	0	2	-8	2	0	-8	21	-8	1	2	-8	2	0	0	0	0	0
35	0	0	0	0	1	0	0	2	-8	2	1	-8	22	-8	0	2	-8	2	0	0	0	0
36	0	0	0	0	0	0	0	0	0	0	0	0	0	1	0	0	0	0	0	0	0	0
37	0	0	0	0	0	0	2	0	0	0	-16	4	0	0	21	-8	1	0	0	0	0	0
38	0	0	0	0	0	0	0	2	0	0	4	-16	4	0	-8	20	-8	1	0	0	0	0
39	0	0	0	0	0	0	0	0	2	0	0	4	-16	4	1	-8	21	-8	0	0	0	0
40	0	0	0	0	0	0	0	0	0	0	0	0	0	0	0	0	0	1	0	0	0	0
41	0	0	0	0	0	0	0	0	0	0	0	0	0	0	0	0	0	0	1	0	0	0
42	0	0	0	0	0	0	0	0	0	0	0	0	0	0	0	0	0	0	0	1	0	0
43	0	0	0	0	0	0	0	0	0	0	0	0	0	0	0	0	0	0	0	0	1	0
44	0	0	0	0	0	0	0	0	0	0	0	0	0	0	0	0	0	0	0	0	0	1

$\mathbf{b} =$

0	0
1	0
2	0
3	0
4	23.75
5	0
6	0
7	0
8	45
9	0
10	0
11	0
12	63.75
13	0
14	0
15	0
16	80
17	0
18	0
19	0
20	93.75
21	0
22	0
23	0
24	105
25	0
26	0
27	0
28	113.75
29	0
30	0
31	0
32	120
33	0
34	0
35	0
36	123.75
37	0
38	0
39	0
40	125
41	-7.813
42	-25
43	-42.188
44	-50

Fig.3.33 Matrices of the Finite Difference Method equations system

Figure 3.34 shows comparison of stress values in the section at the coordinate ξ=0.45, which are obtained with use of finite difference method and analytical method with use of the stress function as 5th degree polynomial (Eqn.3.32).

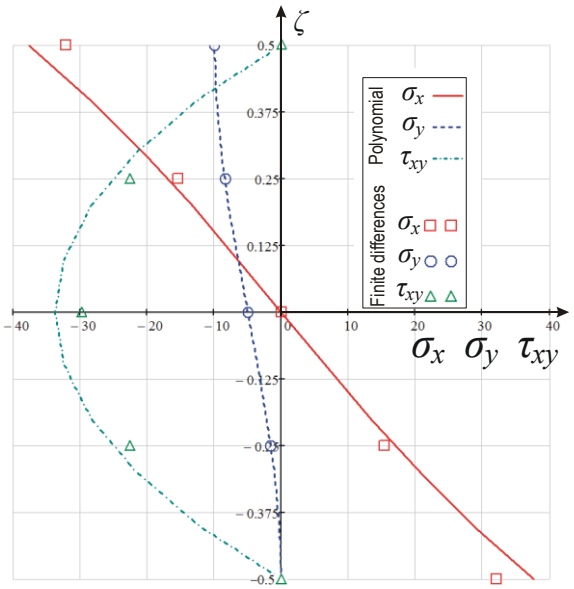

Fig. 3.34 Comparison of stresses in the slab at ξ=0.45, obtained by various methods

4. Theory of Plates

Plates are one of the most commonly used elements in structures. They can be found in almost every building or mechanical structure. The geometric shape of a plate can be defined similarly to a 2D element (Chapter 3), but they differ in the way of loading. Plates are loaded with normal loads to their surfaces which cause bending. Bending is not present in the case of the deformation of the 2D element.

Analytical methods of determining both deflections and internal forces were described by Euler, Bernoulli, Germain, Lagrange, Poisson and especially by Navier in papers which appeared at the end of the 18th century described by Rao (1982). Literature devoted to the theory of plates is unusually rich, the books of Kączkowski (1980), Nowacki (1979), Timoshenko and Woinowsky-Krieger (1962) are recommended to interested readers.

Many important statics and dynamics problems of plates were solved by analytical methods (mainly by the method of the Fourier series), but they are inaccurate both in the case of problems with complex boundary conditions and complicated shapes of plates. However, the finite element method has proved to be universal and although it gives approximate solutions, they are precise enough for practical applications.

4.1. Classifications of Various Plate Theories

- Classical Plate Theory
- Shear deformation included
    - FSDT (First order Shear Deformation Theory)
    - TSDT (Third order Shear Deformation Theory)

Classical Plate Theory:

- Assumptions:
    - All layers in plane state of stress
    - Transverse normal strain ε_3 negligible compared to in-plane normal strains ε_1 and ε_2 (no transverse interaction of layers)
    - Transverse shear strains ε_4 and ε_5 negligible (straight lines normal to the middle surface remain so after deformation – Kirchhoff hypothesis)

$$\psi_1\left(x_1,x_2\right)=-\frac{\partial w}{\partial x_1} \qquad \psi_2\left(x_1,x_2\right)=-\frac{\partial w}{\partial x_2}$$

- Displacements:

$$u_1\left(x_1,x_2,x_3\right)=u\left(x_1,x_2\right)-x_3\frac{\partial w\left(x_1,x_2\right)}{\partial x_1}$$

$$u_2\left(x_1,x_2,x_3\right)=v\left(x_1,x_2\right)-x_3\frac{\partial w\left(x_1,x_2\right)}{\partial x_2}$$

$$u_3\left(x_1,x_2,x_3\right)=w\left(x_1,x_2\right)$$

- Strain:

$$\varepsilon_1=\frac{\partial u}{\partial x_1}-x_3\frac{\partial^2 w}{\partial x_1^2} \qquad \varepsilon_2=\frac{\partial v}{\partial x_2}-x_3\frac{\partial^2 w}{\partial x_2^2} \qquad \varepsilon_3=\varepsilon_4=\varepsilon_5=0$$

$$\varepsilon_6=\frac{\partial u}{\partial x_2}+\frac{\partial v}{\partial x_1}-2x_3\frac{\partial^2 w}{\partial x_1\partial x_2} \qquad \varepsilon_i\left(x_1,x_2,x_3\right)=\epsilon_i\left(x_1,x_2\right)+x_3\kappa_i \qquad i=1,2,6$$

$$\epsilon_1=\frac{\partial u}{\partial x_1} \qquad \epsilon_2=\frac{\partial v}{\partial x_2} \qquad \epsilon_6=\frac{\partial u}{\partial x_2}+\frac{\partial v}{\partial x_1}$$

$$\kappa_1 = -\frac{\partial^2 w}{\partial x_1^2} \qquad \kappa_2 = -\frac{\partial^2 w}{\partial x_2^2} \qquad \kappa_6 = -2\frac{\partial^2 w}{\partial x_1 \partial x_2}$$

Shear deformation should be taken into account for moderately thick plates.

- Reissner-Mindlin theory:
  - Relaxation of the Kirchhoff's plate theory assumptions: Transverse normals before deformation are no longer perpendicular to the middle surface after deformation – translation + rotation.

First order shear deformation theory:

$$u_1(x_1, x_2, x_3) = u(x_1, x_2) + x_3 \psi_1(x_1, x_2)$$

$$u_2(x_1, x_2, x_3) = v(x_1, x_2) + x_3 \psi_2(x_1, x_2)$$

$$u_3(x_1, x_2, x_3) = w(x_1, x_2)$$

Higher order theories (TSDT):

$$u_1(x_1, x_2, x_3) = u(x_1, x_2) + x_3 \psi_1(x_1, x_2) - c_1 x_3^3 \left(\psi_1 + \frac{\partial w}{\partial x_1} \right)$$

$$u_2(x_1, x_2, x_3) = v(x_1, x_2) + x_3 \psi_2(x_1, x_2) - c_1 x_3^3 \left(\psi_2 + \frac{\partial w}{\partial x_1} \right)$$

$$u_3(x_1, x_2, x_3) = w(x_1, x_2)$$

Theories of higher orders than 3 are not used. Too much computational effort, to small gain in precision of results.

4.2. Basic assumptions and equations of the classical plate theory

We accept the following assumptions of the classic theory of thin plates (Timoshenko and Woinowsky-Krieger (1962)):

a) thickness of a plate is small in comparison with its other dimensions;
b) deflections of plates are small in comparison with its thickness;
c) middle plane does not undergo lengthening (or shortening);

d) points lying on the lines which are perpendicular to the middle plane before its deformation lie on these lines after the deformation;
e) components of stress which are perpendicular to the plane of the plate can be neglected.

From point d) of the above assumptions it follows that the displacement of points lying within the plate varies linearly with its thickness (Fig. 4.3):

$$u_x = -z\frac{\partial w}{\partial x}, \quad u_y = -z\frac{\partial w}{\partial y}, \quad u_z = w(x,y). \tag{4.13}$$

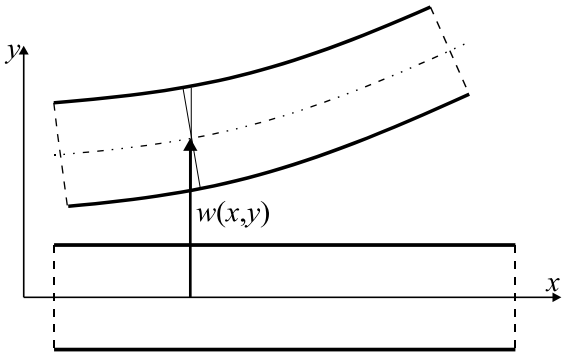

Fig. 4.3. The plate segment deformation scheme.

Thus stains are expressed by the relations:

$$\varepsilon_x = \frac{\partial u_x}{\partial x} = -z\frac{\partial^2 w}{\partial x^2}, \quad \varepsilon_y = \frac{\partial u_y}{\partial y} = -z\frac{\partial^2 w}{\partial y^2}, \quad \gamma_{xy} = \frac{\partial u_x}{\partial y} + \frac{\partial u_y}{\partial x} = -2z\frac{\partial^2 w}{\partial x \partial y}. \tag{4.14}$$

The strain vector can be presented in the form:

$$\boldsymbol{\varepsilon} = -z\,\boldsymbol{\partial} w(x,y), \tag{4.15}$$

where vector $\boldsymbol{\partial}$ is the vector of differential operators:

$$\boldsymbol{\partial} = \begin{bmatrix} \partial_{xx} \\ \partial_{yy} \\ 2\partial_{xy} \end{bmatrix}, \; \partial_{xx} = \frac{\partial^2}{\partial x^2}, \; \partial_{yy} = \frac{\partial^2}{\partial y^2}, \; \partial_{xy} = \frac{\partial^2}{\partial x \partial y}.$$

Let us assume that there is a plane stress condition in the plate, so the stress vector can be determined as follows:

$$\boldsymbol{\sigma} = \mathbf{D} \cdot \boldsymbol{\varepsilon} = -z\,\mathbf{D}\,\boldsymbol{\partial} w(x,y), \tag{4.16}$$

where $\mathbf{D}$ is the matrix of material constants determined for plane stress (Eqn. (13)).

Now we introduce in the expression of internal forces (moments and shearing forces – Figure 4)

$$M_x = \int_{-h/2}^{h/2} \sigma_x z dz, \quad M_y = \int_{-h/2}^{h/2} \sigma_y z dz, \quad M_{xy} = \int_{-h/2}^{h/2} \tau_{xy} z dz,$$
$$Q_x = \int_{-h/2}^{h/2} \tau_{xz} dz, \quad Q_y = \int_{-h/2}^{h/2} \tau_{yz} dz. \tag{4.17}$$

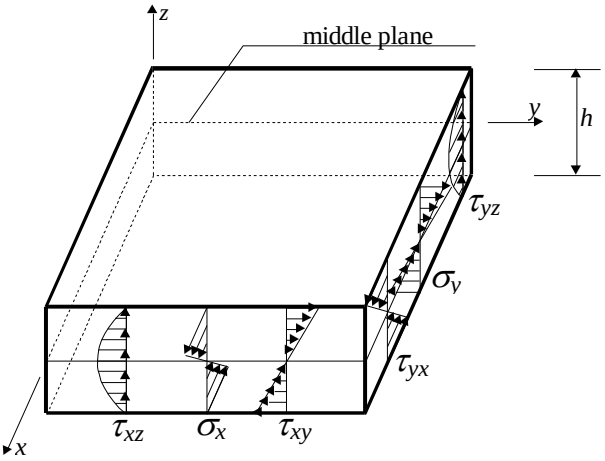

a) stresses

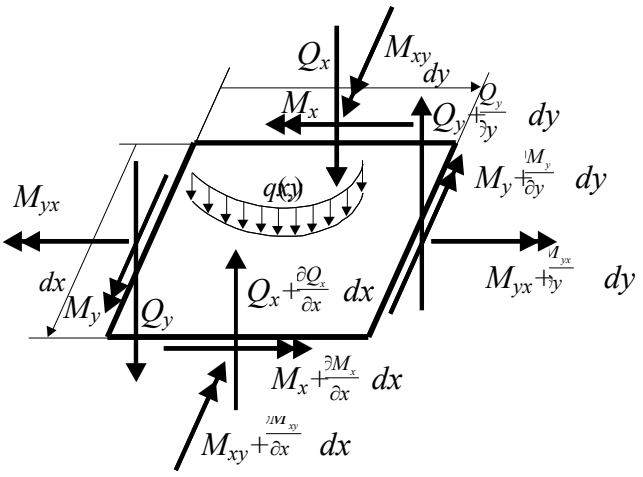

b) internal forces

Figure 4. The distribution of stresses, external loads and internal forces in the plate element.

The equilibrium of an infinitesimal plate element shown in Figure 4b leads to the set of equations:

$$\frac{\partial Q_x}{\partial x} + \frac{\partial Q_y}{\partial y} + q(x,y) = 0, \tag{4.18}$$

$$\frac{\partial M_x}{\partial x}+\frac{\partial M_{xy}}{\partial y}=Q_x \,,$$

$$\frac{\partial M_{xy}}{\partial x}+\frac{\partial M_y}{\partial y}=Q_y \,.$$

After integration Eqn. (4.17) taking into consideration Eqn. (4.16), we obtain

$$\begin{aligned} M_x &= -D\left(\frac{\partial^2 w}{\partial x^2}+\nu\frac{\partial^2 w}{\partial y^2}\right), \\ M_y &= -D\left(\frac{\partial^2 w}{\partial y^2}+\nu\frac{\partial^2 w}{\partial x^2}\right), \\ M_{xy} &= -D(1-\nu)\frac{\partial^2 w}{\partial x \partial y}, \end{aligned} \tag{4.19}$$

where D denotes the plate stiffness defined by the equation

$$D=\frac{Eh^3}{12\left(1-\nu^2\right)} \,. \tag{4.20}$$

From the last two Eqn. (4.18), we obtain relations for the shearing forces:

$$\begin{aligned} Q_x &= -D\left(\frac{\partial^3 w}{\partial x^3}+\frac{\partial^3 w}{\partial x \partial y^2}\right), \\ Q_y &= -D\left(\frac{\partial^3 w}{\partial x^2 \partial y}+\frac{\partial^3 w}{\partial y^3}\right). \end{aligned} \tag{4.21}$$

Inserting the above equation describing shearing forces into the first Eqn. (4.18) we obtain

$$\frac{\partial^4 w}{\partial x^4}+2\frac{\partial^4 w}{\partial x^2 \partial y^2}+\frac{\partial^4 w}{\partial y^4}=\frac{q(x,y)}{D} \,. \tag{4.22}$$

It is a biharmonic partial differential equation which should be satisfied by the function of deflection $w(x,y)$ within the plate. The following boundary conditions should be realised at the edges of the plate:

a) $w = 0$, $\frac{\partial w}{\partial n}=0$ – on the fixed edge,

b) $w = 0$, $\frac{\partial^2 w}{\partial n^2} = 0$ – on the free supported edge,

c) $M_n = 0$, $V_n = 0$ – on the free edge.

In the above equations n defines the direction of the line which is perpendicular to the edge and V_n is the reduced force introduced by Kirchhoff in 1850, described by Timoshenko and Woinowsky-Krieger (1962). This force joins the influence of the torsion moment M_{ns} and the shearing force Q_n on the free edge Figure 4b:

$$V_n = Q_n - \frac{\partial M_{ns}}{\partial s} = -D\left[\frac{\partial^3 w}{\partial n^3} + (2-\nu)\frac{\partial^3 w}{\partial n \partial s^2}\right] \tag{4.23}$$

where n describes the direction of the line which is perpendicular to the edge and s is the direction of the line which is parallel to the edge of the plate.

The modification of the boundary conditions is necessary here because the fourth order Eqn. (4.22) cannot be solved for three boundary conditions coming from the requirement of zero stress on the free edge: $M_{ns} = 0$, $M_n = 0$, $Q_n = 0$.

5. Analytical methods

There are many analytical methods.

5.1. Thin Plates

Only selected cases of plates with particular shapes and loading can be solved analytically. In other cases, iterative solution in the shape of infinite series can be found. These iterative methods are:

- Plate strip;
- Double Fourier series expansion;
- Single Fourier series expansion.

5.1.1. Plate strip

Cylindrical bending applies only in the following conditions:

- a/b<<1,
- long opposite edges support conditions independent of x_2.

5.1.2. Navier solution

Double Fourier series expansion is called Navier solution and can be obtained in case of rectangular, simply supported plates.

The load of the rectangular plate of the dimensions *a* x *b*, perpendicular to the plate surface, can be expressed as double Fourier series, with use of the following formula:

$$p_3\left(x_1, x_2\right) = \sum_{r=1}^{\infty}\sum_{s=1}^{\infty} p_{rs} \sin \alpha_r x_1 \sin \beta_s x_2 \tag{19}$$

where the coefficients can be calculated as:

$$\alpha_r = \frac{r\pi}{a} \quad \beta_s = \frac{s\pi}{b} \qquad r, s = 1, 2, 3, \ldots$$

After integration at the whole surface of the plate, the coefficients for the series expansion can be expressed as follows:

$$p_{rs} = \frac{4}{ab}\int_0^b \int_0^a p_3\left(x_1, x_2\right) \sin \alpha_r x_1 \sin \beta_s x_2 dx_1 dx_2 \tag{20}$$

In the case of the uniform plate $p_3\left(x_1, x_2\right) = p = const$, the following simplification can be obtained:

$$p_{rs} = \frac{16p}{\pi^2 rs} \qquad r, s = 1, 3, 5, \ldots. \tag{21}$$

Assuming the function of the plate deflection as the double series expansion:

$$w\left(x_1, x_2\right) = \sum_{r=1}^{\infty}\sum_{s=1}^{\infty} w_{rs} \sin \alpha_r x_1 \sin \beta_s x_2 \tag{22}$$

and substitution into the differential equation of the plate (10), we obtain the following equation:

$$D\sum_{r=1}^{\infty}\sum_{s=1}^{\infty}\left(\alpha_r{}^2 + \beta_s{}^2\right)^2 w_{rs} \sin \alpha_r x_1 \sin \beta_s x_2 = \sum_{r=1}^{\infty}\sum_{s=1}^{\infty} q_{rs} \sin \alpha_r x_1 \sin \beta_s x_2 \tag{23}$$

To make the equation fulfilled for each coefficient x_1 and x_2, we finally get the relation:

$$w_{rs} = \frac{q_{rs}}{\Delta} \tag{24}$$

where:

$$\Delta = D\left(\alpha_r{}^2 + \beta_s{}^2\right)^2$$

Knowing the deflected surface (22), on the basis of equations (4.19) and (4.21), we can find formulae for calculation of internal forces:

$$M_x = D\sum_{r=1}^{\infty}\sum_{s=1}^{\infty}\left(\alpha_r{}^2 + \nu\beta_s{}^2\right) w_{rs} \sin\alpha_r x_1 \sin\beta_s x_2 \tag{25}$$

$$M_y = D\sum_{r=1}^{\infty}\sum_{s=1}^{\infty}\left(\nu\alpha_r{}^2 + \beta_s{}^2\right) w_{rs} \sin\alpha_r x_1 \sin\beta_s x_2 \tag{26}$$

$$M_{xy} = -D(1-\nu)\sum_{r=1}^{\infty}\sum_{s=1}^{\infty}\alpha_r\beta_s w_{rs} \cos\alpha_r x_1 \cos\beta_s x_2 \tag{27}$$

$$Q_x = D\sum_{r=1}^{\infty}\sum_{s=1}^{\infty}\alpha_r\left(\alpha_r{}^2 + \beta_s{}^2\right) w_{rs} \cos\alpha_r x_1 \sin\beta_s x_2 \tag{28}$$

$$Q_y = D\sum_{r=1}^{\infty}\sum_{s=1}^{\infty}\beta_s\left(\alpha_r{}^2 + \beta_s{}^2\right) w_{rs} \sin\alpha_r x_1 \cos\beta_s x_2 \tag{29}$$

5.1.1. Nádai-Lévy solution

Single series expansion is called Nádai-Lévy solution and can be used in case of rectangular plates with simply supported long edges and arbitrary other boundary conditions.

The following assumptions are used in this method:

- The load is changing only along the x axis;
- Both sides of the plate (x=0 and x=L_x) are simply supported.

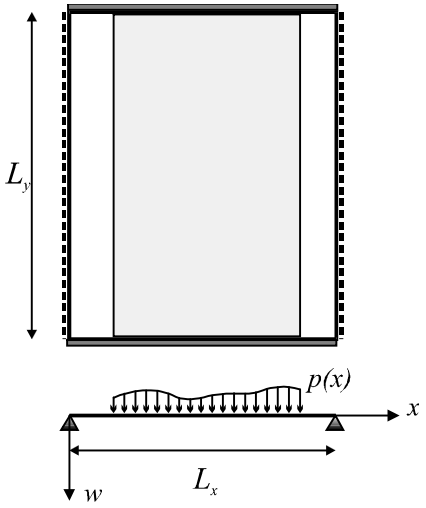

Figure 5. The plate load scheme.

These assumptions allow 6 essentially different schemes of plate support which have been shown in Figure 6.

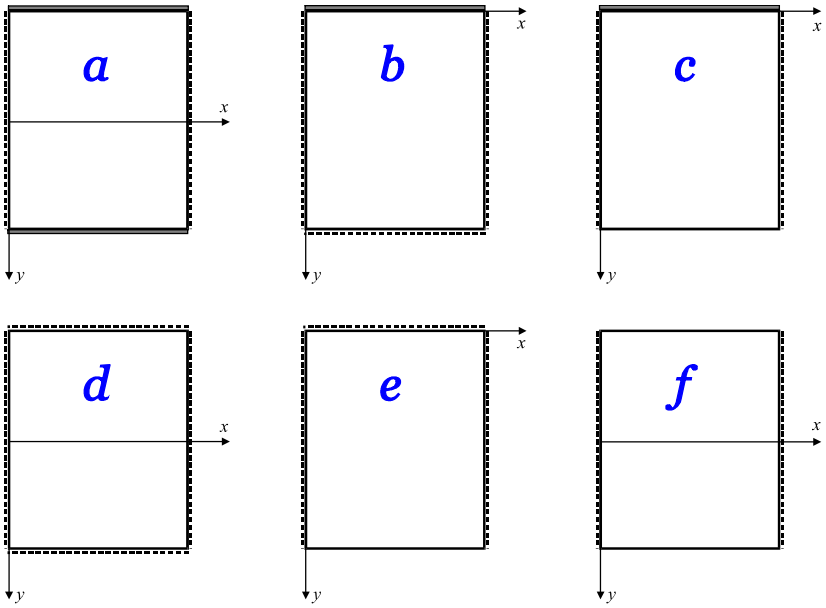

Figure 6. The plate support schemes.

5.1.1.1. Equation of the deflected plate

The plate deflection can be described with use of the following equation:

$$w(x,y) = w_1(x,y) + w_2(x) \tag{30}$$

After substitution of this equation to the equilibrium equation of the plate, we obtain:

$$\nabla^4 \left[w_1(x,y) + w_2(x) \right] = \frac{p(x)}{D} \tag{31}$$

which allows writing this equation in the following form:

$$\nabla^4 w_1(x,y) = 0 \tag{32}$$

$$\frac{\mathrm{d}^4 w_2(x)}{\mathrm{d}x^4} = \frac{p(x)}{D} \tag{33}$$

Seeking the solution of the equation (33) as a series:

$$w_2(x) = \sum_{i=1}^{\infty} E_i \sin \alpha_i x \tag{34}$$

we expand the load into sine series:

$$p(x)=\sum_{i=1}^{\infty} p_i \sin \alpha_i x \tag{35}$$

where $p_i=\frac{2}{L_x}\int_0^{L_x} p(x)\sin\alpha_i x\,\mathrm{d}x$, $\alpha_i=\frac{i\pi}{L_x}$.

After substitution to the equation (33) we obtain:

$$\sum_{i=1}^{\infty}\alpha_i^{\,4}E_i \sin\alpha_i x=\frac{1}{D}\sum_{i=1}^{\infty} p_i \sin\alpha_i x \tag{36}$$

and consequently:

$$E_i=\frac{p_i}{D\alpha_i^{\,4}} \tag{37}$$

Solution of the equation (32) is also sought as a sine series:

$$w_1(x)=\sum_{i=1}^{\infty} f_i(y)\sin\alpha_i x \tag{38}$$

which after substitution into equation (32) gives the condition describing the function $f_i(y)$:

$$\frac{\mathrm{d}^4 f_i}{\mathrm{d}y^4}-2\alpha_i^{\,2}\frac{\mathrm{d}^2 f_i}{\mathrm{d}y^2}+\alpha_i^{\,4} f_i=0 \tag{39}$$

Solution of the linear differential equation (32) can be put down in the following form:

$$f_i(y)=A_i \operatorname{sh}\alpha_i y+B_i \operatorname{ch}\alpha_i y+C_i\alpha_i y \operatorname{sh}\alpha_i y+D_i\alpha_i y \operatorname{ch}\alpha_i y, \tag{40}$$

$$\operatorname{sh}\alpha_i y=\sinh\alpha_i y,\ \operatorname{ch}\alpha_i y=\cosh\alpha_i y.$$

where the constants A_i, B_i, C_i, D_i should be taken to fulfil all boundary conditions for both edges y = const.

The following derivatives of the function $f(y)$ will be commonly used in the following considerations:

$$f_i'(y)=\alpha_i[A_i \operatorname{ch}\alpha_i y+B_i \operatorname{sh}\alpha_i y+C_i(\operatorname{sh}\alpha_i y+\alpha_i y \operatorname{ch}\alpha_i y)+D_i(\operatorname{ch}\alpha_i y+\alpha_i y \operatorname{sh}\alpha_i y)], \tag{41}$$

$$f_i''(y)=\alpha_i^{\,2}[A_i \operatorname{sh}\alpha_i y+B_i \operatorname{ch}\alpha_i y+C_i(2\operatorname{ch}\alpha_i y+\alpha_i y \operatorname{sh}\alpha_i y)+D_i(2\operatorname{sh}\alpha_i y+\alpha_i y \operatorname{ch}\alpha_i y)], \tag{42}$$

$$f_i'''(y)=\alpha_i^{\,3}[A_i \operatorname{ch}\alpha_i y+B_i \operatorname{sh}\alpha_i y+C_i(3\operatorname{sh}\alpha_i y+\alpha_i y \operatorname{ch}\alpha_i y)+D_i(3\operatorname{ch}\alpha_i y+\alpha_i y \operatorname{sh}\alpha_i y)], \tag{43}$$

where:

$$f' = \frac{df}{dy}, \quad f'' = \frac{d^2 f}{dy^2}, \quad f''' = \frac{d^3 f}{dy^3}.$$

5.1.1.2. Exemplary solutions with use of Nádai-Lévy method

5.1.1.2.1. Two opposite edges fixed and other two simply supported

The following boundary conditions are in force for both edges fixed:

$y = \pm\frac{1}{2} L_y$:

$$w = 0, \varphi_x = \frac{\partial w}{\partial y} = 0, \tag{44}$$

Symmetry of the deflected surface about the x axis results in disappearing of the terms with non-symmetrical functions from the equation (40), i.e. $A_i = 0$ and $D_i = 0$. Equation (40) after substitution of boundary conditions (44) obtains the following form:

$$f_i(y) = B_i \operatorname{ch} \alpha_i y + C_i \alpha_i y \operatorname{sh} \alpha_i y, \tag{45}$$

The equation of the deflected plate (30) can be simplified then:

$$w(x,y) = w_1(x,y) + w_2(x) = \sum_{i=1}^{\infty} \left(B_i \operatorname{ch} \alpha_i y + C_i \alpha_i y \operatorname{sh} \alpha_i y + E_i \right) \sin \alpha_i x \tag{46}$$

Substitution of the boundary conditions results in:

$$\sum_{i=1}^{\infty} \left(B_i \operatorname{ch} \lambda_i + C_i \lambda_i \operatorname{sh} \lambda_i + E_i \right) \sin \alpha_i x = 0 \tag{47}$$

$$\sum_{i=1}^{\infty} \alpha_i \left[B_i \operatorname{sh} \lambda_i + C_i \left(\operatorname{sh} \lambda_i + \lambda_i \operatorname{ch} \lambda_i \right) \right] \sin \alpha_i x = 0 \tag{48}$$

where: $\lambda_i = \frac{\alpha_i L_y}{2} = \frac{i \pi L_y}{2 L_x}$.

To make this system of equations be in force for each x, the following conditions should be fulfilled:

$$B_i \operatorname{ch} \lambda_i + C_i \lambda_i \operatorname{sh} \lambda_i + E_i = 0 \tag{49}$$

$$B_i \operatorname{sh} \lambda_i + C_i \left(\operatorname{sh} \lambda_i + \lambda_i \operatorname{ch} \lambda_i \right) = 0 \tag{50}$$

After solution of system of equations (49) and (50) we obtain:

$$C_i = \frac{E_i}{\operatorname{ch}\lambda_i + \dfrac{\lambda_i}{\operatorname{sh}\lambda_i}} \tag{51}$$

$$B_i = -C_i\left(1+\lambda_i \operatorname{ch}\lambda_i\right) \tag{52}$$

Eventually, by using equations (37), (51) and (52) all constants can be found, and finally we can calculate the plate deflection with use of the equation (46).

5.1.1.2.2. One edge fixed and all other simply supported

The following boundary conditions are in force for the edges at y=const:

$y = 0$:

$$w(x,0) = 0, \tag{53}$$

$$\varphi_x(x,0) = \left.\frac{\partial w}{\partial y}\right|_{y=0} = 0, \tag{54}$$

$y = L_y$:

$$w(x,L_y) = 0, \tag{55}$$

$$M_y(x,L_y) = D\left(\frac{\partial^2 w}{\partial y^2} + \nu\frac{\partial^2 w}{\partial x^2}\right)_{y=L_y} = 0, \tag{56}$$

Condition (56) after introduction of (55) can be reduced to the following equation:

$$\left.\frac{\partial^2 w}{\partial y^2}\right|_{y=L_y} = 0. \tag{57}$$

The deflected surface is non-symmetrical, so the equation of the deflected plate (30) obtains the following form:

$$w(x,y) = \sum_{i=1}^{\infty}\left(A_i \operatorname{sh}\alpha_i y + B_i \operatorname{ch}\alpha_i y + C_i\alpha_i y \operatorname{sh}\alpha_i y + D_i\alpha_i y \operatorname{ch}\alpha_i y + E_i\right)\sin\alpha_i x. \tag{58}$$

Introduction of the conditions (53) and (54) gives equations:

$$B_i + E_i = 0, \tag{59}$$

$$A_i + D_i = 0. \tag{60}$$

Conditions (55) and (57) give equations:

$$A_i \operatorname{sh}\lambda_i + B_i \operatorname{ch}\lambda_i + C_i\lambda_i \operatorname{sh}\lambda_i + D_i\lambda_i \operatorname{ch}\lambda_i + E_i = 0, \tag{61}$$

$$A_i \operatorname{sh}\lambda_i + B_i \operatorname{ch}\lambda_i + C_i\left(2\operatorname{ch}\lambda_i + \lambda_i \operatorname{sh}\lambda_i\right) + D_i\left(2\operatorname{sh}\lambda_i + \lambda_i \operatorname{ch}\lambda_i\right) = 0, \tag{62}$$

where $\lambda_i = \alpha_i L_y = \dfrac{i\pi L_y}{L_x}$.

System of equations (59)÷(62) has got the solution:

$$A_i = -E_i \frac{1 + \frac{1}{2}\lambda_i \operatorname{th}\lambda_i - \operatorname{ch}\lambda_i}{\operatorname{sh}\lambda_i[1 - \lambda_i(\operatorname{cth}\lambda_i - \operatorname{th}\lambda_i)]},\ C_i = A_i \operatorname{th}\lambda_i + \frac{E_i}{2\operatorname{ch}\lambda_i},$$

$$B_i = -E_i,\ D_i = -A_i \tag{63}$$

where E_i is described by equation (37) and $\operatorname{th}\lambda_i = \tanh\lambda_i$, $\operatorname{cth}\lambda_i = \coth\lambda_i$.

Substitution of the calculated constants into equation (58) leads us to the calculation of the deflected surface.

5.1.1.2.3. One edge fixed, opposite one – free, and two other simply supported

The following boundary conditions are in force for the edges parallel to the *x* axis:

$y = 0$:

$$w(x,0) = 0, \tag{64}$$

$$\varphi_x(x,0) = \left.\frac{\partial w}{\partial y}\right|_{y=0} = 0, \tag{65}$$

$y = L_y$:

$$M_y(x,L_y) = D\left(\frac{\partial^2 w}{\partial y^2} + \nu\frac{\partial^2 w}{\partial x^2}\right)_{y=L_y} = 0, \tag{66}$$

$$V_y(x,L_y) = -D\left[\frac{\partial^3 w}{\partial y^3} + (2-\nu)\frac{\partial^3 w}{\partial y \partial x^2}\right]_{y=L_y} = 0, \tag{67}$$

As in the previous example, the deflected surface is non-symmetrical, so the equation of the deflected plate (30) obtains the following form:

$$w(x,y) = \sum_{i=1}^{\infty}\left(A_i \operatorname{sh}\alpha_i y + B_i \operatorname{ch}\alpha_i y + C_i\alpha_i y \operatorname{sh}\alpha_i y + D_i\alpha_i y \operatorname{ch}\alpha_i y + E_i\right)\sin\alpha_i x. \tag{68}$$

Introduction of the conditions (64) and (65) gives equations:

$$B_i + E_i = 0, \tag{69}$$

$$A_i + D_i = 0. \tag{70}$$

Condition (66) after taking into account (69) and (70) reduces to the following form:

$$-A_i\left[\frac{1+\nu}{1-\nu}\operatorname{th}\lambda_i + \lambda_i\right] + C_i\left[\lambda_i \operatorname{th}\lambda_i + \frac{2}{1-\nu}\right] = E_i\left[1 + \frac{\nu}{(1-\nu)\operatorname{ch}\lambda_i}\right], \tag{71}$$

and condition (67) after introduction of (69) and (70) gives equation:

$$A_i\left[\frac{2}{1-\nu}\operatorname{cth}\lambda_i - \lambda_i\right] - C_i\left[\frac{1+\nu}{1-\nu} - \lambda_i \operatorname{cth}\lambda_i\right] = E_i, \tag{72}$$

where $\lambda_i = \alpha_i L_y = \dfrac{i\pi L_y}{L_x}$.

If we write down the system of equations (71) and (72) in the matrix form:

$$\begin{bmatrix} g_{1i} & g_{2i} \\ g_{3i} & g_{4i} \end{bmatrix}\begin{bmatrix} A_i \\ C_i \end{bmatrix} = E_i \begin{bmatrix} h_{1i} \\ h_{2i} \end{bmatrix}, \tag{73}$$

where $g_{1i} = -\dfrac{1+\nu}{1-\nu}\operatorname{th}\lambda_i - \lambda_i$, $g_{2i} = \lambda_i \operatorname{th}\lambda_i + \dfrac{2}{1-\nu}$,

$$g_{3i} = \frac{2}{1-\nu}\operatorname{cth}\lambda_i - \lambda_i, \qquad g_{4i} = -\frac{1+\nu}{1-\nu} + \lambda_i \operatorname{cth}\lambda_i,$$

$$h_{1i} = 1 + \frac{\nu}{(1-\nu)\operatorname{ch}\lambda_i}, \qquad h_{2i} = 1,$$

then we obtain the solution in the form:

$$A_i = E_i \frac{h_{1i}g_{4i} - h_{2i}g_{2i}}{G_i},\ C_i = E_i \frac{h_{2i}g_{1i} - h_{1i}g_{3i}}{G_i},\ B_i = -E_i,\ D_i = -A_i, \tag{74}$$

where $G_i = g_{1i}g_{4i} - g_{2i}g_{3i}$.

5.1.1.2.4. All edges simply supported

The following boundary conditions are in force for both edges *y* = const:

$y = \pm\frac{1}{2}L_y$:

$$w(x, \tfrac{1}{2}L_y) = 0, \tag{75}$$

$$M_y(x, \tfrac{1}{2}L_y) = D\left(\frac{\partial^2 w}{\partial y^2} + \nu\frac{\partial^2 w}{\partial x^2}\right)_{y=\frac{1}{2}L_y} = 0, \tag{76}$$

As in the first example (5.1.1.2.1), symmetry of the deflected surface about the *x* axis results in disappearing of the terms with non-symmetrical functions from the equation (40), i.e. $A_i = 0$ and $D_i = 0$.

So the equation (40) after substitution of boundary conditions (75) and (76) obtains the following form:

$$f_i(y) = B_i \operatorname{ch}\alpha_i y + C_i \alpha_i y \operatorname{sh}\alpha_i y, \tag{77}$$

The equation of the deflected plate (30) can be simplified then:

$$w(x, y) = w_1(x, y) + w_2(x) = \sum_{i=1}^{\infty}\left(B_i \operatorname{ch}\alpha_i y + C_i \alpha_i y \operatorname{sh}\alpha_i y + E_i\right)\sin\alpha_i x \tag{78}$$

The second of boundary conditions (76) after taking (75) into account is reduced to:

$$\frac{\partial^2 w}{\partial y^2} = \sum_{i=1}^{\infty} f_i'' \sin\alpha_i x = 0 \tag{79}$$

After introduction of the boundary conditions, we have:

$$\sum_{i=1}^{\infty}\left(B_i \operatorname{ch}\lambda_i + C_i \lambda_i \operatorname{sh}\lambda_i + E_i\right)\sin\alpha_i x = 0 \tag{80}$$

$$\sum_{i=1}^{\infty}\alpha_i^2\left[B_i \operatorname{ch}\lambda_i + C_i\left(2\operatorname{ch}\lambda_i + \lambda_i \operatorname{sh}\lambda_i\right)\right]\sin\alpha_i x = 0 \tag{81}$$

where $\lambda_i = \dfrac{\alpha_i L_y}{2} = \dfrac{i\pi L_y}{2L_x}$.

To make the system of equations (80) and (81) be in force for each *x*, the following conditions should be fulfilled:

$$B_i \operatorname{ch}\lambda_i + C_i \lambda_i \operatorname{sh}\lambda_i + E_i = 0 \tag{82}$$

$$B_i \operatorname{ch}\lambda_i + C_i\left(2\operatorname{ch}\lambda_i + \lambda_i \operatorname{sh}\lambda_i\right) = 0 \tag{83}$$

After solution of system of equations (82) and (83) we have:

$$C_i = \frac{E_i}{2\,\mathrm{ch}\,\lambda_i}, \tag{84}$$

$$B_i = -C_i\left(2 + \lambda_i\,\mathrm{th}\,\lambda_i\right). \tag{85}$$

5.1.1.2.5. Three edges simply supported, the remaining edge free

The following boundary conditions are in force for the edges parallel to the *x* axis:

$y = 0$:

$$w(x,0) = 0, \tag{86}$$

$$M_y(x,0) = D\left(\frac{\partial^2 w}{\partial y^2} + \nu\frac{\partial^2 w}{\partial x^2}\right)_{y=0} = 0, \tag{87}$$

$y = L_y$:

$$M_y(x,L_y) = D\left(\frac{\partial^2 w}{\partial y^2} + \nu\frac{\partial^2 w}{\partial x^2}\right)_{y=L_y} = 0, \tag{88}$$

$$V_y(x,L_y) = -D\left[\frac{\partial^3 w}{\partial y^3} + (2-\nu)\frac{\partial^3 w}{\partial y \partial x^2}\right]_{y=L_y} = 0, \tag{89}$$

Equations (86) and (87) may be reduced into much simpler form:

$$B_i + E_i = 0, \tag{90}$$

$$B_i + 2C_i = 0, \tag{91}$$

which allows easy calculation of constant values: $B_i = -E_i$, $C_i = \frac{1}{2}E_i$.

Equations (88) and (89) may be presented as:

$$A_i + D_i\left[\frac{2}{1-\nu} + \frac{\lambda_i}{\mathrm{th}\,\lambda_i}\right] = E_i\left[\frac{\nu}{1-\nu}\left(\frac{1}{\mathrm{sh}\,\lambda_i} - \frac{1}{\mathrm{th}\,\lambda_i}\right) - \frac{\lambda_i}{2}\right], \tag{92}$$

$$A_i + D_i\left[\lambda_i\,\mathrm{th}\,\lambda_i - \frac{1+\nu}{1-\nu}\right] = \frac{E_i}{2}\left[\frac{3-\nu}{1-\nu}\mathrm{th}\,\lambda_i - \lambda_i\right], \tag{93}$$

where $\lambda_i = \alpha_i L_y = \frac{i\pi L_y}{L_x}$.

In the similar manner as in the example (5.1.1.2.3), it will be more convenient to write down this system of equations in matrix form:

$$\begin{bmatrix} 1 & g_{1i} \\ 1 & g_{2i} \end{bmatrix} \begin{bmatrix} A_i \\ D_i \end{bmatrix} = E_i \begin{bmatrix} h_{1i} \\ h_{2i} \end{bmatrix}, \tag{94}$$

where $g_{1i} = \dfrac{2}{1-\nu} + \dfrac{\lambda_i}{\operatorname{th}\lambda_i}$, $\quad h_{1i} = \dfrac{\nu}{1-\nu}\left(\dfrac{1}{\operatorname{sh}\lambda_i} - \dfrac{1}{\operatorname{th}\lambda_i}\right) - \dfrac{\lambda_i}{2}$,

$$g_{2i} = \lambda_i \operatorname{th}\lambda_i - \frac{1+\nu}{1-\nu}, \quad h_{2i} = \frac{1}{2}\left[\frac{3-\nu}{1-\nu}\operatorname{th}\lambda_i - \lambda_i\right].$$

Finally, we obtain solution of (94) in the following form:

$$A_i = E_i \frac{h_{1i}g_{2i} - h_{2i}g_{1i}}{g_{2i} - g_{1i}}, \; D_i = E_i \frac{h_{2i} - h_{1i}}{g_{2i} - g_{1i}}. \tag{95}$$

5.1.1.2.6. Two opposite edges simply supported, other two free

The following boundary conditions are in force for both edges y = const:

$y = \pm\frac{1}{2}L_y$:

$$M_y(x, \tfrac{1}{2}L_y) = D\left(\frac{\partial^2 w}{\partial y^2} + \nu\frac{\partial^2 w}{\partial x^2}\right)_{y=\frac{1}{2}L_y} = 0, \tag{96}$$

$$V_y(x, \tfrac{1}{2}L_y) = -D\left[\frac{\partial^3 w}{\partial y^3} + (2-\nu)\frac{\partial^3 w}{\partial y \partial x^2}\right]_{y=\frac{1}{2}L_y} = 0, \tag{97}$$

As in examples (5.1.1.2.1) and (5.1.1.2.4), symmetry of the deflected surface about the x axis results in disappearing of the terms with non-symmetrical functions from the equation (40), i.e. $A_i = 0$ and $D_i = 0$.

Boundary conditions (96) and (97) in this case obtain the following form:

$$B_i + C_i\left[\frac{2}{1-\nu} + \lambda_i \operatorname{th}\lambda_i\right] = \frac{\nu}{(1-\nu)\operatorname{ch}\lambda_i}E_i, \tag{98}$$

$$B_i + C_i\left[\lambda_i \operatorname{cth}\lambda_i - \frac{1+\nu}{1-\nu}\right] = 0, \tag{99}$$

where $\lambda_i = \dfrac{\alpha_i L_y}{2} = \dfrac{i\pi L_y}{2L_x}$.

As in example (5.1.1.2.5), it will be more convenient to write down this system of equations in matrix form:

$$\begin{bmatrix} 1 & g_{1i} \\ 1 & g_{2i} \end{bmatrix} \begin{bmatrix} B_i \\ C_i \end{bmatrix} = E_i \begin{bmatrix} h_{1i} \\ 0 \end{bmatrix}, \tag{100}$$

where $g_{1i} = \frac{2}{1-\nu} + \lambda_i \operatorname{th} \lambda_i$, $g_{2i} = \lambda_i \operatorname{cth} \lambda_i - \frac{1+\nu}{1-\nu}$, $h_{1i} = \frac{\nu}{(1-\nu)\operatorname{ch} \lambda_i}$.

Solution of the system of equations (100) is finally given by:

$$B_i = E_i \frac{h_{1i} g_{2i}}{g_{2i} - g_{1i}}, \; C_i = -E_i \frac{h_{1i}}{g_{2i} - g_{1i}}. \tag{101}$$

6. Examples

6.1. Rectangular slab

Rectangular slab loaded with any at the edge – determination of displacements and stress field

6.2. Rectangular plate

In this chapter, we will present some solutions for rectangular plates with use of previously presented analytical methods.

6.2.1. Navier solution

6.2.1.1. Constant distributed load over limited rectangular area of the plate

Let us consider simply supported rectangular plate with constant load $p0 = 10kPa$ over limited rectangular area of the plate. The plate dimensions are:

- Length: $Lx = 5m;$
- Width: $Ly = 4m;$
- Thickness: $h = 10cm.$

The material parameters are:

- Young's modulus: $E = 20GPa;$
- Poisson's ratio: $\nu = 0.2.$

We can calculate plate stiffness as: $D0 = \frac{E \cdot h^3}{12\left(1 - \nu^2\right)} = 1736.111 \cdot kN \cdot m.$

The load is distributed at the area limited by the coordinates:

- at *x* axis: $Lx1 < x < Lx2, \quad Lx1 = 1.5m, Lx2 = 3.5m;$
- at *y* axis: $Ly1 < y < Ly2; \quad Ly1 = 1m, \quad Ly2 = 3m.$

We can calculate the resultant of the distributed load:

$$Q = p0 \cdot \left(\int_{Lx1}^{Lx2} \int_{Ly1}^{Ly2} q(x, y)\, dy\, dx \right) \qquad Q = 40 \cdot kN$$

We will solve the plate with use of Navier method. First we calculate the coefficients to be used in expanding the load into double Fourier series. The number of terms used in this expansion is limited:

$N = 20 \qquad i = 1,3..N \quad j = 1,3..N$

The coefficients are expressed with use of the formulae:

$$\lambda_i = i \cdot \pi \qquad \alpha_i = \frac{\lambda_i}{Lx} \qquad \beta_i = \frac{\lambda_i}{Ly}$$

These coefficients obtain values presented in arrays:

$\lambda_i =$

3.141593
9.424778
15.707963
21.991149
28.274334
34.557519
40.840704
47.12389
53.407075
59.69026

$\alpha_i =$

0.628319	$\frac{1}{m}$
1.884956	
3.141593	
4.39823	
5.654867	
6.911504	
8.168141	
9.424778	
10.681415	
11.938052	

$\beta_i =$

0.785398	$\frac{1}{m}$
2.356194	
3.926991	
5.497787	
7.068583	
8.63938	
10.210176	
11.780972	
13.351769	
14.922565	

The coefficients of the load expansion in a double Fourier series can be calculated with use of the formula:

$$p_{i,j} = \frac{4}{Lx \cdot Ly} \left(\int_{Lx1}^{Lx2} \int_{Ly1}^{Ly2} q(x, y) \cdot \sin\left(\beta_j \cdot y\right) \cdot \sin\left(\alpha_i \cdot x\right) dy\, dx \right)$$

The coefficients of the load expansion can be shown as the following matrix:

$p =$

	1	2	3	4	5	6	7	8
1	0.674	0.000	-0.225	0.000	-0.135	0.000	0.096	0.000
2	0.000	0.000	0.000	0.000	0.000	0.000	0.000	0.000
3	-0.363	0.000	0.121	0.000	0.073	0.000	-0.052	0.000
4	0.000	0.000	0.000	0.000	0.000	0.000	0.000	0.000
5	0.000	0.000	0.000	0.000	0.000	0.000	0.000	0.000
6	0.000	0.000	0.000	0.000	0.000	0.000	0.000	0.000
7	0.156	0.000	-0.052	0.000	-0.031	0.000	0.022	0.000
8	0.000	0.000	0.000	0.000	0.000	0.000	0.000	0.000
9	-0.075	0.000	0.025	0.000	0.015	0.000	-0.011	0.000
10	0.000	0.000	0.000	0.000	0.000	0.000	0.000	0.000
11	-0.061	0.000	0.020	0.000	0.012	0.000	-0.009	0.000
12	0.000	0.000	0.000	0.000	0.000	0.000	0.000	0.000
13	0.084	0.000	-0.028	0.000	-0.017	0.000	0.012	0.000
14	0.000	0.000	0.000	0.000	0.000	0.000	0.000	0.000
15	0.000	0.000	0.000	0.000	0.000	0.000	0.000	0.000
16	0.000	0.000	0.000	0.000	0.000	0.000	0.000	...

Now we can approximate the load with use of the double Fourier series:

$$p1(x,y) = \sum_i \left[\sum_j \left(p_{i,j} \cdot \sin(\alpha_i \cdot x) \cdot \sin(\beta_j \cdot y) \right) \right]$$

The load can be presented in the graph:

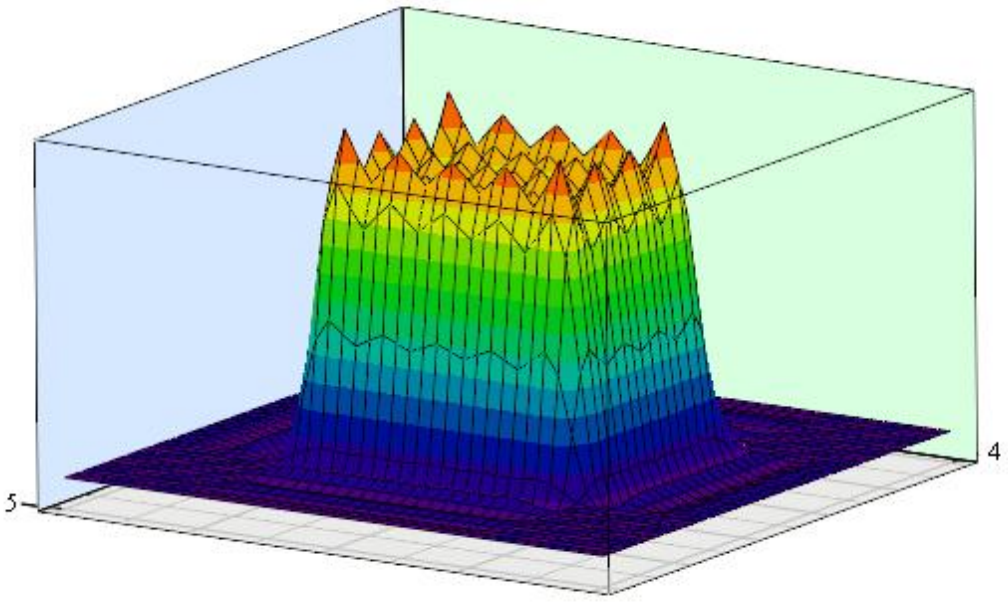

p1

The function representing plate deflection approximated with double Fourier series expansion is expressed as follows:

$$w(x,y) = \frac{1}{\kappa 0}\cdot\left[\sum_i\left[\sum_j\left(a_{i,j}\cdot sin\left(\alpha_i\cdot x\right)\cdot sin\left(\beta_j\cdot y\right)\right)\right]\right]$$

where:

$$a_{i,j} = \frac{p_{i,j}}{\left[\left(\alpha_i\right)^2+\left(\beta_j\right)^2\right]^2}$$

$$\kappa 0 = \frac{D0}{p0} \qquad \kappa 0 = 173.611\cdot m^3$$

The plate deflection can be presented in the graph:

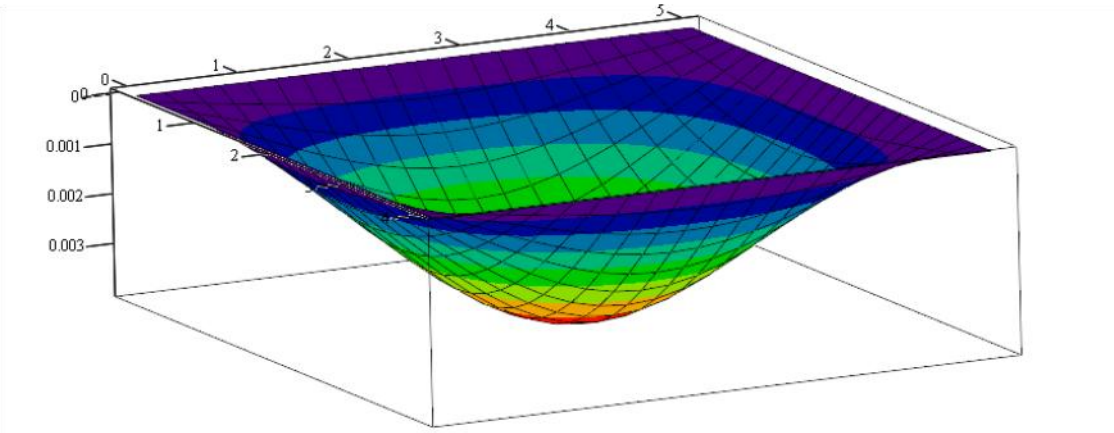

w

Maximum deflection occurs at the middle of the plate:

$$w\left(\frac{Lx}{2},\frac{Ly}{2}\right) = 3.95\cdot mm$$

Next we will find the internal forces:

- bending moments:

$$Mx(x,y) = -D0\cdot\left(\frac{d^2}{dx^2}w(x,y)+\nu\cdot\frac{d^2}{dy^2}w(x,y)\right)$$

$$Mx(x,y) = p0\left[\sum_i\left[\sum_j\left[a_{i,j}\cdot\left[\left(\alpha_i\right)^2+\nu\cdot\left(\beta_j\right)^2\right]\cdot sin\left(\alpha_i\cdot x\right)\cdot sin\left(\beta_j\cdot y\right)\right]\right]\right]$$

$$My(x,y) = -D0\cdot\left(\frac{d^2}{dy^2}w(x,y)+\nu\cdot\frac{d^2}{dx^2}w(x,y)\right)$$

$$My(x,y) = p0\left[\sum_i\left[\sum_j\left[a_{i,j}\cdot\left[\nu\cdot(\alpha_i)^2+(\beta_j)^2\right]\cdot sin(\alpha_i\cdot x)\cdot sin(\beta_j\cdot y)\right]\right]\right]$$

- torsional moment:

$$Mxy(x,y) = -D0\cdot(1-\nu)\cdot\left[\frac{d}{dx}\left(\frac{d}{dy}w(x,y)\right)\right]$$

$$Mxy(x,y) = p0\cdot(1-\nu)\left[\sum_i\left[\sum_j\left(a_{i,j}\cdot\alpha_i\cdot\beta_j\cdot cos(\alpha_i\cdot x)\cdot cos(\beta_j\cdot y)\right)\right]\right]$$

Bending moments and torsional moments can be presented in graphs with maximum values:

- bending moments:

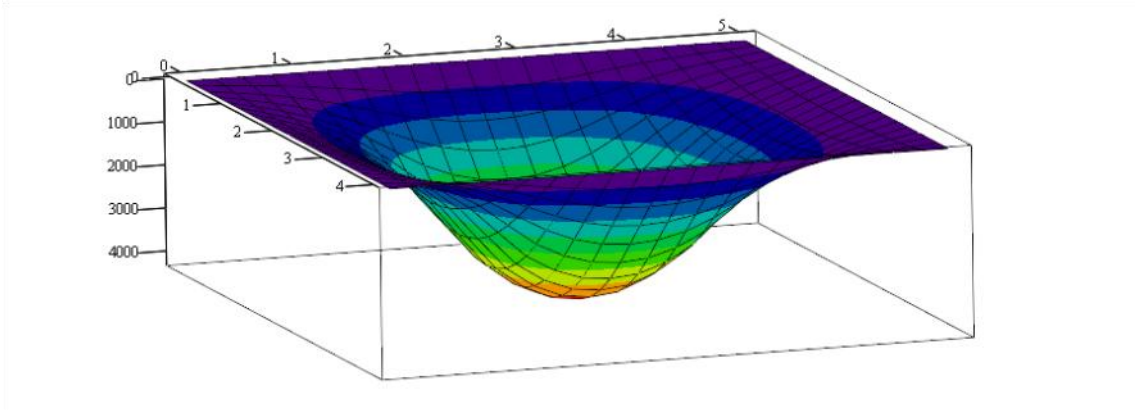

Mx

$$Mx\left(\frac{Lx}{2},\frac{Ly}{2}\right) = 4.213572\times 10^{0}\cdot\frac{kN\cdot m}{m}$$

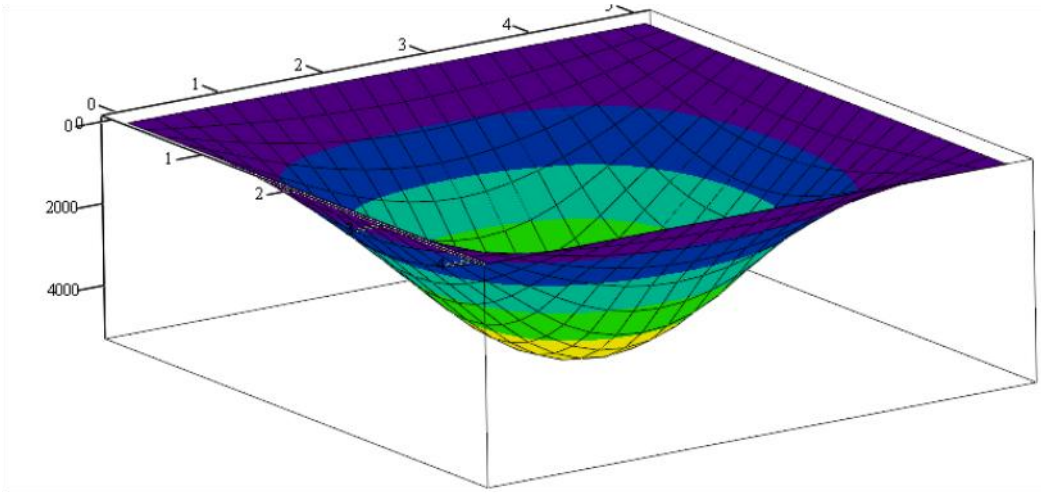

My

$$My\left(\frac{Lx}{2},\frac{Ly}{2}\right) = 5.152556\times 10^{0}\cdot\frac{kN\cdot m}{m}$$

- torsional moment:

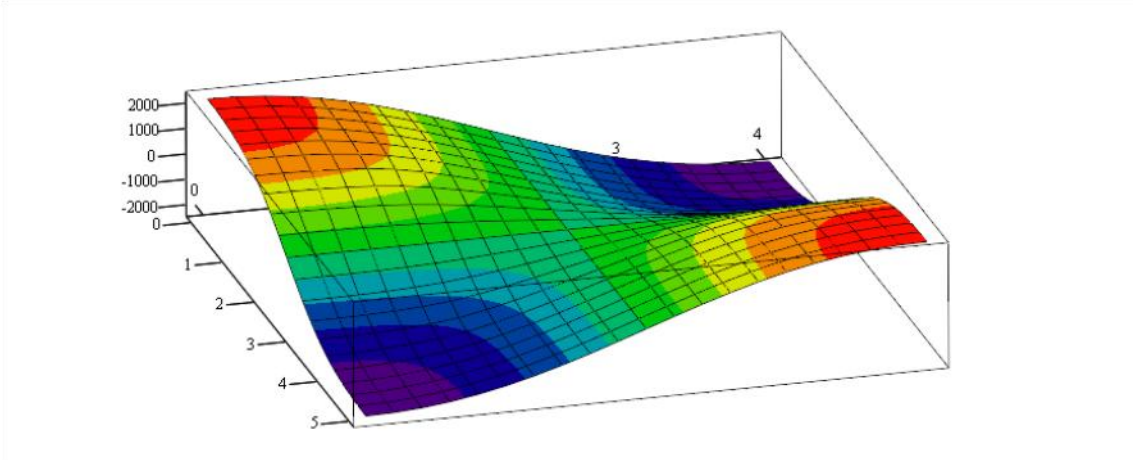

Mxy

$$Mxy(0,0) = 2.330655\times 10^{0}\cdot\frac{kN\cdot m}{m}$$

The next step will be calculation of shear forces:

$$Qx(x,y) = -D0\cdot\left[\frac{d^3}{dx^3}w(x,y)+\frac{d}{dx}\left(\frac{d^2}{dy^2}w(x,y)\right)\right]$$

$$Qx(x,y) = p0\left[\sum_i\left[\sum_j\left[a_{i,j}\cdot\alpha_i\cdot\left[(\alpha_i)^2+(\beta_j)^2\right]\cdot cos(\alpha_i\cdot x)\cdot sin(\beta_j\cdot y)\right]\right]\right]$$

$$Qy(x,y) = -D0\cdot\left[\frac{d^3}{dy^3}w(x,y)+\frac{d}{dy}\left(\frac{d^2}{dx^2}w(x,y)\right)\right]$$

$$Qy(x,y) = p0\left[\sum_i\left[\sum_j\left[a_{i,j}\cdot\beta_j\cdot\left[(\alpha_i)^2+(\beta_j)^2\right]\cdot sin(\alpha_i\cdot x)\cdot cos(\beta_j\cdot y)\right]\right]\right]$$

Shear forces can be presented in graphs with maximum values:

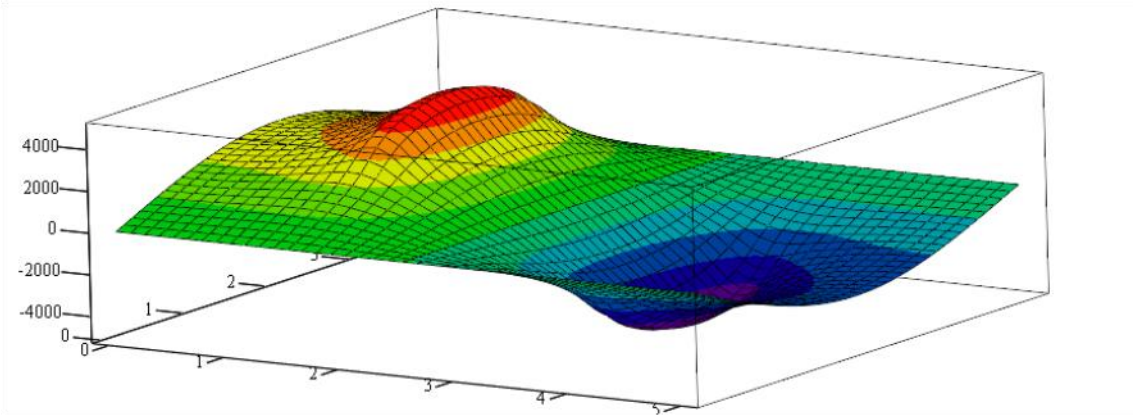

Qx

$$Qx\left(\frac{\mathrm{Lx}}{4},\frac{Ly}{2}\right) = 4.452033\times 10^{0}\cdot\frac{kN}{m}$$

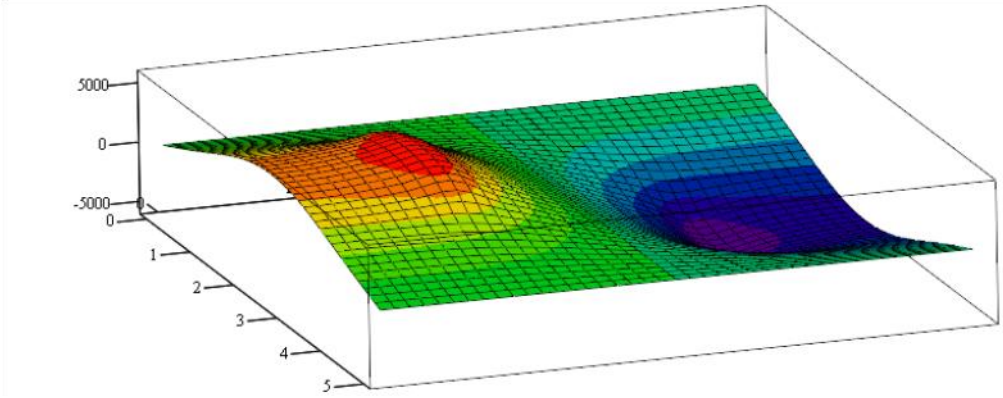

Qy

$$Qy\left(\frac{Lx}{2},\frac{Ly}{4}\right) = 5.725398\times 10^{0}\cdot\frac{kN}{m}$$

The next will be calculation of principal moments. First we calculate the parameters of Mohr's circle for principal moments:

- horizontal component of Mohr's circle radius:

$$U(x,y) = \frac{Mx(x,y) - My(x,y)}{2}$$

- circle radius:

$$R(x,y) = \sqrt{U(x,y)^2 + Mxy(x,y)^2}$$

- location of the circle center at the horizontal axis of bending moments:

$$S(x,y) = \frac{Mx(x,y) + My(x,y)}{2}$$

The functions of principal moments are calculated with use of formulae:

$$Mmax(x,y) = S(x,y) + R(x,y)$$

$$Mmin(x,y) = S(x,y) - R(x,y)$$

These functions of principal moments can be presented in the graphs:

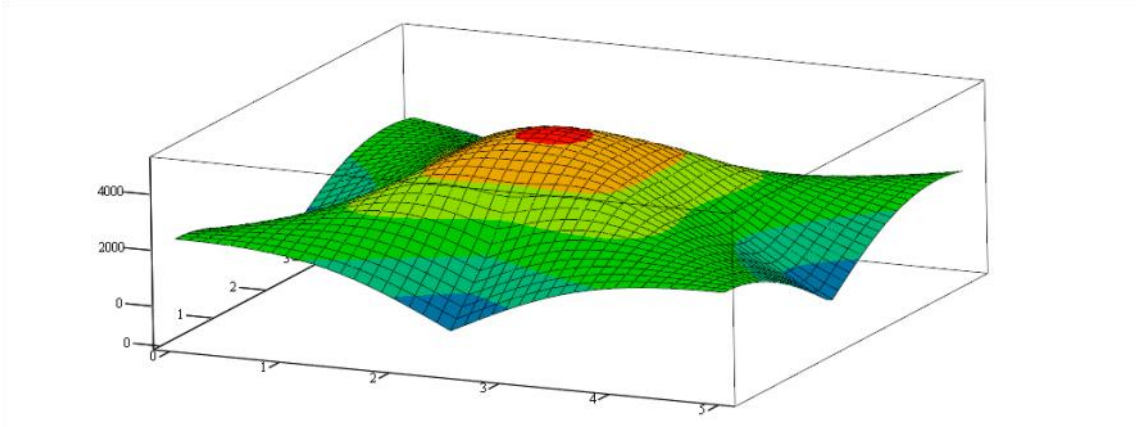

Mmax

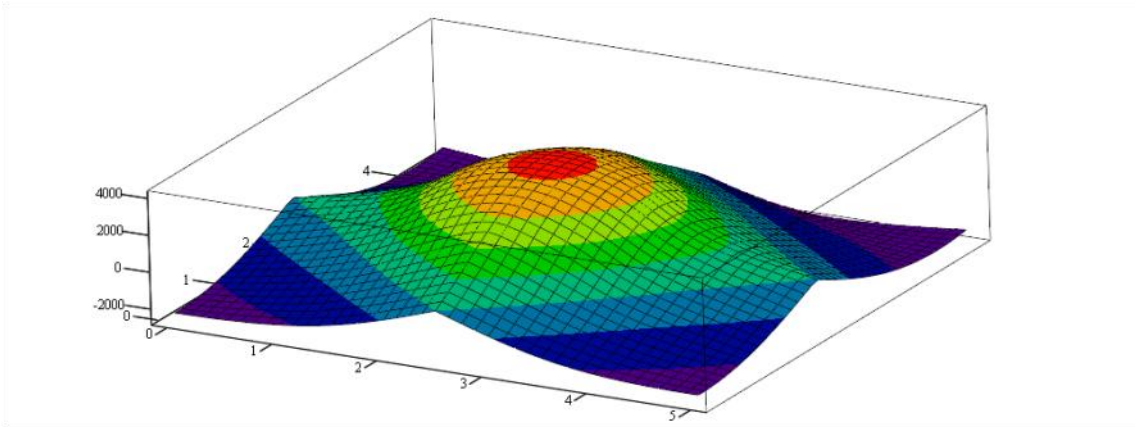

Mmin

Finally, we can calculate the angle for the principal direction in relation to the *x* axis direction:

$$\Phi(x,y) = 0.5 \cdot atan2(U(x,y), Mxy(x,y))$$

This direction can be presented as a vector plot:

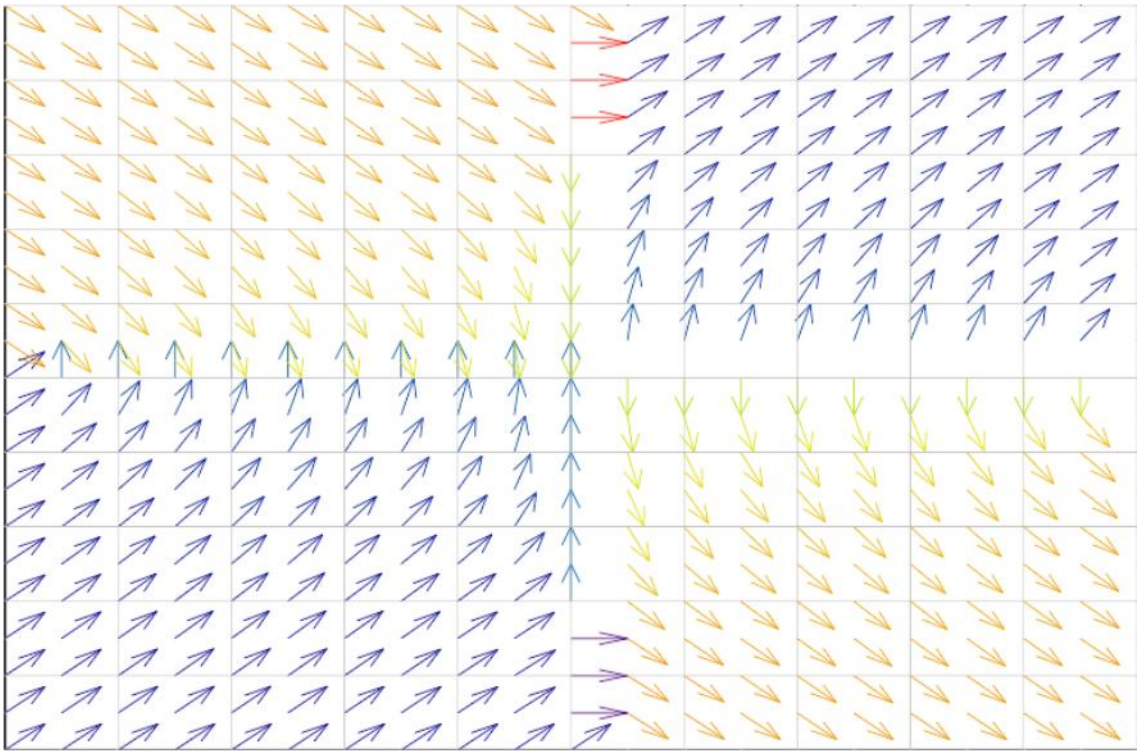

(X, Y)

6.2.2. Nádai-Lévy solution

6.2.2.1. Two opposite edges simply-supported, two others - fixed

Let us consider a rectangular plate with constant load which includes dead load $p0 = -5kPa - \gamma \cdot h$ over the whole area of the plate. The plate is simply supported at two opposite edges and fixed at other ones. The plate dimensions are:

- Length: $Lx = 5m;$
- Width: $Ly = 6m;$
- Thickness: $h = 7cm.$

The material parameters are:

- Young's modulus: $E = 30GPa;$
- Poisson's ratio: $\nu = 0.2;$
- Material specific weight: $\gamma = 25\frac{kN}{m^3}.$

We can calculate plate stiffness as: $D0 = \frac{E \cdot h^3}{12\left(1 - \nu^2\right)} = 893.229 \cdot kN \cdot m.$

The load is distributed at the whore area of the plate:

- at *x* axis: $Lx1 < x < Lx2, \qquad Lx1 := 0m, \quad Lx2 := Lx;$
- at *y* axis: $0 < y < Ly.$

We can calculate the resultant of the distributed load:

$$Q0 := p0 \cdot Ly \cdot \left(\int_{Lx1}^{Lx2} q(x)\, dx \right) \qquad Q0 = -202.5 \cdot kN$$

We will solve the plate with use of Nádai-Lévy method. First we calculate the coefficients to be used in expanding the load into single Fourier series. The number of terms used in this expansion is limited:

$N := 15 \qquad i := 1, 3 .. N$

The coefficients are expressed with use of the formulae:

$$\alpha_i := \frac{i \cdot \pi}{Lx} \qquad \lambda_i := \alpha_i \cdot \frac{Ly}{2}$$

These coefficients obtain values presented in arrays:

$\alpha_i =$

0.628319	$\frac{1}{m}$
1.884956	
3.141593	
4.398230	
5.654867	
6.911504	
8.168141	
9.424778	

$\lambda_i =$

1.885
5.655
9.425
13.195
16.965
20.735
24.504
28.274

The coefficients of the load expansion in a single Fourier series can be calculated with use of the formula:

$$p_i := \frac{2}{Lx} \cdot \left(\int_{Lx1}^{Lx2} p0 \cdot \sin\left(\alpha_i \cdot x\right) dx \right)$$

The coefficients of the load expansion can be shown as the following vector:

$p_i =$

	1
1	-8.594
2	-2.865
3	-1.719
4	-1.228
5	-0.955
6	-0.781
7	-0.661
8	-0.573

$\cdot kPa$

Now we can approximate the load with use of the single Fourier series:

$$p1(x) = \sum_i \left(p_i \cdot sin\left(\alpha_i \cdot x\right)\right)$$

The load can be presented in the graph:

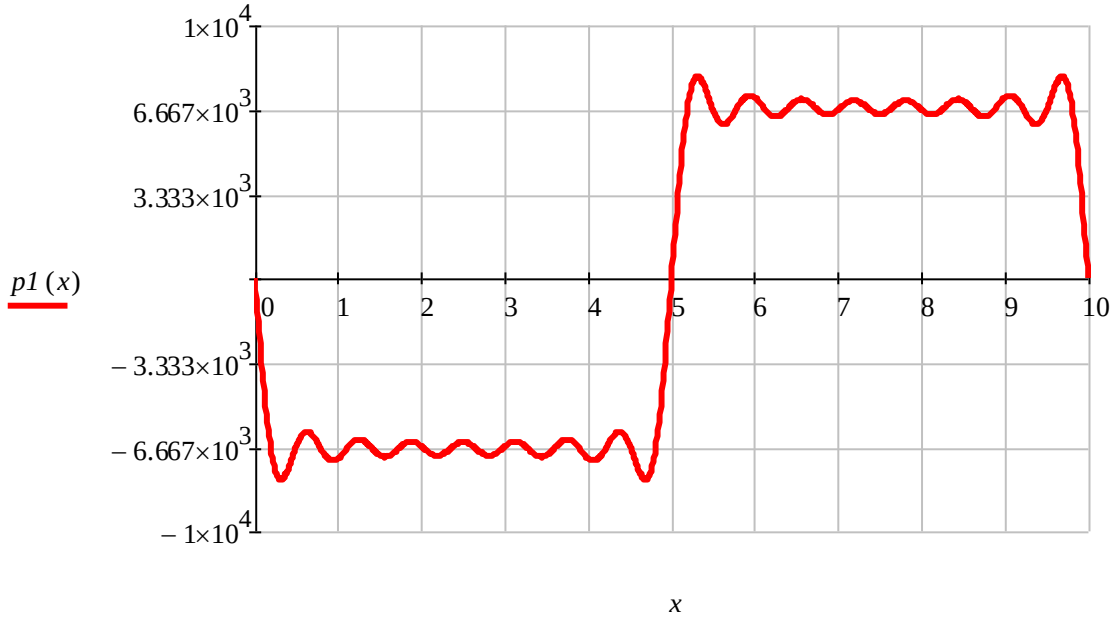

The coefficients of the cylindrical component of the plate deflection can be calculated as:

$$E_i = \frac{p_i}{D0 \cdot \left(\alpha_i\right)^4}$$

and presented in as a vector:

$E_i =$

	1
1	-61.735010
2	-0.254054
3	-0.019755
4	-0.003673
5	-0.001045
6	-0.000383
7	-0.000166
8	-0.000081

$\cdot mm$

The cylindrical deflection of the plate is now described with use of the formula:

$$w2(x) = \sum_i \left(E_i \cdot \sin\left(\alpha_i \cdot x\right)\right)$$

and can be presented in the following graph:

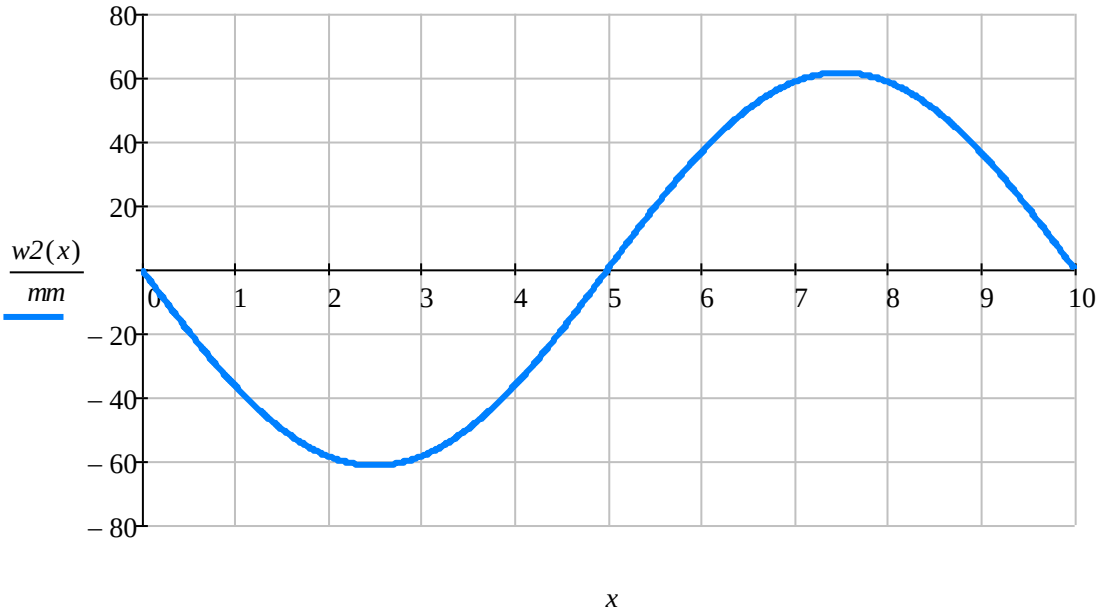

The maximum value of this cylindrical deflection occurs at x=2.5 m:

$w2max = w2(2.5m)$ $\quad w2max = -61.498 \cdot mm$

To find the total deflection of the plate, firs we calculate other four coefficients with use of the formulae:

$A_i = 0 \qquad D_i = 0$

$$C_i = \frac{E_i}{\lambda_i \cdot csch\left(\lambda_i\right) + \cosh\left(\lambda_i\right)} \qquad B_i = -C_i \cdot \left(1 + \lambda_i \cdot \coth\left(\lambda_i\right)\right)$$

These coefficients can be presented as the following vectors:

$A_i =$ $B_i =$ $C_i =$ $D_i =$

A_i		B_i		C_i		D_i	
$0 \cdot 10^0$	$\cdot mm$	$4.642255 \cdot 10^1$	$\cdot mm$	$-1.560989 \cdot 10^1$	$\cdot mm$	$0 \cdot 10^0$	$\cdot mm$
$0 \cdot 10^0$		$1.183315 \cdot 10^{-2}$		$-1.778083 \cdot 10^{-3}$		$0 \cdot 10^0$	
$0 \cdot 10^0$		$3.323909 \cdot 10^{-5}$		$-3.18847 \cdot 10^{-6}$		$0 \cdot 10^0$	
$0 \cdot 10^0$		$1.940066 \cdot 10^{-7}$		$-1.366755 \cdot 10^{-8}$		$0 \cdot 10^0$	
$0 \cdot 10^0$		$1.611143 \cdot 10^{-9}$		$-8.968435 \cdot 10^{-11}$		$0 \cdot 10^0$	
$0 \cdot 10^0$		$1.647647 \cdot 10^{-11}$		$-7.580785 \cdot 10^{-13}$		$0 \cdot 10^0$	
$0 \cdot 10^0$		$1.933413 \cdot 10^{-13}$		$-7.580698 \cdot 10^{-15}$		$0 \cdot 10^0$	
$0 \cdot 10^0$		$2.501526 \cdot 10^{-15}$		$0 \cdot 10^0$		$0 \cdot 10^0$	

The following functions will be used in order to calculate the total deflection of the plate:

$$f(i,y) = A_i \cdot \sinh(\alpha_i \cdot y) + B_i \cdot \cosh(\alpha_i \cdot y) + C_i \cdot \alpha_i \cdot y \cdot \sinh(\alpha_i \cdot y) + D_i \cdot \alpha_i \cdot y \cdot \cosh(\alpha_i \cdot y)$$

$$f0(i,y) = f(i,y) + E_i$$

Additionally we calculate the derivatives of the function $f(i,y)$:

- first derivative:

$$f1(i,y) = \frac{d}{dy} f(i,y)$$

$$f1(i,y) = \alpha_i \cdot \begin{bmatrix} A_i \cdot \cosh(\alpha_i \cdot y) + B_i \cdot \sinh(\alpha_i \cdot y) \ ... \\ + C_i \cdot \left(\sinh(\alpha_i \cdot y) + \alpha_i \cdot y \cdot \cosh(\alpha_i \cdot y)\right) \ ... \\ + D_i \cdot \left(\cosh(\alpha_i \cdot y) + \alpha_i \cdot y \cdot \sinh(\alpha_i \cdot y)\right) \end{bmatrix}$$

- second derivative:

$$f2(i,y) = \frac{d^2}{dy^2} f(i,y)$$

$$f2(i,y) = (\alpha_i)^2 \cdot \begin{bmatrix} A_i \cdot \sinh(\alpha_i \cdot y) + B_i \cdot \cosh(\alpha_i \cdot y) \ ... \\ + C_i \cdot \left(2 \cdot \cosh(\alpha_i \cdot y) + \alpha_i \cdot y \cdot \sinh(\alpha_i \cdot y)\right) \ ... \\ + D_i \cdot \left(2 \cdot \sinh(\alpha_i \cdot y) + \alpha_i \cdot y \cdot \cosh(\alpha_i \cdot y)\right) \end{bmatrix}$$

- third derivative:

$$f3(i,y) = \frac{d^3}{dy^3} f(i,y)$$

$$f3(i,y) = (\alpha_i)^3 \cdot \begin{bmatrix} A_i \cdot \cosh(\alpha_i \cdot y) + B_i \cdot \sinh(\alpha_i \cdot y) \ ... \\ + C_i \cdot \left(3 \cdot \sinh(\alpha_i \cdot y) + \alpha_i \cdot y \cdot \cosh(\alpha_i \cdot y)\right) \ ... \\ + D_i \cdot \left(3 \cdot \cosh(\alpha_i \cdot y) + \alpha_i \cdot y \cdot \sinh(\alpha_i \cdot y)\right) \end{bmatrix}$$

The functions can be presented in the graph:

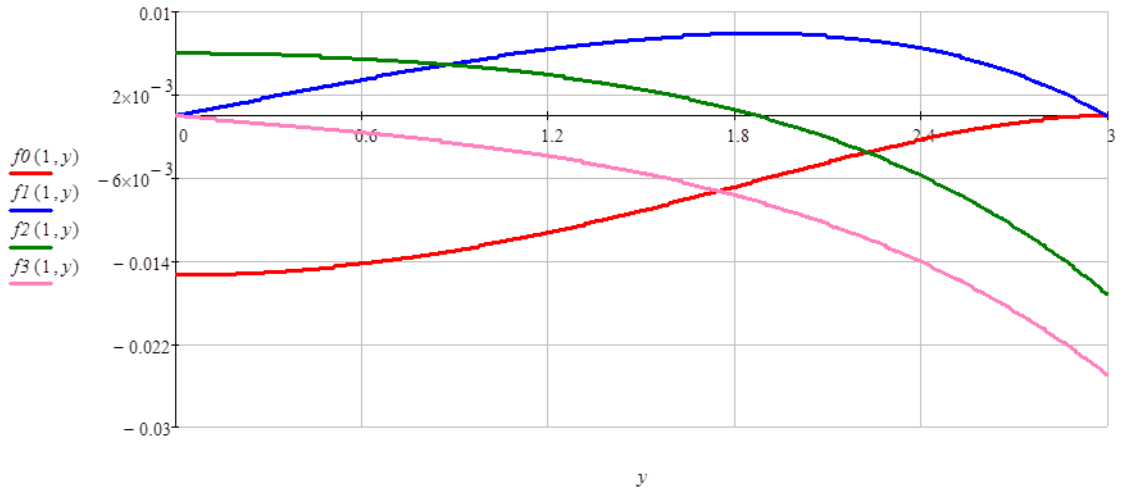

The function representing plate deflection can be expressed on the basis of the presented functions as follows ($w(x,y)=w1(x,y)$):

$$w1(x,y) = \sum_i \left(f0(i,y)\cdot \sin\left(\alpha_i \cdot x\right)\right)$$

$$w(x,y) = \sum_i \left[\left(A_i\cdot\sinh\left(\alpha_i\cdot y\right) + B_i\cdot\cosh\left(\alpha_i\cdot y\right) + C_i\cdot\alpha_i\cdot y\cdot\sinh\left(\alpha_i\cdot y\right) + D_i\cdot\alpha_i\cdot y\cdot\cosh\left(\alpha_i\cdot y\right) + E_i\right)\cdot\sin\left(\alpha_i\cdot x\right)\right]$$

The plate deflection can be presented in the graph:

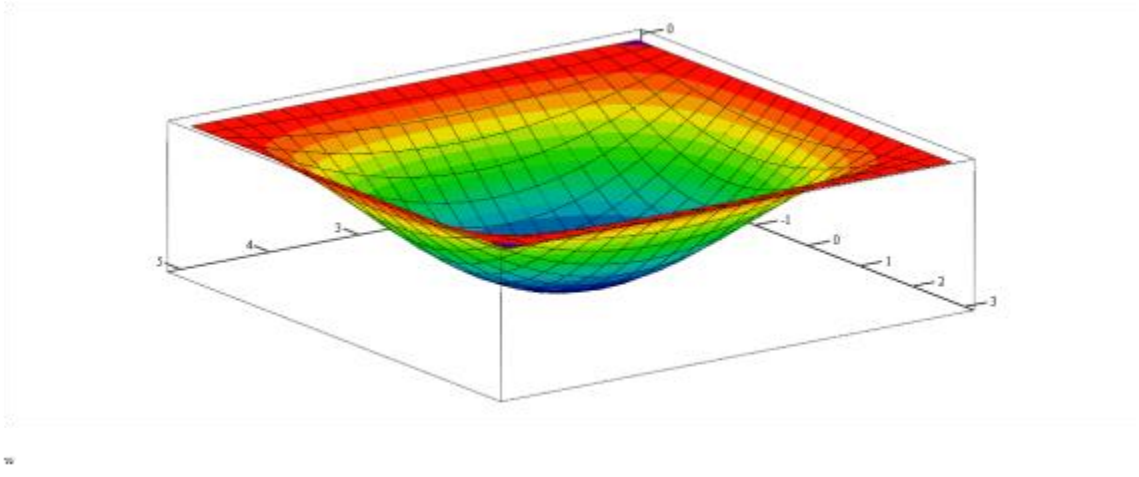

Maximum deflection occurs at the middle of the plate:

$$w\left(\frac{Lx}{2},0\right) = -15.087\cdot mm \qquad w1\left(\frac{Lx}{2},0\right) = -15.087\cdot mm$$

Next we will find the internal forces:

- bending moments:

$$Mx(x,y) = -D0\cdot\left(\frac{d^2}{dx^2}w(x,y) + \nu\cdot\frac{d^2}{dy^2}w(x,y)\right)$$

$$Mx(x,y) = D0\cdot\left[\sum_i\left[\left[(\alpha_i)^2\cdot f0(i,y) - \nu\cdot f2(i,y)\right]\cdot sin(\alpha_i\cdot x)\right]\right]$$

$$My(x,y) = -D0\cdot\left(\frac{d^2}{dy^2}w(x,y) + \nu\cdot\frac{d^2}{dx^2}w(x,y)\right)$$

$$My(x,y) = D0\cdot\left[\sum_i\left[\left[\nu\cdot(\alpha_i)^2\cdot f0(i,y) - f2(i,y)\right]\cdot sin(\alpha_i\cdot x)\right]\right]$$

- torsional moment:

$$Mxy(x,y) = -D0\cdot(1-\nu)\cdot\left[\frac{d}{dx}\left(\frac{d}{dy}w(x,y)\right)\right]$$

$$Mxy(x,y) = -D0\cdot(1-\nu)\cdot\left[\sum_i\left(\alpha_i\cdot f1(i,y)\cdot cos(\alpha_i\cdot x)\right)\right]$$

Bending moments and torsional moments can be presented in graphs with maximum values:

- bending moments:

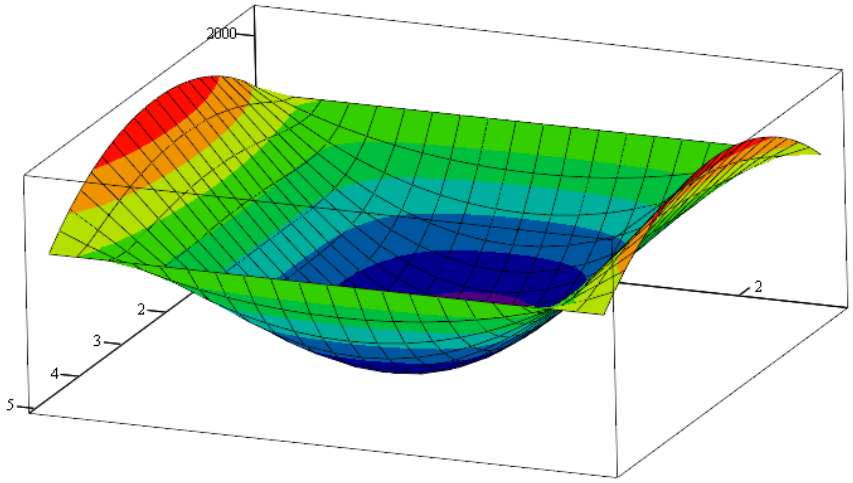

Mx

$$Mx\left(\frac{Lx}{2},0\right) = -5.82530\cdot\frac{kN\cdot m}{m}$$

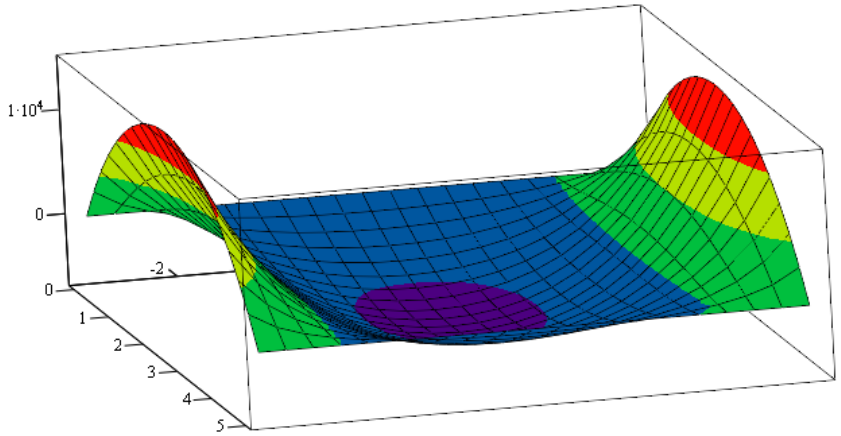

My

$$My\left(\frac{Lx}{2},0\right) = -6.28662\cdot\frac{kN\cdot m}{m}$$

- torsional moment:

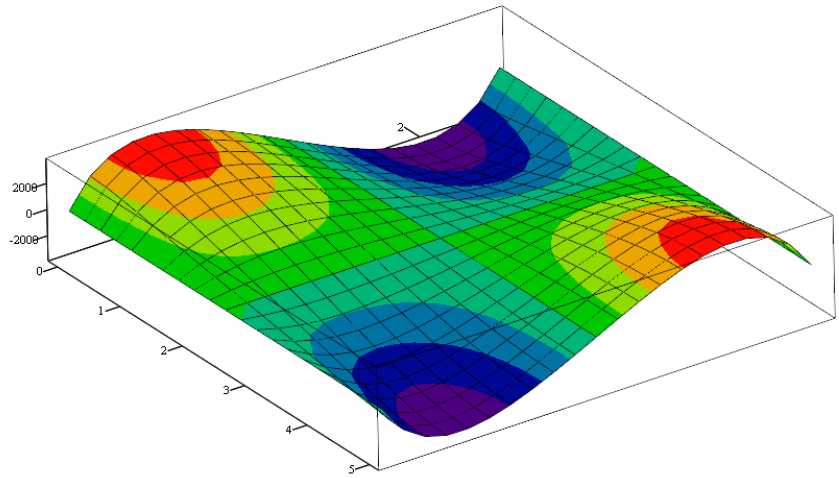

Mxy

$$Mxy\left(Lx,\frac{Ly}{2}\right) = 0.00000\cdot\frac{kN\cdot m}{m}$$

The next step will be calculation of shear forces:

$$Qx(x,y) = -D0\cdot\left[\frac{d^3}{dx^3}w(x,y) + \frac{d}{dx}\left(\frac{d^2}{dy^2}w(x,y)\right)\right]$$

$$Qx(x,y) = D0\cdot\left[\sum_i\left[\left[(\alpha_i)^3\cdot f0\,(i,y) - \alpha_i\cdot f2\,(i,y)\right]\cdot\cos(\alpha_i\cdot x)\right]\right]$$

$$Qy(x,y) = -D0\cdot\left[\frac{d^3}{dy^3}w(x,y) + \frac{d}{dy}\left(\frac{d^2}{dx^2}w(x,y)\right)\right]$$

$$Qy(x,y) = D0\cdot\left[\sum_i\left[\left[(\alpha_i)^2\cdot f1\,(i,y) - f3\,(i,y)\right]\cdot\sin(\alpha_i\cdot x)\right]\right]$$

Shear forces can be presented in graphs with maximum values:

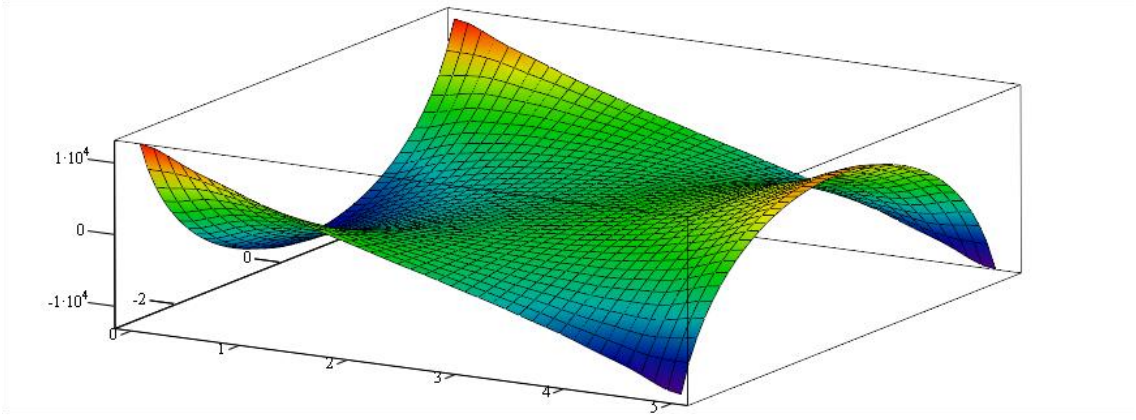

Qx

$$Qx(\mathrm{Lx},0) = 9.509418\cdot\frac{kN}{m}$$

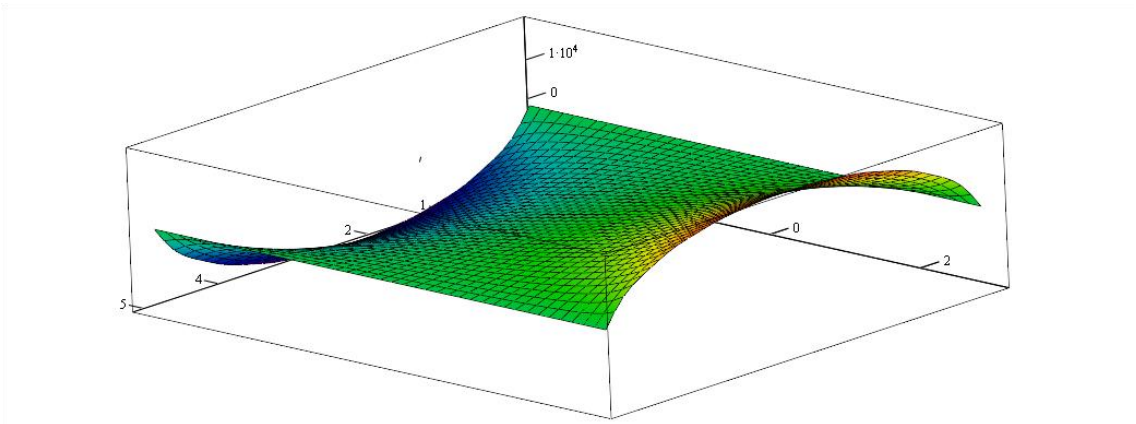

Qy

$$Qy\left(\frac{Lx}{2},\frac{\mathrm{Ly}}{2}\right) = 19.902710\cdot\frac{kN}{m}$$

The next will be calculation of principal moments. First we calculate the parameters of Mohr's circle for principal moments:

- horizontal component of Mohr's circle radius:

$$U(x,y) = \frac{Mx(x,y) - My(x,y)}{2}$$

- circle radius:

$$R(x,y) = \sqrt{U(x,y)^2 + Mxy(x,y)^2}$$

- location of the circle center at the horizontal axis of bending moments:

$$S(x,y) = \frac{Mx(x,y) + My(x,y)}{2}$$

The functions of principal moments are calculated with use of formulae:

$$Mmax(x,y) = S(x,y) + R(x,y)$$

$$Mmin(x,y) = S(x,y) - R(x,y)$$

These functions of principal moments can be presented in the graphs:

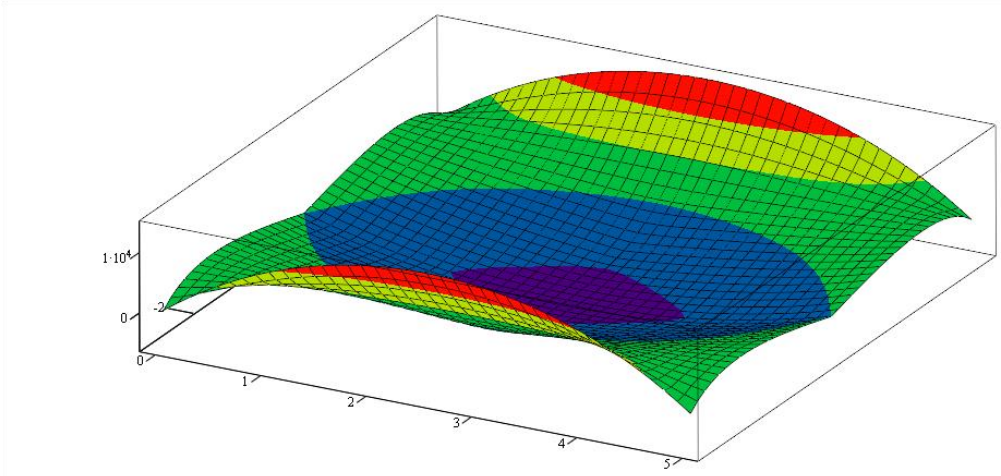

Mmax

$$Mmax(3m,2m) = 1.082430 \cdot \frac{kN \cdot m}{m}$$

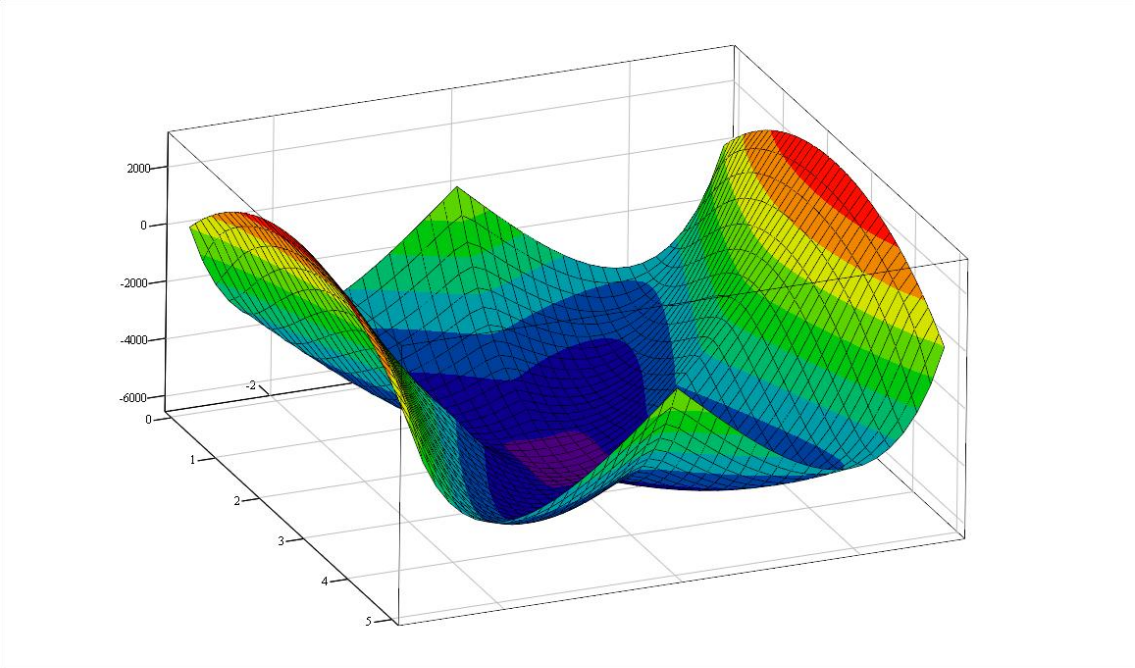

Mmin

$$Mmin(2.5m, 0m) = -6.286619 \cdot \frac{kN \cdot m}{m}$$

Finally, we can calculate the angle for the principal direction in relation to the *x* axis direction:

$$\Phi(x, y) = 0.5 \cdot atan2(U(x, y), Mxy(x, y))$$

This direction can be presented as a vector plot:

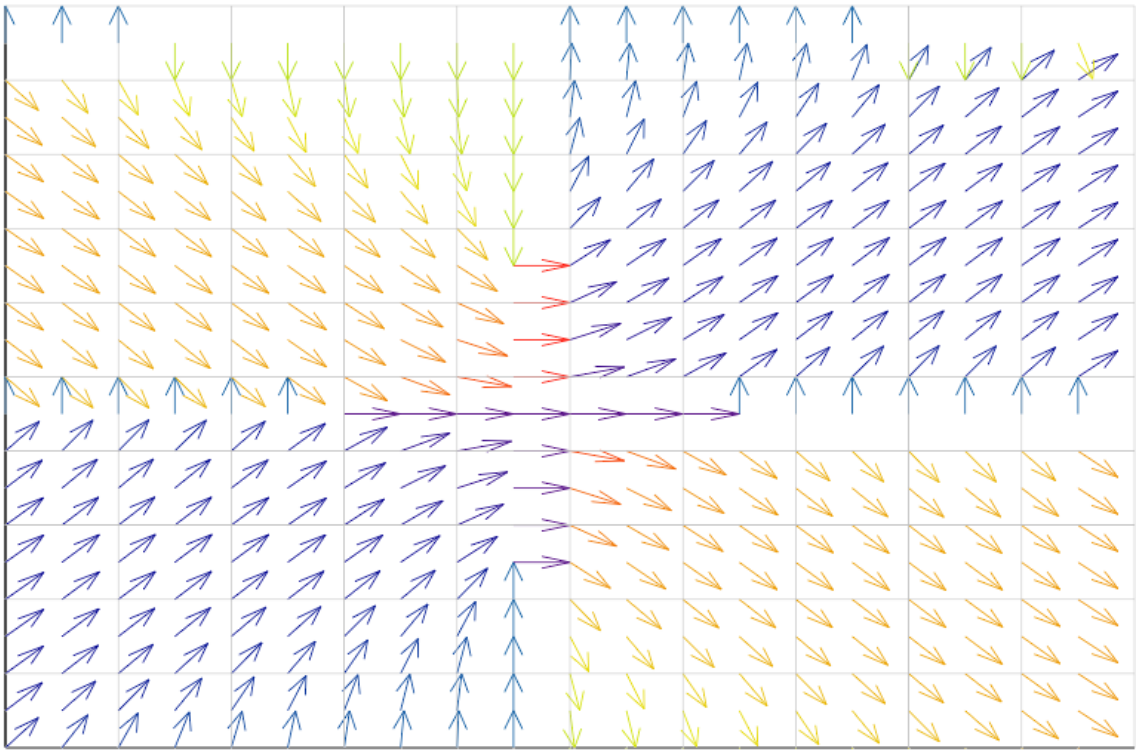

(X, Y)

6.2.3. Finite difference method

6.2.3.1. Two neighboring edges simply-supported, two others - fixed

Let us consider a rectangular plate with constant load $q = 4kPa$ over the area of the plate. The plate is simply supported at two neighboring edges and fixed at other ones. The plate dimensions are:

- Length: $L_x = 4m;$
- Width: $L_y = 3m;$
- Thickness: $h = 6cm.$

The material parameters are:

- Young's modulus: $E = 20GPa;$
- Poisson's ratio: $\nu = 0.17.$

We can calculate plate stiffness as: $D = \frac{E \cdot h^3}{12 \cdot \left(1 - \nu^2\right)} = 370.714 \cdot kN \cdot m.$

The load is distributed at the whore area of the plate:

- at x axis: $0 < x < Lx;$

- at y axis: $0 < y < Ly$.

We divide the plate area into $\Delta = 1m$ divisions. This leads to the nodal mesh, which can be presented in figure:

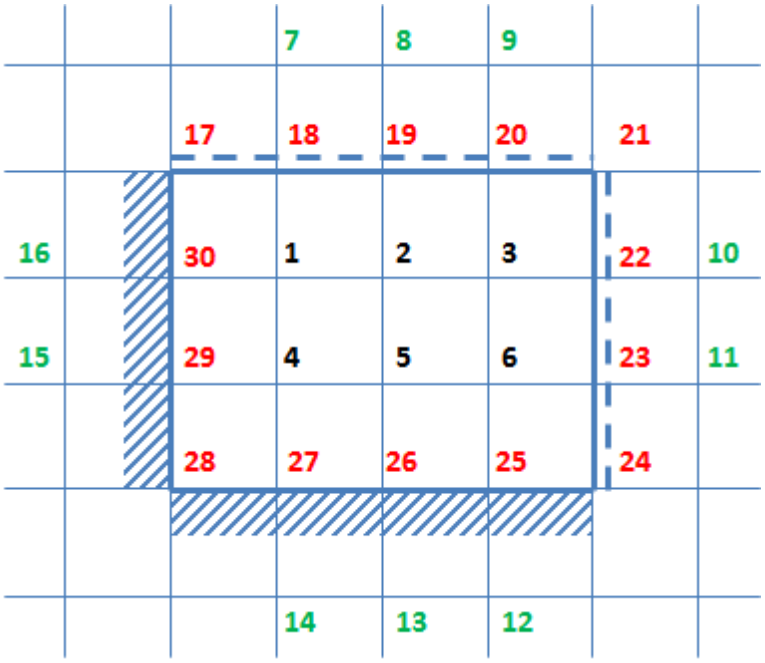

The following differential scheme will be used in order to approximate differential equations:

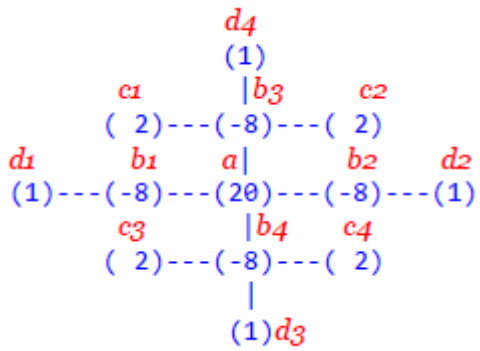

The equations approximating the plate deflection are written in every point inside the plate area (marked in black), so we obtain the system of six equations:

$$20 \cdot w_1 - 8 \cdot (w_2 + w_4 + w_{30} + w_{18}) + 2(w_{17} + w_{19} + w_5 + w_{29}) + (w_7 + w_3 + w_{27} + w_{16}) = \alpha_0$$

$$20 \cdot w_2 - 8 \cdot (w_1 + w_{19} + w_3 + w_5) + 2(w_{18} + w_{20} + w_6 + w_4) + (w_8 + w_{22} + w_{26} + w_{30}) = \alpha_0$$

$$20 \cdot w_3 - 8 \cdot (w_2 + w_{20} + w_{22} + w_6) + 2(w_{19} + w_{21} + w_5 + w_{23}) + (w_9 + w_{10} + w_{25} + w_1) = \alpha_0$$

$$20 \cdot w_4 - 8 \cdot (w_1 + w_5 + w_{27} + w_{29}) + 2(w_{30} + w_2 + w_{26} + w_{28}) + (w_{18} + w_6 + w_{14} + w_{15}) = \alpha_0$$

$$20 \cdot w_5 - 8 \cdot (w_2 + w_6 + w_{26} + w_4) + 2(w_1 + w_3 + w_{27} + w_{25}) + (w_{19} + w_{23} + w_{13} + w_{29}) = \alpha_0$$

$$20 \cdot w_6 - 8 \cdot (w_3 + w_{23} + w_{25} + w_5) + 2(w_2 + w_{22} + w_{24} + w_{26}) + (w_{20} + w_{11} + w_{12} + w_4) = \alpha_0$$

There is a total number of 30 unknowns in this system of equations. Only the deflection components at the points inside of the plate are the "real" unknowns. Other values will be calculated on the basis of boundary conditions.

First we put down the condition for the nodes marked in red. These nodes are positioned at edges that are fixed or simply supported, so we know the deflection at these nodes is equal to 0, so we can state:

$w_{17}= w_{18}= w_{19}= w_{20}= w_{21}= w_{22}= w_{23}= w_{24}= w_{25}= w_{26}= w_{27}= w_{28}= w_{29}= w_{30}=0$

In this way we eliminate the unknowns $w_{17} \div w_{30}$ from the system of equation. Additional relations coming from boundary conditions are:

- for the fixed edges: the deflection at the point outside the plate is equal to value of the deflection in the plate area, opposite to the analyzed node;
- for the simply supported edges: the deflection at the point outside the plate is equal to the negative value of deflection in the plate area, opposite to the analyzed node;

The first condition results with equations:

$$w_{12} = w_6$$

$$w_{13} = w_5$$

$$w_{14} = w_4$$

$$w_{15} = w_4$$

$$w_{16} = w_1$$

And the second one results with:

$$w_7 = -w_1$$

$$w_8 = -w_2$$

$$w_9 = -w_3$$

$$w_{10} = -w_3$$

$$w_{11} = -w_6$$

Introduction of the above relations into the system of equations results with the reduced number of the unknown. The system of equations may be written as:

$$20 \cdot w_1 - 8 \cdot (w_4 + w_2) + 2 w_5 + w_3 + w_1 - w_1 = \alpha_0$$

$$20 \cdot w_2 - 8 \cdot (w_1 + w_3 + w_5) + 2(w_4 + w_6) - w_2 = \alpha_0$$

$$20 \cdot w_3 - 8 \cdot (w_2 + w_6) + 2 w_5 + w_1 - w_3 - w_3 = \alpha_0$$

$$20 \cdot w_4 - 8 \cdot (w_1 + w_5) + 2 w_2 + w_6 + w_4 + w_4 = \alpha_0$$

$$20 \cdot w_5 - 8 \cdot (w_2 + w_4 + w_6) + 2(w_1 + w_3) + w_5 = \alpha_0$$

$$20 \cdot w_6 - 8 \cdot (w_3 + w_5) + 2 w_2 + w_4 + w_6 - w_6 = \alpha_0$$

where there are only six unknowns, the same number as of the number of equations. Solution of the system of equations leads to the following vector of deflection for six nodes inside the plate area:

$$w = \begin{pmatrix} 0 \\ -2.315 \\ -3.537 \\ -2.779 \\ -2.016 \\ -3.067 \\ -2.424 \end{pmatrix} mm$$

These values can be distributed over the plate area to form the matrix of deflection:

$$W = \begin{pmatrix} w_0 & w_0 & w_0 & w_0 & w_0 \\ w_0 & w_1 & w_2 & w_3 & w_0 \\ w_0 & w_4 & w_5 & w_6 & w_0 \\ w_0 & w_0 & w_0 & w_0 & w_0 \end{pmatrix}$$

We can now present the results in the graph:

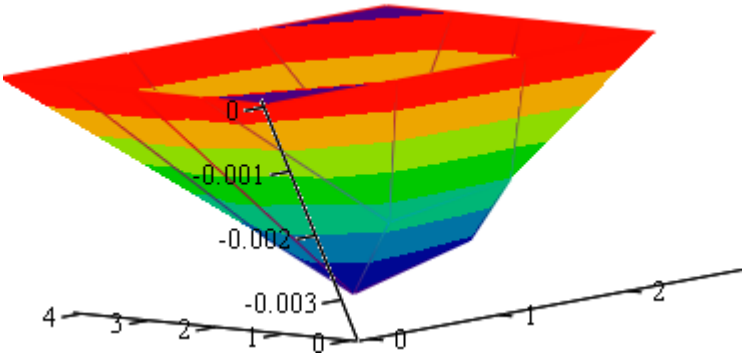

W

The next step is calculation of internal forces. The bending moments in the point i,j of the matrix W can be calculated with the following formulae:

$$M_{x_{i,j}} = \frac{D}{\Delta^2}\cdot\left[W1_{i,j}\cdot 2\cdot(1+\nu) - W1_{i,j-1} - W1_{i,j+1} - \nu\cdot\left(W1_{i-1,j} + W1_{i+1,j}\right)\right]$$

$$M_{y_{i,j}} = \frac{D}{\Delta^2}\cdot\left[W1_{i,j}\cdot 2\cdot(1+\nu) - W1_{i-1,j} - W1_{i+1,j} - \nu\cdot\left(W1_{i,j+1} + W1_{i,j-1}\right)\right]$$

and the torsional moment can be found with use of the formula:

$$M_{xy_{i,j}} = \frac{-D}{4\Delta^2}(1-\nu)\cdot\left(W1_{i+1,j+1} + W1_{i-1,j-1} - W1_{i+1,j-1} - W1_{i-1,j+1}\right)$$

The moments can be put in the matrix of points, including the nodes at the edges:

- bending moments:

$$submatrix\left(M_x,1,4,1,5\right) = \begin{pmatrix} 0 & 0 & 0 & 0 & 0 \\ 1.716 & -0.57 & -0.986 & -0.947 & 0 \\ 1.495 & -0.466 & -0.792 & -0.79 & 0 \\ 0 & 0.254 & 0.387 & 0.305 & 0 \end{pmatrix}\cdot\frac{kN\cdot m}{m}$$

$$submatrix\left(M_y,1,4,1,5\right) = \begin{pmatrix} 0 & 0 & 0 & 0 & 0 \\ 0.292 & -1.038 & -1.61 & -1.289 & 0 \\ 0.254 & -0.697 & -1.07 & -0.879 & 0 \\ 0 & 1.495 & 2.274 & 1.797 & 0 \end{pmatrix}\cdot\frac{kN\cdot m}{m}$$

- torsional moment:

$$submatrix\left(M_{xy},1,4,1,5\right) = \begin{pmatrix} 0.178 & 0.544 & 0.071 & -0.544 & -0.641 \\ 0 & 0.236 & 0.031 & -0.236 & -0.373 \\ 0 & -0.272 & -0.036 & 0.272 & 0.428 \\ 0.155 & 0 & 0 & 0 & 0.186 \end{pmatrix}\cdot\frac{kN\cdot m}{m}$$

Shear forces are calculated as:

$$Q_{x_{i,j}} = \frac{D}{2\Delta^3}\cdot\begin{pmatrix} W1_{i,j+2} - 2\cdot W1_{i,j+1} + 2\,W1_{i,j-1} - W1_{i,j-2} \ldots \\ +-2\cdot W1_{i,j+1} + 2\,W1_{i,j-1} + W1_{i+1,j+1} + W1_{i-1,j+1} - W1_{i+1,j-1} - W1_{i-1,j-1} \end{pmatrix}$$

$$Q_{y_{i,j}} = \frac{D}{2\Delta^3}\cdot\begin{pmatrix} W1_{i+2,j} - 2\cdot W1_{i+1,j} + 2\,W1_{i-1,j} - W1_{i-2,j} \ldots \\ +-2\cdot W1_{i+1,j} + 2\,W1_{i-1,j} + W1_{i+1,j+1} + W1_{i+1,j-1} - W1_{i-1,j+1} - W1_{i-1,j-1} \end{pmatrix}$$

and shown in matrix form:

$$submatrix\left(Q_y,2,3,2,4\right) = \begin{pmatrix} 0.497 & 0.796 & 0.713 \\ -1.434 & -2.247 & -1.854 \end{pmatrix}\cdot\frac{kN}{m}$$

$$submatrix\left(Q_x,2,3,2,4\right) = \begin{pmatrix} 1.968 & 0.269 & -1.11 \\ 1.543 & 0.216 & -0.796 \end{pmatrix}\cdot\frac{kN}{m}$$

7. References

Timoshenko S.P., Goodier J.N. *Theory of Elasticity.* McGraw-Hill Comp., N.Y. 1951

Timoshenko S.P., Woinowsky-Krieger S. *Theory of Plates and Shells.* McGraw-Hill Comp., N.Y. 1959

Ventsel E., Krauthammer Th. *Thin Plates and Shells: Theory: Analysis, and Applications*. CRC Press, 2001

Girkmann K. *Flächentragwerke,* Springer, 1959

Nowacki W. *Dźwigary powierzchniowe,* PWN, Warszawa 1979

Fung Y. C. *Foudations of Solid Mechanics,* Prentice Hall Inc. New York, 1965